DEVELOPMENT OF A LASER INDUCED BREAKDOWN SPECTROMETER FOR DETECTION OF TOXIC ELEMENTS IN COSMETIC PRODUCTS

BY

YASIN WANDHAMI MAGANDA

A Thesis Presented to the

DEANSHIP OF GRADUATE STUDIES

KING FAHD UNIVERSITY OF PETROLEUM & MINERALS

DHAHRAN, SAUDI ARABIA

In Partial Fulfillment of the
Requirements for the Degree of

MASTER OF SCIENCE

In

PHYSICS

NOVEMBER 2013

KING FAHD UNIVERSITY OF PETROLEUM & MINERALS

DHAHRAN- 31261, SAUDI ARABIA

DEANSHIP OF GRADUATE STUDIES

This thesis, written by **YASIN WANDHAMI MAGANDA** under the direction of his thesis advisor and approved by his thesis committee, has been presented and accepted by the Dean of Graduate Studies, in partial fulfillment of the requirements for the degree of

MASTER OF SCIENCE IN PHYSICS

M. A. Gondal

Prof. M.A.Gondal
(Advisor)

Prof. F.F. Al-Adel
(Member)

Dr. Abdul-Aziz Al-Jalal
Department Chairman

Dr. A. Mekki
(Member)

Prof. Salam A. Zummo
Dean of Graduate Studies

2/12/13

Date

Dedicated to my mum

ACKNOWLEDGEMENT

First and foremost thanks to the almighty Allah who gave me the strength, ability and patience to accomplish this research work. Profound appreciation is also due to King Fahd University of Petroleum and Minerals (KFUPM) for supporting this research.

I wish to express my sincere gratitude to Professor M. A. Gondal, who served as my major advisor for his guidance and patience throughout the success of this research work. His continuous support and encouragement are immeasurably appreciated and can never be forgotten. I am greatly indebted to Prof. F. F. Al-Adel, Dr. A. Mekki, Mr. M. A. Dastageer and Mr. M. Pillai for their tremendous and priceless support towards the completion of this work. Thanks are due to the chairman of Physics department Dr. A. M. Al-jalal for all the available departmental research facilities used. I am also grateful to the entire faculty members for their encouragement and their direct or indirect help in one way or the other.

Lastly, I would like to extend my heartfelt thanks to my family and friends for their love, affection and continual moral support.

TABLE OF CONTENTS

LIST OF TABLES

LIST OF FIGURES

LIST OF ABBREVIATIONS

LIBS	**:**	**Laser Induced Breakdown Spectroscopy**
AES	**:**	**Atomic Emission Spectroscopy**
LSS	**:**	**Laser Spark Spectroscopy**
LAS	**:**	**Laser Ablation Spectroscopy**
LIPS	**:**	**Laser Induced Plasma Spectroscopy**
TRIBLIS	**:**	**Time Resolved Laser Induced break down Spectroscopy**
ICP-MS	**:**	**Inductively Coupled Plasma Mass Spectroscopy**
ICP - OES	**:**	**Inductively Coupled Plasma Optical Emission Spectroscopy**
Nd: YAG	**:**	**Neodymium Doped Yttrium Garnet**
KBr	**:**	**Potassium Bromide**
UV	**:**	**Ultra violet**
IR	**:**	**Infrared**
ICCD	**:**	**Intensified Charge Coupled Device**
S/N	**:**	**Signal to Noise ratio**
LTE	**:**	**Local Thermodynamic Equilibrium**
B.P	**:**	**Boltzmann Plot**

LIP	**:**	**Laser Induced Plasma**
NIST	**:**	**National Institute of Standard and Technology**
IUPAC	**:**	**International Union of Pure and Applied Chemistry**
FWHM	**:**	**Full Wavelength at Half Maximum**
RSD	**:**	**Relative Standard Deviation**
LOD	**:**	**Limit of Detection**
EA	**:**	**Environmental Agency**
FDA	**:**	**Food and Drug Administration**

ABSTRACT

Full Name : Yasin Wandhami Maganda

Thesis Title : Development of a Laser Induced Breakdown Spectrometer for detection of toxic elements in cosmetic products

Major Field : Physics

Date of Degree : November 2013

In this research work we developed a highly sensitive analytical Laser Induced Breakdown Spectrometer to detect toxic elements in commercially available cosmetic products. These products are frequently used by many all over the world, therefore there is an increasing demand to determine concentration levels of toxic elements present in them because they cause dangerous diseases and most of them are highly carcinogenic and life threatening. Laser Induced Breakdown Spectroscopy (LIBS) was applied for spectroscopic analysis of cosmetic products such as tooth paste, synthetic hair dye, kohl eyeliners and talcum powder samples. These samples were purchased from the local market within the kingdom of Saudi Arabia. The LIBS method is based on spectroscopic analysis of plasma resulting from the interaction of a high power pulsed laser radiations with a sample medium. In order to improve the sensitivity of the spectrometer, the dependence of the LIBS signal intensity and plasma parameters such as temperature (T) and electron density (n_e) on gate/time delay, laser fluence and wavelength of the excitation source for plasma generated under ambient conditions were studied. During this work Nd: YAG lasers having 266nm, 532 nm and 1064 nm wavelengths operating in Q-switch mode were used as the excitation sources in combination with a spectrograph having a gated ICCD camera. Boltzmann plots and stark broadening for the recorded spectral lines were used to

estimate the plasma temperature and electron density respectively. Temporal evolution of the plasma temperature and electron density showed a t^{-2} dependence. On the other hand plasma temperature and electron density increased with increase in laser fluence but leveled off at higher fluencies. It is worth noting that in both cases 266 nm and 1064 nm excitation wavelengths consistently had the highest and lowest values respectively. Therefore a 266 nm wavelength Nd: YAG laser excitation source was selected to develop a highly sensitive Laser Induced Breakdown spectrometer to detect and quantify the fluoride (F), lead (Pb) and chromium (Cr) content in commercially available toothpaste, synthetic hair dye, kohl eyeliners and talcum powder samples. The experimental parameters such as gate/ delays and laser fluencies were optimized to achieve an optically thin and in local thermodynamic equilibrium plasma (L.T.E) which improved the limit of detection of our spectrometer. The choice of the parameters was validated using the Mcwhirter criterion. For fluoride detection in the toothpaste samples, a strong atomic transition line of fluorine at 731.102 nm was used as the marker line. The LIBS system was able to detect fluoride concentration levels in the range of 1300 – 1750 ppm with a detection limit of 156ppm.In the synthetic hair dye, chromium was detected using a strong atomic transition of chromium (Cr) at a wavelength 427.5 nm as the spectral marker line and the spectrometer with a detection limit of 1.2 ppm was able to detect chromium concentration levels in the range of 5-11 ppm. These results achieved with our LIBS system were compared with those obtained using a standard detection method such as ICP-MS. The results obtained are in excellent agreement with ICP-MS. Lead (Pb) and Chromium (Cr) in kohl were detected using atomic transitions at wavelengths of 405.7 nm and 425.4 nm respectively as the spectral marker lines. The system was calibrated for these toxic metals and it was able to detect Lead and Chromium in the range of 5-14 ppm and 4-9 ppm with detection limits of 1ppm and 2 ppm

respectively. The LIBS results were compared with those obtained using ICP-MS and were in good agreement yielding a relative accuracy in the range 0.05-0.3 which is acceptable. Lead (Pb) and Chromium (Cr) levels in talcum powder samples were detected and quantified using strong transitions at wavelengths of 405.7 nm and 425.4 nm respectively. The LIBS system detected lead and chromium in the range of 15-17 ppm and 23-29 ppm with limits of detection of 1.96 ppm and 1.72 ppm respectively. The concentration levels of fluoride, lead and chromium detected using our LIBS system exceeded the permissible limits set by the Environmental agency and other regulatory organization and hence frequent use of such cosmetic products can be hazardous to human health. The LIBS spectrometer developed through this research work can be applied for analysis of many other samples like pharmaceutical, polymers, iron, volcanic eruption and geological samples for mineral quantification.

ملخص الرسالة

الاسم الكامل: ياسين وندامي ماجاندا

عنوان الرسالة: تطوير مطيافية تفتت من منشأ ليزري للكشف عن مواد سامة في منتجات تجميلية

التخصص: فيزياء

تاريخ الدرجة العلمية: أوكتوبر 2013

في هذا العمل البحثي طورنا مقياس طيفي للتكسير بالليزر حساس للغاية للكشف عن العناصر السامة في منتجات التجميل المتاحة تجاريًا. وكثيرا ما تستخدم هذه المنتجات من قبل العديد في جميع أنحاء العالم، وبالتالي هناك طلب متزايد لتحديد مستويات تركيز العناصر السامة الموجودة فيها لأنها تسبب أمراض خطيرة ومعظمها مسرطن للغاية وتهدد الحياة. تم تطبيق طريقة طيف التكسير بالليزر على مستحضرات التجميل مثل معجون الأسنان، وصبغة الشعر الاصطناعية، وأقلام تكحيل العين، وعينات بودرة التلك. وقد تم شراء هذه العينات من السوق المحلية في المملكة العربية السعودية. ويستند أسلوب طيف التكسير بالليزر على تحليل طيف البلازما الناتجة من تفاعل نبضات ليزر عالية الطاقة مع العينة. من أجل تحسين حساسية المطياف، تم دراسة مدى اعتماد قوة خطوط طيف التكسير بالليزر وعوامل البلازما مثل درجة الحرارة وكثافة الإلكترونات على تأخير فتح البوابة، وفترة فتحها، وكمية الليزر، والطول الموجي للمصدر المثير للبلازما في الظروف المحيطة. خلال هذا البحث استخدمنا ليزر من نوع Nd: YAG بعدة أطوال موجية 266 نانومتر، و532 نانومتر، و1064 نانومتر يعمل في وضعية تسمى تبديل-Q (Q-switch) كمصادر مثيرة، بالإضافة إلى راسم طيف يحتوى كاميرا من نوع ICDD. رسم بولتزمان استخدِم لتقدير حرارة البلازما واستخدِم اتساع ستارك لخطوط الطيف لتقدير كثافة الإلكترونات. اتضح أن حرارة البلازما وكثافة الإلكترونات يتغيران مع الوقت ويتناسبان طرديا مع t^{-2}. على الجانب الآخر درجة حرارة البلازما وكثافة الإلكترونات زادتا مع زيادة كمية الليزر، ولكن استقرتا عند كميات عالية. تجدر الإشارة إلى أن الطول الموجي 266 نانومتر يعطي أعلى قيم، بينما الطول الموجي 1064 نانومتر يعطي أدنى قيم. لذا الطول الموجي 266 نانومتر للمصدر المثير لليزر Nd: YAG اختير لتطوير مقياس طيفي للتكسير بالليزر لكشف وقياس الفلوريد، والرصاص، والكروم الموجودين في معجون الأسنان، وصبغة الشعر الاصطناعية، وأقلام كحل العين، وعينات بودرة التلك المتاحين تجاريًا. تم ضبط عوامل التجربة مثل تأخيرات البوابة وكميات الليزر لإيجاد توازن ديناميكي حراري موضعي لبلازما "رقيقة ضوئيًا" (optically thin)، مما رفع الحد الأدني لقدرة كشف المطياف. اختيار العوامل يتفق مع معيار Mcwhirter. للكشف عن الفلورايد في عينات معجون الأسنان استخدم الخط الانتقالي الذري القوي للفلور عند 731.102 نانومتر كمؤشر. كان لنظام طيف التكسير بالليزر القدرة على الكشف عن مستويات تركيز الفلورايد في حدود 1300 - 1750 جزء في المليون مع حد أدنى للكشف 156 جزء في المليون. في صبغة الشعر الاصطناعية تم الكشف عن الكروم باستخدام الانتقال الذري القوي للكروم عند الطول الموجي 427.5 نانومتر كمؤشر، وكان المطياف الذي له حد أدنى للكشف 1.2 جزء في المليون قادر على الكشف عن مستويات تركيز الكروم في حدود 5-11 جزء في المليون. وتمت مقارنة هذه النتائج من نظام طيف التكسير بالليزر لدينا مع

تلك التي تم الحصول عليها باستخدام طريقة كشف قياسية مثل ICP- MS. النتائج التي تم الحصول عليها في اتفاق ممتاز مع ICP- MS. تم الكشف عن الرصاص في أقلام التكحيل باستخدام الإنتقال الذري عند الطول الموجي 405.7 نانومتر، وكُشف الكروم في أقلام التكحيل باستخدام الإنتقال الذري عند الطول الموجي 425.4 نانومتر. نظام طيف التكسير بالليزر كشف عن الرصاص في حدود 15-17 جزء من مليون والكروم في حدود 23-29، وله حد أدنى للكشف عن الرصاص يساوي 1.96 جزء في المليون وحد أدنى للكشف عن الكروم يساوي 1.72 جزء في المليون. مستويات تركيز الفلورايد والرصاص والكروم المكتشفة باستخدام نظام طيف التكسير بالليزر لدينا تجاوزت الحدود المسموح بها التي وضعتها وكالة البيئة ومنظمات رقابية أخرى، وبالتالي الاستعمال المتكرر لهذه المستحضرات التجميلية قد يشكل خطر على صحة الإنسان. مطياف طيف التكسير بالليزر المطور خلال هذا العمل البحثي يمكن استخدامه لتحليل العديد من العينات الأخرى مثل الأدوية، والبوليمرات، والحديد، والمخرجات البركانية، والعينات الجيولوجية لتقدير كمية المعادن فيها.

CHAPTER 1

INTRODUCTION

1.1 Laser induced breakdown spectroscopy (LIBS)

LIBS has been extensively developed as an analytical technique over the last decade. In this technique a low energy laser is focused on the target using a lens of an appropriate focal length, the material is ablated from the target and plasma is generated. The light emitted by the atomic and ionic species in the plasma is collected by a spectrograph interfaced with a computer to generate a LIBS spectrum for spectral analysis.

Ablation of the material occurs when the laser power irradiance exceeds the breakdown threshold of the target sample. When the laser induced plasma is formed, it decays over an interval of about one to several microseconds depending on the energy of the excitation source. After initiation the plasma radiates a continuum which decays rapidly in a few hundred nanoseconds, here weak lines show up which are mostly identified as ionic lines of the plume. This is followed by the emission spectrum in which neutral atoms (atomic lines) are dominant whose line strength is proportional to the concentration of the atoms emitting the radiation. Inspection of the LIBS spectrum reveals immediate qualitative information about sample composition. To measure the concentration of the metals, calibration curves are usually used. The slope of such a curve defines the sensitivity of the analytical method according to IUPAC (International Union of Pure and Applied Chemistry) definition [1].

Conventional techniques such as inductively coupled plasma optical emission spectroscopy (ICP-OES), ICP- Mass spectroscopy (ICP-MS) and atomic absorption spectroscopy have good analytical performance, but their sample pretreatment methods require acid digestion under very high temperatures and pressure. It also involves usage and disposal of hazardous chemicals which create more environmental problems. Hence these analytical methods are destructive, time consuming and environmentally hazardous. In contrast LIBS has various advantages such as simplicity, versatility, extremely flexible experimental set up and capability of multi elemental analysis for any kind of substance with little or no pretreatment and sample preparation. Due to the inherent unique advantages of LIBS, it has developed rapidly since the invention of lasers in the 1960's and has been successfully applied for both qualitative and quantitative analysis in a wide range of areas such as environmental monitoring [2-4], Industrial applications[5,6], medical field [7,8] forensic field [9,10] and space exploration [11].

1.2 Theory of LIBS

1.2.1 Introduction

LIBS is a multi- elemental analytical technique based on Atomic Emission Spectroscopy (AES) used to qualitatively and quantitatively analyze samples in solid, liquid and gaseous form. This analytical technique has other acronyms like Laser Induced Plasma Spectroscopy (LIPS), Laser Spark Spectroscopy (LSS), Laser Ablation Spectroscopy (LAS) and Time Resolved Laser Induced Breakdown Spectroscopy (TRLIBS) [1, 12]. AES is based on the discrete energy level structure of atoms whereby excited atoms de-excite to radiation with frequencies characteristic of the radiating species and with intensities related to the concentrations of the atoms emitting the radiation. Therefore AES can be used to quantitatively and qualitatively analyze a sample [13]. The three basic components of AES apparatus are the excitation source, wavelength selector and a detector. The excitation source is required to produce and excite free atoms from the sample. The wavelength selector provides information on the specific wavelength recoded by the detector and the detector quantifies the intensity of radiation emitted by the excited atoms at a given frequency pre-determined by the wavelength selector.

1.2.2 Principle of LIBS

In LIBS, a high power pulsed laser beam is focused on the target surface; this laser pulse momentarily creates plasma on the surface of the target through multi-photon and collisional processes. The initial temperature of the multi-colored plasma reaches as high as 25 kilo Kelvin and rapidly falls, which we technically refer to as plasma cooling [14-17]. The plasma emission is directed to a monochromator/spectrograph for wavelength dispersion, which in turn deciphers the presence of any element based on its characteristic atomic emission wavelength. The timing

of the detection after the laser excitation is a key parameter to deal with. As time passes by up until a few micro seconds, the components of the plasma recapture electron and becomes excited neutral atoms and after few microseconds, these atoms transfer from the excited states to lower states by emitting the characteristic wavelengths inherent to the elements present in the sample [18]. In addition to the emission from the neutral atoms, emission from the singly ionized atomic species can be detected provided the detection time window is restricted to an earlier time. The detection time gate is adjusted by tuning the delay between the laser and the detector.

1.2.3 LIBS as an Analytical technique

Over the past three decades there has been intense activity in the study and development of the LIBS [19-27]. This is due to its unique capabilities which allow analysis of materials under conditions not possible previously by using other analytical techniques. Firstly, the ability of the laser pulse to prepare and excite the sample in one step as a result of the high power densities ($>10^8$ Wcm^{-2}) required to initiate plasma. Secondly, the region of analysis can be defined accurately due to the very small spot size provided by the high degree of collimation of the laser beam. This capability is useful for some applications such as spatial mapping of elements (micro-analysis). Thirdly, the plasma can be formed on a remotely located target and in harsh environments by transmitting the laser pulse over long distances either through open path or through a fiber optic. However, inspite of all these capabilities, it cannot directly compete with established laboratory based analytical methods in terms of the usual analytical figures of merit (detection limits, accuracy and precision). Also the quality of quantitative analysis is subject to a number of operating parameters that may or may not be controlled to maximize LIBS analytical measurements. For example the mass ablated and the characteristics of the resultant laser plasma are strongly dependent on operational parameters such as laser properties, target properties,

geometrical set up, laser pulse irradiance/fluence, time window observation, ambient conditions. Changes in these parameters affect the analyte signals as well as relative intensities of the emission lines hence the sensitivity of the LIBS system as discussed below [28].

1.2.3.1 Factors affecting the LIBS plasma

The interaction of a high power focused laser-radiation with solids is a complex phenomenon depending on a multi dimensional matrix of parameters such as laser properties, properties of the target material (composition) and the ambient conditions (pressure).

1.2.3.2 Laser properties

Various types of lasers are used in LIBS ranging from UV Excimer lasers to infrared solid state lasers. Each laser has a different absorption characteristic during plasma formation which affects the behavior of the resulting plasma. There are two main mechanisms for electron generation and growth before plasma generation. The first involves absorption of laser radiation by the free electrons, which collide with neutral atoms in the target vapor. When they gain sufficient energy, they impact and ionize atoms/ molecules in the vapor. The electron concentration increases with time due to cascade break down. The second mechanism is the multi photon ionization which involves absorption of a sufficient number of photons by atoms/ molecules to cause ionization. Multi photon ionization plays an important role for only short wavelength lasers < 1µm. Both cascade and multi-photon ionization require very high irradiances typically $\geq 10^8$ Wcm^{-2}. Also plasma formation takes place when the laser intensity exceeds a threshold value characteristic of the target material easily attained by proper focusing of the laser beam [1]. When nanosecond lasers interact with solids, the energy is transferred to the electrons of the lattice resulting in melting and vaporization of the target followed by an expanding vapor plume of the material. The expanding plume forms a shock wave which assists the ionization of the surrounding gas.

Furthermore, the laser pulse interacts with the plasma resulting in a more efficient re heating of the plasma by inverse bremsstralung absorption. When Ps lasers interact with solids, at first an air break down plasma is formed on a Pico second time scale, followed by an expanding plume of a material on a nanosecond time scale. Therefore the laser plasma interaction using nanosecond laser is fundamentally different from that under Pico second excitation [29].

1.2.3.3 Properties of the target material.

The shape and size of the laser induced plasma plume is dependent on thermal, physical and mechanical properties of the target material. The mass removed from the target depends not only on the laser intensity but also on the properties of the target material [30]. A relationship for ablated mass *m (t)* on the basis of heat conduction mechanism is as given in equation 1[31]

$$m(t) = A(aIt) + B(AI)^2 t^{3/2} \tag{1}$$

where *A* and *B* are proportional to the target thermal properties, *a* is energy coupling factor, *I* is laser intensity and *t* is the laser pulse duration.

For formation of plasma, the fluence should exceed a threshold value typically of order of several Jcm^{-2} for *ns* laser pulses. Plasma formation requires vaporization of the material as the first step and vaporization of the sample occurs when the energy deposited on the target exceeds the latent heat of vaporization of the target L_v. This threshold fluence (F_{th}) below which no evaporation will occur is given by

$$F_{th} = \rho l_v a^{1/2} w^{1/2}, \; a = K / \rho C_p \tag{2}$$

where ρ is the sample density, L_v is the latent heat of vaporization of the target, a is the thermal diffusivity, K is thermal conductivity, C_p is specific heat and w is the laser pulse width.

It’s worth mentioning that a threshold intensity of a material is related to its thermal properties such as thermal conductivity, melting and boiling temperature implying that thermal effects play an important role during laser ablation [32]. The physical and mechanical properties of the material have an influence on the shape and size of the crater on its surface hence the size and shape of the plasma plume. Specifically, reflectivity of the target material determines the fraction of the laser energy coupled to the surface of the target material. Laser energy can be absorbed effectively by a reflecting surface due to the phase change of the material at high temperatures which is possible only at high laser intensities [33]. Reflectivity of the sample surface, density, specific heat and boiling temperature influence the size and shape of the craters and is given by the following relation [34]

$$D = \frac{A(1-R)}{\rho C_p T_b} \tag{3}$$

where D is the diameter of the crater, A is proportionality constant, R is the reflectivity of the surface, T_b is the boiling temperature and all other symbols have their usual meaning. The volume heated by the laser pulse also depends on the thermal conductivity of the material [35].

1.2.3.4 Geometrical set up

The shape of the plasma and spatial emission intensity profile are dependent on the optical alignment for focusing the laser and collecting the emission from the plasma plume for recording the spectrum. Therefore it’s important to understand the dependence of the LIBS signal on the optical alignment and the collection light for recording the spectrum. In LIBS cylindrical lenses are preferred to spherical ones to focus the laser beam on the sample because, they have a better precision [36]. For analysis of solids the laser is focused perpendicular to the target surface and for the case of liquids, it’s usually focused slightly off the normal so as to protect the lens from

the splashes of produced by the liquid due to the shock waves. The high laser intensity causes break down in air before focusing on the sample surface; this affects the intensity reaching the surface of the target especially when some dust particles are occasionally irradiated. To avoid this, the distance between the focusing lens and the target surface is made a little shorter than the focal length to produce a stable break down while maximizing the interaction area [37, 38].

The collection of the plasma emission is performed axially, that's along the perpendicular to the surface of the target because of its simplicity and reproducibility. This configuration is less sensitive to the change is surface to lens distance which occurs when several shots are fired at the same position on the sample. With on- axis collection the change in surface to lens distance causes minimum perturbations in the LIBS signal because of the depth of focus of direction optics which is typically longer than the crater depth [39]. Hence focal lengths having a few centimeters are best suited for LIBS. The most important technique to collect light from the plasma plume is using a fiber optic by placing it a few centimeters from the plume to avoid damage due to heating. The collection angle allows gathering light from a broad volume of the plasma plume [40].

1.2.3.5 Time window observation

Initially the plasma has a very high temperature, but when the plasma expands away from the target surface its temperature decreases. It's observed that early stages of the plasma evolution are dominated by a continuum radiation. The evolution of the line intensities are observed after the expansion of the plasma followed by a decrease in temperature. These line emissions are superimposed on the continuum emission. Only the line emission is important during compositional analysis of materials using LIBS. Usually the continuum emission decays very

fast in comparison to the line emission. Therefore an appropriate time delay when the line emission to background noise is very high is very vital when using LIBS [37, 41].

1.2.3.6 Ambient conditions

The shape and size of the plasma also depend on the ambient conditions such as surrounding pressure and gas composition. The emission intensity of laser induced plasma increases with increase in pressure. This is due to the confinement of the plasma which produces denser and hotter plasma. However at moderately high pressures, the absorption effects become significant due to the increase in concentration of the absorbing species surrounding the hot plasma which makes it thin and expands rapidly, resulting in a decrease in the emission intensity. This effect can be minimized by using moderate pressures in the range $50 < P < 500$ torr in air [42].

1.2.3.7 Binding materials

The binding material plays a vital role in the preparation of samples for LIBS. The samples should have adequate mechanical strength for LIBS analysis due to the fact that when a high power pulsed laser beam interacts with the sample; it disintegrates during laser ablation by mechanical shocks resulting into target breakage and crumbling into original particulate material. For homogenous target sample preparation, the sample is first broken down into unconsolidated particles by grinding to an extremely fine powder. Then, pellets are prepared using a binding material [1]. In order to achieve a higher sensitivity and more precise analysis with LIBS, an appropriate binding material should be selected. This can be achieved by mixing the actual powder material with suitable binders, such as KBr, Ag, Al, starch or poly (vinyl alcohol) and then pressing in a special die. One of the parameter of a binding material is bond strength defined as a measure of strength between particles that bind a sample together to resist ablation therefore it influences the matrix of the sample. Higher bond strength causes resistance to various changes

in a target sample hence increases the analytical stability of the sample [1]. Study of various binding materials like potassium bromide, polyvinyl alcohol, starch, silver and aluminum was carried out using LIBS [2]. The role of the matrix effects using these five binders on LIBS signal intensity and crater depth produced was investigated for better performance of LIBS technique as a quantitative analytical tool. For comparative study of various binders, the signal intensity of different Mg, lines at 518.3, 517.2, 383.8 and 279.5 nm wavelengths were recorded for pellets prepared with known concentrations of Mg in these binders. Optical scanning microscopy images of the ablated crater were studied to understand the laser ablation process. The relative signal intensity measured for a standard Mg line (at 518.3 nm) were 735, 538, 387, 227 and130 for potassium bromide, starch, poly (vinyl alcohol), silver and aluminum as binders, respectively. This indicates clearly that potassium bromide was better as a binder for LIBS studies of powder samples.

1.2.4 Breakdown phenomena on solid surfaces

When the laser irradiance is high enough to cause a plasma plume, the leading edge of the pulse rapidly heats, melts and vaporizes material into a layer above the target surface. Some of the laser energy then heats the evaporated material. While the plasma is weakly ionized, part of the laser energy continues to the surface and part of it is absorbed by the plasma. At high enough energies the plasma can become opaque to the laser beam and the surface is shielded, while the plasma front grows towards the laser. This occurs when the plasma frequency becomes greater than the laser frequency.

1.2.5 Laser ablation

Ablation depends on a multidimensional matrix of parameters including material properties and laser properties. Laser fluencies of micro joules to millijoules can cause removal of atoms and ions with no obvious physical change to the surface. At higher fluencies different mechanisms come into play because, for subsequent pulses, the laser energy is incident upon melted and condensed matter. The surface reflectivity changes and an ablation crater with or without elevated walls forms. The elements of the previous sample may have been selectively evaporated so that the re-deposited material no longer exhibits the original composition. Important issues in ablation are minimum power density to initiate vaporization, effects of shorter or longer laser pulse lengths, the rate at which ablation proceeds, and the goal of retaining the composition of the sample after ablation into the plasma. An estimate of the minimum power density within a laser required to produce vaporization is given as [45]

$$I_{\min} = \frac{\rho L_v \kappa^{1/2}}{\Delta t^{1/2}} \left(w / cm^2 \right) \tag{4}$$

where, ρ is the density of the target material, L_v is the latent heat of vaporization, κ is the thermal diffusivity of the target and Δt is the laser pulse length. For pure aluminum for example $I_{\min}$ is about $1.75 X 10^8 W cm^{-2}$ [46]. The effect of the laser wavelength is partly described through the critical density given by equation 1 but this should be coupled with the temporal length of the laser pulse. The potential advantage of picosecond and femtosecond pulses is that absorption and interaction with the surface could be finished before plasma or plume forms to absorb the laser energy. Material ablated into the plasma can have the form particles (fresh, melted, and cooled) as well as atoms and/or molecules. Because of the different volatilities of elements and their compounds, the vaporization of elements doesn't necessarily mirror the samples composition

[47]. It's therefore apparent to minimize selective vaporization in order to retain stoichiometry is critical. When the energy deposited into the sample is much higher than the latent heat of vaporization for all the constituents, it's likely that all the constituents can be vaporized and removed. This is because target thermal properties and constants no longer play a major role. At $> 10^9$ Wcm^{-2} and nanosecond pulses, the pressure over the surface inhibits further vaporization until the substrate reaches a critical temperature. Because of the more uniform heating and a more explosive release, the melt ejected is closer to the sample composition.

1.2.6 Plasma generation and expansion

When the laser intensity exceeds the ablation threshold of the target material, the laser beam causes evaporation and ionization of the material creating a plasma plume just above the surface of the material. Initially the atoms, molecules and ions undergo collisions in the high density region near the target forming the Knudsen layer [48]. This leads to a highly directional expansion of the plasma plume perpendicular to the target. In the initial stage, the interaction of the laser beam with the bulk target results in the evaporation of the surface layer. Further interaction of the laser beam with the material leads to formation of an isothermally expanding plasma. This expansion persists until the termination of the laser pulse [48]. The vapor particles are pushed forward in the lateral direction exclusively by the high pressure emanating from the target surface when the ejected plume is considered transparent to the incident laser beam. Strong laser plasma interaction creates an additional high pressure kinetic energy region fuelling further expansion of the plume. After the termination of the laser pulse no further particles are ejected from the target surface. The forward directed nature of the laser evaporation process results from anisotropic expansion velocities of different species governed by the initial dimensions of the expanding plasma. The thermal energy is rapidly converted to kinetic energy

with the plasma attaining extremely high expansion velocity. During the initial stages of plasma expansion, when the particle density is high (~10^{19} cm^{-3}), the mean free path of the particles is short (~1μm) and the plasma behaves as a continuum fluid. As the plasma expands the temperature drops very rapidly (within 100ns), However the rate of temperature drop is smaller at later times (> 100ns) because energy is regained due to recombination of ions.

1.2.7 Qualitative Analysis

Qualitative analysis of chemical elements using LIBS begins with the identification of the strong emission lines in the LIBS spectra. There are several data bases for atomic spectra wavelengths and relative intensities but the most commonly used is NIST (National Institute of Standards and Technology) which provides line spectra database and dependable LIBS research tools that are informative and easy to use. Both weak and strong emission lines are compiled in the NIST site for more than 100 elements referenced from various atomic line emission spectroscopy references. For identification of an element by strong line emission, wavelengths resolutions of 0.03 nm to 0.2 nm are required and its identification is verified by the presence of at least three strong to moderate relative intensity lines [1].

1.2.8 Plasma opacity

Plasma is a local assembly of atoms, electrons and ions overly electrically neutral. They are characterized by a number of parameters but the most basic is the degree of ionization. A weakly ionized plasma is one in which the ratio of electrons to other species is less than 10%. It's worth noting that LIBS plasma typically fall in the weakly ionized plasmas. At early times the ionization is very high, this is followed by electron ion recombination, neutral atoms and finally molecules form. During the temporal evolution of the plasma, on the LIBS spectrum the spectral lines are observed to be superimposed on the background (continuum) however it decays faster

than the spectral lines. Time resolution of the plasma light in LIBS allows discrimination of the region where the spectral lines dominate the spectrum. The main objective of LIBS is to create optically thin plasma and in local thermodynamic equilibrium whose composition is the same as that of the sample. Plasma is optically thin when the emitted light traverses and escapes from the plasma without significant absorption or scattering. The intensity of radiation emitted by plasma is given by

$$I(\lambda) = \left[\frac{\varepsilon(\lambda)}{\alpha(\lambda)}\right]\left\{1 - \exp\left[1 - \alpha(\lambda) L\right]\right\} \tag{5}$$

where $\varepsilon(\lambda)$ is the emissivity, $\alpha(\lambda)$ is the absorption coefficient/cm, L is the plasma length along the sight of the observer. For optically thin plasma, $\alpha(\lambda)$ is small, therefore $I(\lambda) \sim \varepsilon(\lambda) L$.

In order to check the optical thickness of plasma, strong spectral lines of elements with known relative intensities are used. When self absorption becomes noticeable, the observed intensities will depart from the expected values and this poses a problem for converting line intensities to concentrations. Intensity ratio of two spectral lines of the same species of ionization stage Z is expressed as

$$\frac{I_1}{I_2} = \left(\frac{\lambda_{nm,z}}{\lambda_{ki,z}}\right)\left(\frac{A_{ki,z}}{A_{nm,z}}\right)\left(\frac{g_{k,z}}{g_{n,z}}\right)\exp\left(\frac{-E_{k,z} - E_{n,z}}{K_B T}\right) \tag{6}$$

where I_1 is the line intensity from the k - i transition and I_2 is that from the n – m transition. If two emission spectral lines have the same or approximately the same upper energy levels, the effect of the Boltzmann factor on the line intensity ratio is minimized [1].Neglecting the exponential factor, the theoretical value of the intensity ratio of the two spectral lines is

determined using the atomic parameters of the transitions from the NIST database and the measured value is obtained using the experimental signal intensity values of the spectral lines. The region in which both ratios are the same is known as the temporal window for the optically thin plasma.

1.2.9 Local thermodynamic equilibrium

Laser induced plasmas (LIP) are generated by the interaction between matter and a laser radiation with irradiance above the breakdown threshold (> 1GW/cm^2). A LIP is plasma expanding at supersonic speeds whose density and temperature change with time. During its temporal evolution, the ablated material undergoes a transition between plasma typologies, passing from warm dense matter, immediately after the ablation to non equilibrium plasma such as corona plasma. In the late expansion stages it's important to note that during the plasma expansion it's possible to find a temporal window in which the system exists in thermodynamic equilibrium. In this case, plasma properties such as relative populations in the energy levels, distribution of the speed of particles are described using thermodynamic parameters i.e. populations in the energy levels follow Boltzmann statistics , particles have Maxwellian velocity distribution, ionization processes are described by Saha's equation and the radiation density obeys planks law. A valid approximation for the Local Thermodynamic Equilibrium (L.T.E) a condition where by the light emitted the laser induced plasma is not scattered or reabsorbed and also the plasma its self doesn't absorb the laser beam exists after a sufficient number of collisions have occurred to thermalize the plasma. It's common for heavy species (atoms and ions) and light species (electrons) to equilibrate separately more quickly and then later in time with each other because, energy between collision partners is shared more equally the closer the masses of the colliding particles. Along the boundary of the plasma where number densities are low and

movement of the boundary region is very rapid, the LTE is not a good assumption. However slightly deeper into the plasma where conditions change more slowly and collisions occur more frequently, this assumption is valid. Clearly for LTE to hold, the electron density must be sufficiently high. The minimum density condition for plasma to exist in local thermodynamic equilibrium can be checked using the Mcwhirter criterion given by the relation in equation 7 [49]

$$n_e \geq 1.4\times10^{14} T^{1/2} \left(\Delta E\right)^3 cm^{-3} \tag{7}$$

where n_e is the critical electron density and its dependence on the largest energy gap $\left(\Delta E\right)$ between two adjacent levels of the considered species i.e. the energy of the shortest wavelength transition used in the temperature determination. T is the plasma temperature and n_e is the electron density.

1.2.10 Plasma temperature

To determine the plasma temperature, the laser induced plasma should be optically thin and in LTE. Under these conditions, the energy level population of the species in such plasma is given by Boltzmann distribution law.

$$\frac{n_{k,z}}{n_z} = \frac{g_{k,z}}{p_z} \exp\left(\frac{-E_{k,z}}{K_B T}\right) \tag{8}$$

The index z refers to the ionization stage of the species, K_B is the Boltzmann constant, T is the plasma temperature, $n_{k,z}$, $E_{k,z}$ and $g_{k,z}$ are the population, energy and degeneracy of the upper level k respectively, n_z is the number density and P_z is the statistical partition function of the species in the ionization stage z. The integrated intensity I_z of the spectral line occurring between the upper energy level k and the lower energy level i of the species in the ionization stages z in optically thin plasma [50] is given by

$$I_z = \frac{hc}{4\pi\lambda_{ki,z}} A_{ki,z} n_{k,z} L \tag{9}$$

where *h* is the Planck constant, *c* is the speed of light; *L* is the characteristic length of the plasma, $A_{ki,z}$ is the transitional probability and $\lambda_{ki,z}$ is the transition line wavelength. From the equations above

$$I_z = \frac{hc}{4\pi\lambda_{ki,z}} A_{ki,z} L \frac{n_z}{P_z} g_{k,z} \exp\left(\frac{-E_{k,z}}{K_B T}\right) \tag{10}$$

Taking the natural logarithm of equation 10

$$ln\left(\frac{I_z \lambda_{ki,z}}{A_{ki,z} g_{k,z}}\right) = \frac{-1}{K_B T} E_{k,z} + ln\left(\frac{-hcLn_z}{4\pi P_z}\right) \tag{11}$$

Plotting a graph of magnitude of the component on the left hand side of the equation 11, for several transitions as a function of the energy for the upper level of the species in ionization stage *z* yields a Boltzmann plot. The value of plasma temperature *(T)* is then deduced from the slope of the plot.

1.2.11 Electron density

In highly dense plasmas generated under atmospheric pressure, stark broadening is the only dominant form of broadening and therefore is used to determine electron density of the plasma. Stark broadening of spectral lines in plasma is due to collisions of electrons and atoms with charged species resulting into broadening and a corresponding shift in the peak wavelength of the line. The line profile for stark broadening is described by a Lorentzian function [51-55] and has a full width at half maximum $\Delta\lambda_{1/2}$ related to the electron density (n_e) as shown in equation 12.

$$\Delta\lambda_{1/2} = 2W\left[\frac{n_e}{10^{16}}\right] + 3.5A\left[\frac{n_e}{10^{16}}\right]^{1/4}\left[1-\frac{3}{4}N_D^{-1/3}\right]W\left[\frac{n_e}{10^{16}}\right]A^0 \qquad (12)$$

where W is the electron impact parameter, A is the ion broadening parameter and N_D is the number of particles in the Debye sphere [51-55]. The first term on the right hand side of equation 12 represents broadening due to electron contribution and the second term is the ion contribution factor. For non hydrogenic ions, stark broadening is predominantly caused by the electron impact, since the perturbations by the ions are negligible as compared to those from the electrons. Therefore the correction factor can safely be neglected reducing the equation to

$$\Delta\lambda_{1/2} = 2W\left[\frac{n_e}{10^{16}}\right] \qquad (13)$$

1.2.12 Quantitative analysis

Quantitative analysis with high precision and accuracy to determine the concentration of an analyte in a given sample is the ultimate aim of any analytical technique. In LIBS, atomic emission intensity is used for analysis and quantification. From equation 10 a plot of Intensity as a function of concentration yields a calibration curve. The region in which the curve is linear is the dynamic range and its slope is called the sensitivity [1]. Therefore one can determine an unknown concentration of an analyte at any intensity provided its concentration is within the dynamic range of the curve and the same experimental conditions (time delay, laser energy, collecting fiber optics and incidence focusing distance, target rotation speed, atmospheric pressure) are observed [50].

1.2.13 Detection limit

The estimation of the limit of detection (LOD) is very significant for any spectroscopic analytical instrument. A detection limit is defined as the lowest amount of concentration of an analyte that can be reliably detected by the Laser Induced Breakdown Spectroscopy system developed. The calculation of the detection limits is based on the $2\sigma_B$ where σ_B is the noise of the background. In our case we define the noise of the background as the standard deviation of the experimental data over a spectral range free from the dynamic peaks. The limit of detection is then given as the concentration yielding net line intensity equal to two times the standard deviation [56].

$$LOD = 2\left(\frac{\sigma_B}{S}\right) \tag{14}$$

where S is the slope of the calibration curve which is the ratio of the intensity to the concentration. The limits of detection obtained in this study were estimated using equation 14.

1.2.14 Precision

The short to short variation caused by fluctuation in the laser pulses significantly distorts the analytical results of a sample hence the averaging mode is used to determine the optimum number of laser pulses for generation of the LIBS spectrum. The fluctuation is due to plasma perturbations which are attributed to the sampling techniques involved, sample homogeneity and target surface condition. Precision is the closeness of agreement between the results obtained by repeating the analytical procedure a large number of times under the same conditions [1]. It's expressed in terms of standard deviation (S), the deviation of a set of measurements (n) from the arithmetic mean (M) of the set of repeated measurements as shown below.

$$S = \sqrt{\frac{\sum\left(x_i - M\right)^2}{n-1}} \tag{15}$$

Using S, the percentage relative deviation (%RSD) can be calculated as

$$\%RSD = 100\% \times \left(S \middle/ M \right) \tag{16}$$

1.2.15 Accuracy

Accuracy of an analytical system is defined as how close the measured values are to the acceptable ones. It depends on the sample composition, homogeneity, surface condition and particle size. It's worth mentioning that sample matrix can affect the amount of material ablated and hence the intensity of the signal. The error in accuracy is defined as the difference between the measured value (x_m) and the acceptable value (x_{atv}) [1].

$$Error = x_m - x_{atv} \tag{17}$$

The accuracy of an analytical instrument is usually expressed as the percentage of the accuracy error as shown in equation 18.

$$Error = \left[(x_m - x_{atv}) \middle/ x_{atv} \right] \times 100\% \tag{18}$$

1.2.16 Advantages of LIBS

LIBS like other methods of Atomic Emission Spectroscopy (AES) have the following advantages as compared to some of the non-AES methods of elemental analysis: simultaneous multi-elemental detection capability and uses focused optical radiation rather than a physical devise such as electrodes to generate plasma [57]. In comparison with conventional analytical techniques such as inductively coupled plasma- mass spectroscopy and graphite furnace atomic absorption spectroscopy, LIBS is fast, simple and requires minimal or no sample preparation. These advantages are valuable particularly in the analysis of chemically and radiologically hazardous samples, where sample preparation is time consuming, tedious, contamination prone,

costly and frequently generate undesirable and toxic chemical wastes like perchloric and hydrofluoric acids. LIBS can also be coupled with fiber optics for remote and in situ applications [58]. No other technique is capable of real time detection of all kinds of chemical compounds in all states of matter without sample preparation [59].

1.3 Motivation

The presence of toxic metals beyond safe permissible limits in cosmetic products used daily by many people around the globe is of great concern. These toxic elements can be added as byproducts to the cosmetics during the manufacturing process or could be a natural part of the raw materials used. Hence developing an analytical technique for rapid detection and quantification of traces of such metals in the cosmetic products so as to provide baseline data to help determine their levels of toxicity is worthwhile.

1.4 Objectives of this study

1. To develop a laser induced breakdown spectrometer for elemental analysis and detection of toxic metals in cosmetic products.
2. To optimize the LIBS system by studying the LIBS signal dependence on the time delay and laser fluence and excitation wavelength.
3. To determine the concentration levels of the toxic metals present in the cosmetic products.

4. To study theoretical aspects of LIBS and plasma parameters (plasma temperature and electron density).

CHAPTER 2

LITERATURE REVIEW

2.1 General review

The first experiments of LIBS were achieved in the 1960s and involved producing vapor from a solid target by laser beam irradiation and then exciting the ablated plume by an electrical spark [60]. These experiments can be considered as early origin of LIBS and since then LIBS has shown its huge potential as an effective fast multi elemental analytical technique. Starting from the 1980s, significant achievements have been made in both laser and detector technology, which have made reliable and relatively cheap instruments available to research laboratories [61]. This has promoted a huge development of the technique and its adaptation to qualitative and quantitative analysis of a wide variety of samples [62].

During the past several years, there has been constant development in the interest of usage and improvement of the LIBS technique. This is due to its unique features which are not available in many other analytical techniques. Essentially simplicity, versatility, extremely flexible set up and multi elemental analysis for any kind of substance with little or no pretreatment are some of its advantages. Also the LIBS technique is fast, micro destructive and analysis can be performed in air, vacuum, in fluids and even under extreme conditions such as high temperature and pressure environments [63-66]. All these features make LIBS particularly suitable for various analytical applications.

2.2 Applications of LIBS

In this section, a review of some of the experimental applications of LIBS for detection and analysis of heavy metals and other contaminants in solids and liquids is presented below.

Ciucci et al [67] investigated the presence of heavy metals in soil samples in air using LIBS. The soil samples in this study were pressed to form pellets prior to the LIBS analysis. Elemental composition of samples and experimental signal/noise ratio for detection of the characteristic emission lines of the elements were measured. According to the authors LIBS allows direct analysis of a wide range of soil samples and has great capabilities to perform a routine non destructive identification of solid samples. In this study (UV excitation source), atomic transitions are observed clearly after a delay time of 400 ns. Emission lines have been found to last for more than 1μs and make it possible to the increase S/N ratio by choosing a large gate width (larger than 100 ns) provided that the background doesn't increase.

Geological samples were analyzed by Vallido and Laserna et al [68]. Four geological samples of different structural families were selected (vanadite, pyrite, garnet and quartz) and were directly taken from the field and analyzed without any pre treatment. The samples were washed using de-ionized water in order to remove dust and mud. A 532 nm wavelength Nd: YAG laser with an irradiance of 18 x 10^{11} Wcm^{-2} was used as the excitation source and typical spectra of the samples recorded. Precise focus of the beam allowed microanalysis of a 0.02 mm^2 surface area working in single laser shot mode to differentiate between the chemical composition of garnet and quartz. All the experiments were performed in a vacuum chamber so as to increase the life time of the ionic lines. Fe, Mn, Mg and Si were detected in these rocks but a detailed comparison

revealed an aluminum line 281.8 nm in garnet which wasn't in the spectrum for compostela quartz.

In another study, rock samples were analyzed using Q-switched Nd: YAG laser by Song et al [69]. Signal acquisition and analysis was carried out using Instaspec V software supplied by the ICCD camera manufacturer. Experimental conditions were optimized in order to obtain the best signal to noise ratio. A time delay of the gate of 1.0 ns was used and spectra for the rock samples recorded. Calibration curves were established and the qualitative results reported. In this study, applicability of the LIBS to characterize solid samples has been illustrated.

Analysis of low ash lignite was performed using LIBS by Fiona et al [70], a 1064 nm Nd: YAG with pulse width of 5ns, repetition rate 5Hz and operating in Q-switch mode was focused by a 50 mm focal length spherical lens to a 200 μm diameter spot on the surface of the lignite pellet. An optimum time delay of 1μs was selected as most of the broadband emission produced by the plasma decay in the initial microsecond. However elemental lines, which are generally more persistent than broadband emission still, can be detected at longer delays. The optimum time delay varies between elements and each atomic transition hence 1μs was selected as an appropriate compromise that yielded a good signal to noise ratio for the elements under investigation. A detector integration time of 5 μs efficiently collects all elemental emission and further ensures that the system was immune to interference from ambient light. The plasma temperature was calculated to be 9000 +/- 300K at 1.0 μs, then it dropped to 8600 +/-100K, at 1.5 μs the plasma had a temperature of 8000 +/ 100 K with a typical electron density of 5 x10^{17} cm^{-3}.

Fichet et al [71] applied LIBS to evaluate the potential of this method for the determination of trace amounts of elements in various types of liquids, in the framework of nuclear applications. A special set up using a pulsed laser was focused with a tilted angle on the liquid surface. Elements such as Pb, Si, Ca, Na, Zn, Sn, Al, Cu, Ni and Cr were detected in two different liquid matrices that is water and oil. Detection limits (0.3-120μgml^{-1}) and reproducibility for Ca, 3 % were reported. The author proposed the use of echelle spectrometer for such elemental analysis. In terms of detection limit and reproducibility, no significant differences were observed between results obtained from oil and water samples.

Charif and Harith etal [72] applied LIBS to estimate its potential for simultaneous determination of major, minor and trace concentrations in water. A combination of an Echelle spectrometer with an ICCD camera was used. Multi-elemental spectra (200-1000 nm) wavelength region was recorded and analyzed at delay times between (0.2-10ms) and gate width (1-10 ms). Temporal and spatial measurements were carried out on the laser induced plasma and trend of the obtained curves was found to be analyte dependent. Optimized values for delay time, gate width, laser pulse energy, number of accumulated single shot spectra and the geometrical arrangements were fixed thoroughly in these experiments. Other physical parameters such as plasma temperature and electron density were estimated from the spectra obtained under the optimized experimental conditions. Aqueous Na and Mg solutions of various concentrations were used to draw linear calibration curves and LODS estimated. LODs obtained for Mg and Na concentrations in bottled potable water showed a good agreement between the measured and labeled values.

Quantitative analysis of ceramic samples was carried with LIBS by Kuzuya et al [73]. A Q-switched Nd: YAG laser of 1064 nm wavelength with a repetition rate of 10 Hz and laser/pulse energy of 90mJ was focused on a ceramic sample in a low pressure argon atmosphere. Emission

spectra was measured using time resolved LIBS. The experimental results showed that at an argon pressure of 200 Torr and a time delay of 0.4 μs, the spectral line intensity and S/N ratio were minimized. Standard ceramic samples were analyzed for Mg, Al, Ca, Fe, and Ti. Linear calibration curves were obtained using the same experimental optimum parameters.

Corsi et al [74] studied the morphology of plasmas induced by single and double laser pulses. The objective of the study was to improve the understanding of the formation and evolution of the plume in single and double laser pulses and to find the reasons for the increase of sensitivity and detection limits in double pulse configuration. Single and double pulse LIBS experiments were carried out on a brass sample in air. Spectrally, temporally and spatially resolved measurements were performed on the plume. In single pulse, only the major elements in the matrix were observed whereas in a double pulse even minor emission lines were measurable. Values of the line emission intensity, plasma temperature and electron density were estimated at different positions in the plume for both configurations. An appreciable deference in plume dimensions and electron density values was observed but the maximum temperature in the plasma core was the same in both cases. In single pulse configuration, they were able to detect only major elements in the sample (Cu, Zn) and in double pulse even minor elements such as Pb, Sn, Al, Fe and Mn were detected.

Boudjemal et al [75] studied spark generated on liquid samples using a fundamental Nd: YAG laser of 10HZ repetition rate, maximum output energy 100mJ and pulse width 18 ns. Different liquid samples were studied, in order to know the proper conditions and limitations of laser plasma productions. Plasma was generated in distilled, tap, neutral, sea water and aqueous solution of $CuSO_4$ and NaCl. The break down threshold observed in air was 90 mJ, distilled water 45 mJ, neutral water samples and salt aqueous solutions was typically 9-12 mJ range.

Spectral measurements were carried out using $CuSO_4$ and NaCl aqueous solutions with concentrations of 1-20 gl^{-1}. The temporal dependence of the plasma emission was recorded and resonance lines 327 nm and 589 nm for Cu and Na respectively were investigated. These preliminary experimental results demonstrate that analysis of bulk liquids using laser induced break down spectroscopy was possible and was particularly applicable to situations requiring real time and non invasive analytical method. It was observed by the author that the sensitivity of this method was not as high as that of some of the traditional ones such atomic absorption spectrometry. This situation was however improved by introduction of successive spark pairs, increasing the number of averaged laser shots, decreasing the spectral band width of the detection, using gated integration over the decaying part of the signal and evaluating the difference between spectrally on and off resonant radiation.

Lazic et al [76] investigated the underwater plasma produced by applying a double pulsed excitation at 1064 nm, with different sets of laser pulse energies. LIBS spectra were recorded separately for each couple of laser pulses in order to monitor shot to shot plasma behavior and to apply signal post processing. The study was aimed at improving the detection limits for elemental analyses. For bulk water, a poor correlation was observed between the peak line intensities and the plasma continuum emission making the S/N ratio unsuitable for internal standardization purposes. Strong shot to shot oscillations of the plasma intensity have been observed both for water solutions and for immersed samples. In the first case, for different laser pulses, LIBS emissions were sometimes not observed even at maximum laser energy. The capabilities of LIBS for bulk liquid was also affected by the spatial fluctuations of the breakdown locations a phenomena known as moving break down, which was responsible for the

signal depletion in the detection region. In preliminary measurements on water solutions, the detection limit of 0.2 mgl^{-1} for Mg was obtained after data processing.

Russell et al [77] studied many different types of geological materials (rocks, minerals and soils).Temperature of the plasma generated by the Laser spark was investigated on soil samples. In this experiment 200 laser shots were accumulated for lead (Pb) in metal, dry soil and moist soil. The resultant temperature estimated were 11300 +/-300K for Pb in metal, 6500+/600K for Pb in dry soil and 5580+/-847 K for Pb in moist soil using Pb lines 357, 364, 368 and 374nm respectively. For the most soil the data indicates that plasma temperature and therefore resultant line intensities showed more variations as one moves from homogeneous to heterogeneous materials and from dry to moist conditions.

LIBS was used to detect and estimate the concentration of heavy metals in the Arabian crude oil residue by Gondal et al [78]. An Nd: YAG laser operating at a wavelength of 1064nm, an optical fiber cable connected to a CCD camera interfaced with a computer. Optimization of experimental parameters prior to the quantitative analysis was done and the effects of time delay and laser energy dependence were also studied. Trace elements such as Ca, Fe, Mg, Cu, Zn, Na, Ni, K and Mo were recorded and the results achieved were compared to those obtained using ICP. The author clearly remarks from this study that LIBS requires little or no preparation.

Lawrence –Snyder et al [79] studied liquid samples analyzed in a high pressure steel sample chamber. The purpose of the study was to provide high sensitivity LIBS measurements at elevated pressures. Estimations of detection limits were made as a qualitative indication of the suitability of LIBS for in situ vent fluid measurements. LIBS spectra were recorded and LODS of Li, Ca and Mn estimated as 5, 54 and 85 ppm respectively. The estimated detection limits

were within the measured concentration ranges of 0.27-8.7, 40-1900 and 3-55 ppm for Li, Ca and Mn respectively. The detection limits estimated in this study were much higher than those reported in the previous studies due to the fact that measurement conditions were not optimized to provide the highest sensitivity for each element but were chosen so that all elements could be measured at the same time. The main reason was that the spectra were measured using a very low throughput echelle spectrometer. This study reveals that LIBS spectral features, specifically intensity were affected by pressure.

In another study, Hussein et al [80] used LIBS to determine and measure nutrients in green house soils, an Nd: YAG laser at a wavelength of 1064nm, an optical fiber cable with a CCD camera interfaced with a computer was used. Also time delay of the detection system and laser energy as vital parameters was optimized experimental parameters such as time delay, laser energy of the system were optimized prior to quantitative measurements. The results obtained were compared with the results from the inductive coupled plasma.

In other studies, LIBS also was used to determine and estimate the concentration of the toxic metals in petroleum, cultivated land and ore samples by Gondal et al [81]. An Nd: YAG laser of 1064nm wavelength, an optical fiber cable connected to an ICCD camera interfaced with a computer were used during the study. The major elements detected in the samples were Mg, Cu, Zn, Na, S, Ni, K and Mo. The concentrations of these elements as measured by the LIBS system were then verified by ICP-MS technique and both results were comparable.

LIBS was also used to determine toxic metals in water waste collected from local paint manufacturing plants by Gondal et al [82]. A system consisting of a fundamental an Nd: YAG laser, four spectrometer modules and an ICCD camera was used. Experimental parameters such

as laser energy, time delay, number of shots accumulated, distance between the plasma and the collecting fiber were optimized prior to the analysis. Major elements detected in the waste samples included Ca, Si, Fe, Na, K and their respective concentrations were counter verified using ICP-MS which were above the safe levels set by FDA and other organizations.

Hussein et al [83] used LIBS to detect and estimate concentrations of toxic metals in gulf war oil spilled contaminated soils. A fundamental Nd: YAG laser was used as the excitation source to generate plasma, an optical fiber cable connected to a CCD camera interfaced with a computer as the detection system. Experimental parameters such as laser energy, time delay were optimized prior to the quantitative analysis. Environmentally important elements like Al, Mg, Ca, Cr, Ti, Fe, Ba, Na, Zr and K were detected. These results were validated using ICP and the concentration of Ba and Cr were found to be higher than the permissible limits.

Siddiqui et al [84] used LIBS to detect trace elements in non degradable part of plastics (insoluble organic material) obtained from thermal and catalytic degradation of plastics. An Nd: YAG laser operating at a wave length of 1064nm, an optical fiber cable connected to a CCD camera interfaced with a computer were used. Experimental parameters such as laser energy, delay time, focusing lens for induced plasma emission were optimized prior to quantitative analysis of the samples. Ag, Al, Fe, Co, V, Ni, Pb, Mn and Cd were identified in the samples and the concentrations were then verified using the ICP which were higher than the permissible safe limits.

LIBS was used to detect and estimate the concentration of highly toxic contaminants chrome tanned leather by Nasr et al [85], An Nd: YAG laser operating at a wave length of 1064nm was used as the excitation source and an optical fiber cable connected to a CCD camera interfaced

with a computer for detection and processing of the signal. Experimental parameters such as laser energy, time delay were optimized prior to the quantitative analysis. Heavily toxic elements such as chromium and Arsenic were detected and their respective concentrations determined. These results were proved by the ICP- MS measurements as a conventional technique. In this study the author stresses the fact that the LIBS technique is fast, in situ and more accurate without any lengthy preparations.

Gondal et al [86] used LIBS detect and measure concentrations of potentially dangerous elements in the electrical cables (new and faulty) and raw materials used in manufacturing cable insulation such as PVC, PP and LDPE that form the water tree which causes electrical break down along the coastal areas of Saudi Arabia. A fundamental Nd: YAG laser, four spectrometer modules and an ICCD camera were used. Vital experimental parameters were optimized prior to the analysis. Elements detected were Ba, Ca, Cr Fe, Cl, Mg, Mn, Na and Ti. The LIBS results were counter checked using ICP-MS. It was observed that, in the manufactured and faulty cables noticeable amounts of Na, K, Mg, Cl and other undesirable elements were detected. And in the raw materials levels of Na and Cl were very high which implies that such cable would more readily absorb water inside the insulation which could lead faster degradation and water tree-formation. This study revealed the major cause of insulation failure in electrical cables along the coastal region of Saudi Arabia.

CHAPTER 3

EXPERIMENTAL METHODS

3.1 Introduction

In order to detect and quantify toxic elements in the cosmetic products, a LIBS spectrometer was designed and optimized to get a preferable performance (obtain the best Limit of detection by maximizing the IBS signal and at same time minimize the signal to noise ration). The selected experimental set up, operating conditions and material were chosen on the basis of the literature survey study and our preliminary experiments. Also the samples used in our study were appropriately prepared using standard procedures described below.

3.2 LIBS system set up.

The LIBS technique is a plasma based method of Atomic Emission Spectroscopy (AES) that uses instrumentation similar to that used by other methods of AES. In this technique, a powerful laser is used to both prepare the target sample and excite the constituent atoms to emit light. Sample preparation results from focusing a high power laser onto the surface of the target sample which removes a very small mass (μg) of the target in the form of atoms and small particles. Coincident with the ablation is the formation of the micro plasma in the focal volume of the laser pulse that excites the ablated atoms. The small particles in the plasma are also vaporized which excites the atoms.

The main components include the following

i) The Nd: YAG pulsed laser to generate powerful optical pulses used to form the micro plasma.

ii) The focusing system of the mirror and the lens to direct and focus the laser pulse on the target sample.

iii) Target holder or container.

iv) The light collecting system (lens, mirrors or optical fiber to collect the spark light and transport it to the detection system).

v) Detection system consisting of a method to spectrally filter or disperse the light such as a spectrograph or detector that records the light.

vi) Computer and electronics to gate the detector, fire the laser and to record the spectrum.

3.2.1 Laser system

A fourth harmonic (266nm) Nd: YAG laser (Big sky Laser Technologies), operating in Q-switched mode, giving a maximum of 50mJ/pulse in 8ns duration at a repetition rate of 20Hz and with pulse stability of +/-3% is used as the excitation source to generate plasma during analysis of the cosmetic products that is tooth paste, cosmetic hair dye and Kohl which were obtained from the local market in Saudi Arabia. The laser system consists of ultra CFR laser head, integrated cooler and electronics. Since the lazing action is relatively inefficient, the system generates more heat than light and therefore it uses a closed loop cooling system with distilled water to keep the laser rod and flash lamp cool. The ICE provides the charging supply to flash pump the laser rod. It also provides system timing, synchronization, controls and safety interlocks. Some electronic assemblies, such as lamp trigger transformer and Q-switch driver are

in the laser head. The ICE includes all controls and indicators necessary to operate the system. Also the fundamental, second harmonic Nd: YAG lasers were also used for the plasma parametric study in addition to the fourth harmonic.

3.2.1.1 Principle of operation

A flush lamp is fired to produce a broadband light [pumping light] over the near UV, Visible and the near IR special regions. A small percentage of this pumping light is absorbed by ions doped in the lasing material [Nd ions in a YAG crystal matrix]. Due the electronic energy levels of the Nd ions in the laser rod, if the flush lamp pumping is sufficiently strong a population inversion is established in which the upper level of the lasing atomic transition is populated than the lower terminating level of the transition. In this case a photon passing through the laser rod at the same frequency as the lasing transition will experience a gain or amplification by the inducing decay of some of the ions from the upper to the lower state (simulated emission). The rod is surrounded by a resonant cavity composed of two mirrors in which some of the amplified light is directed back into the rod. Significant amplification of light at wavelength of the lasing transition can be achieved. An electro optic Q switch shutter positioned in the cavity prevents photons at 266nm wavelength from making a complete path through the cavity and inducing simulated emission hence the population inversion between the upper and lower levels of the lasing transitions becomes very large. When the Q switch is activated by a suitably timed gate pulse, the Q switch becomes transparent allowing photons to make traverses of the laser cavity resulting in a high power pulse of a short duration. A portion of this pulse leaves the cavity through a partially transmitting mirror [output coupler]. The Q switched pulsed length is of the order of 5-10ns. The pulse is of short duration because once lasing begins the population inversion is rapidly depleted and lasing terminates. The Q switch is intentionally closed shortly after the laser pulse to prevent

generation of additional laser pulses. The selection of other wavelength (532 and 1064 nm) can be done efficiently.

3.2.1.2 Properties of Lasers

3.2.1.2.1 Irradiance

Lasers are unique sources of high irradiance light required to generate laser plasma. The unit for irradiance is W/cm^2 or $photons/cm^2$. The pulsed energies used for LIBS typically range from 10mJ to 500mJ. Given that the energy in a visible photon is ~ 10^{-19} J, the number photons in a laser pulse used for LIBS ranges from 10^{17}- 5 $X10^{18}$ photons. Note that these photons will be in a pulse having duration of 10 ns for the usual LIBS experiment. For comparison, a thermal light source (blackbody) at a temperature of 1000K will produce about1012 photons/s from a $1cm^2$ surface area within a bandwidth of 100 nm (a solid-state laser will have a bandwidth <0.001nm), or for comparison, only 104 photons in 10 ns.

3.2.1.2.2 Directionality

The ability of the laser pulse to propagate over long distances as a collimated beam is important for stand-off and remote LIBS measurements. Here stand-off represents the projection of the laser pulse through the atmosphere or free space over a distance of many meters. Remote indicates transport of the laser pulse through a fiber optic cable. Both methods require a laser pulse with good directional beam qualities. A high quality laser which operates in a single lowest order mode (Gaussian mode) produces a laser beam that replicates closely a uniform plane wave having a constant phase distribution across the wave front. Such a beam, emerging from the output coupler of the laser of diameter *d* will propagate as a highly directional, parallel beam for a distance given by $\pi d^2/\lambda$ often termed as the Rayleigh range. After this distance, the beam will

begin to expand with an angular spread of $\Delta\theta$ where $\Delta\theta = d/\lambda$ is specified as the beam divergence.

3.2.1.2.3 Monochromaticity

Conventional light sources are broadband, generating light over a wide range of wavelengths. A laser on the other hand, has the ability to generate the majority of its output energy within a very narrow spectral range due to the laser light originating from a well-defined transition in the lasing medium. As noted above, for a solid state laser the bandwidth will typically be < 0.001 nm. In terms of excitation properties of the laser plasma, monochromaticity is not typically important. Analytically useful laser plasmas can be generated with IR, visible and UV wavelengths. Certain wavelengths couple more strongly into specific materials making wavelength important for ablation but a highly monochromatic beam is not important because the absorption spectra of bulk materials are usually slowing varying functions of wavelength. Monochromaticity may be important, however, in LIBS instrument design. That is, in some configurations, it may be desirable to use optical components that reflect the narrow band laser wavelength and then pass the broad spectrum of the laser plasma which is collected for analysis.

3.2.2 Focusing and light collecting

The high power laser beam is focused on the surface of the target sample using a UV convex lens. The lens focuses the beam to a sufficiently small spot of diameter 0.1 mm so as to achieve analytically useful plasma and a fiber optic cable is used to collect the plasma light which is directed to the detection system (ICCD) for processing.

3.2.3 Lens

A lens of focal length 30mm and diameter 8mm is used in this study. The lens is made of quartz and has maximum transmission at the laser wavelength. It's a double convex lens which helps in minimizing spherical aberration. It also has Anti reflection coatings to minimize back reflection hence maximize energy on the target.

3.2.4 Optical fiber and small miniature lens system

Particularly in this application where by the detection system cannot be poisoned close to the target, a small miniature lens fitted with an optic fiber cable is used to collect plasma light and transmits it to the detector. The optic fiber is put at an appropriate distance of 20 mm from the plasma plume and fixed at an optimal angle of 45^0 with respect to the normal of the surface of the target sample. The fiber transmits the light using total internal reflection and those light rays entering the fiber through the optical aperture are reflected through the fiber with high efficiency.

3.2.5 Target holder

The target holder is a very vital component of the LIBS system. It has a manually controlled X-Y stage and is made of an eye protective polymer that provides a clear view of the sample. It also has an exhaust system to evacuate any particles created by the ablation process and an inert gas induction port for ablation area purge. The chamber door is magnetically latched and interacts with the safety interlock that prevents the laser from firing when the door is open. A 12 Volt DC power supply is included for chamber lighting and exhaust fan power. As any minor variation in the focal length can make a great deal of change in the laser fluence on the sample and consequently on the LIBS signal, care was taken to minimize the size of the crater on the sample surface. This was achieved by constantly moving the rotator sample holder along X and Y directions to provide a fresh surface for every laser shot during the analysis.

3.2.6 LIBS spectrometer

A spectrograph (Andor SR 500i-A) with grating groove densities of 600, 1200 and 1800 lines/mm is connected to an ICCD camera (Andor iStar) through a built in delay generator which is synchronized to the Q-switch sync out of the exciting Nd: YAG laser. It should be noted that all spectrometers are triggered to acquire and read out data simultaneously. Our spectrometer is responsive for a wavelength range of 200-1000 nm and has a spectral resolution ~ 0.1nm. To further improve on the spectral resolution and minimize the signal to noise ratio, a grating of groove density1200 lines/mm, a slit width of 100 µm, gate width of 200 µs, gate delay of 500 ns, exposure time of 4s and as many as 20 accumulations were used as the spectrometer parameters. Hence the spectral lines in all the recorded spectra were very distinct and visible.

3.2.7 Energy meter (Ophir model 300)

This is used to measure laser energy/pulse in Laser induced breakdown spectrometry. A pulse of laser energy 45 mJ with a sport diameter of 0.1 mm yielding a fluence of 23.5 Jcm^{-2} on the surface of a sample was used to generate LIBS spectra. A laser energy/pulse in the range of 35 mJ to 50 mJ corresponding to a laser fluence of 17.5 Jcm^{-2} to 25.5 Jcm^{-2} was used to study the LIBS signal dependence on laser fluence in order to establish optimum laser fluencies generating the highest signal intensities for each specific spectral line of interest.

3.2.8 Oven

This was used for annealing of the toothpaste samples prior to the LIBS analysis.

3.2.9 Inductively Coupled Plasma (ICP) Spectrometer

The ICP spectrometer is comprised of a nebulizer, spray chamber, plasma torch, interface and a detector. The sample in liquid form after preparation is pumped at ml/min with a peristaltic pump

into the nebulizer in which its converted to a fine aerosol with argon gas at 1L/min. Fine droplets of aerosol (1-2%) of the sample are separated from the large droplets using the spray chamber[87]. The fine aerosol then exits from the spray chamber into the plasma torch via a simple injector. In the ICP-MS, the plasma torch is positioned horizontally and used to generate positively charged ions and are directed to the mass spectrometer via the interface region which is maintained at a vacuum pressure of 1-2 torr. The interface region helps the ions to be transported efficiently and with electrical integrity from the plasma (760 torr) to the spectrometer (10^{-6} torr). The ions are successfully extracted from the interface region and directed into the main vacuum chamber by electrostatic lenses called ion optics. A turbo molecular pump maintains the vacuum in the region of 10^{-2} torr, ion optics focus the ion beam towards the mass separation device and to stop photons, particulates and neutral species from reaching the detector. The ions then move to the heart of the spectrometer, the mass separation device (quadrupole magnetic sector) where a second turbo molecular pump maintains a pressure of 10^{-6} torr. The quadruple magnetic sector allows analyte ions of a particular mass to charge ratio (M/Z) through the detector and to also filter out all the non analyte and interfering matrix ions. Finally the ion detector converts the ions into an electrical signal which is then processed by the data handling system in the conventional way and converted into analyte concentration using ICP-MS calibration standards [88].

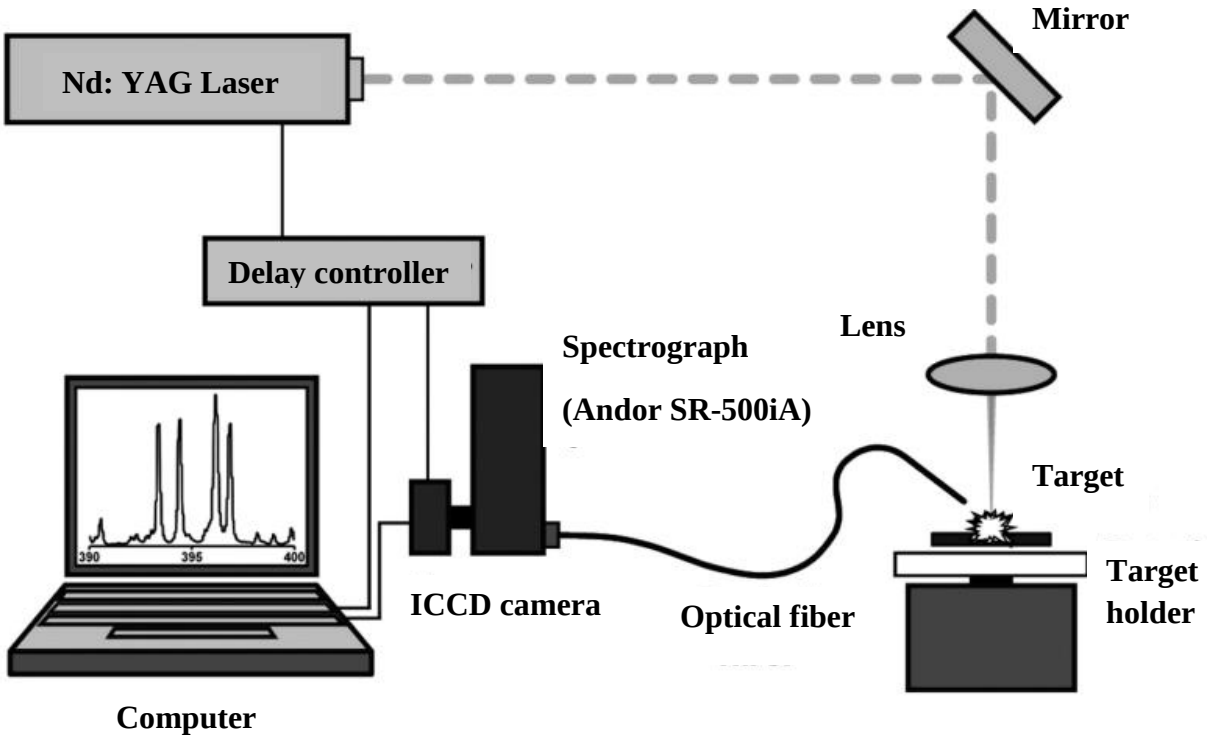

Figure 3. 1: LIBS schematic diagram

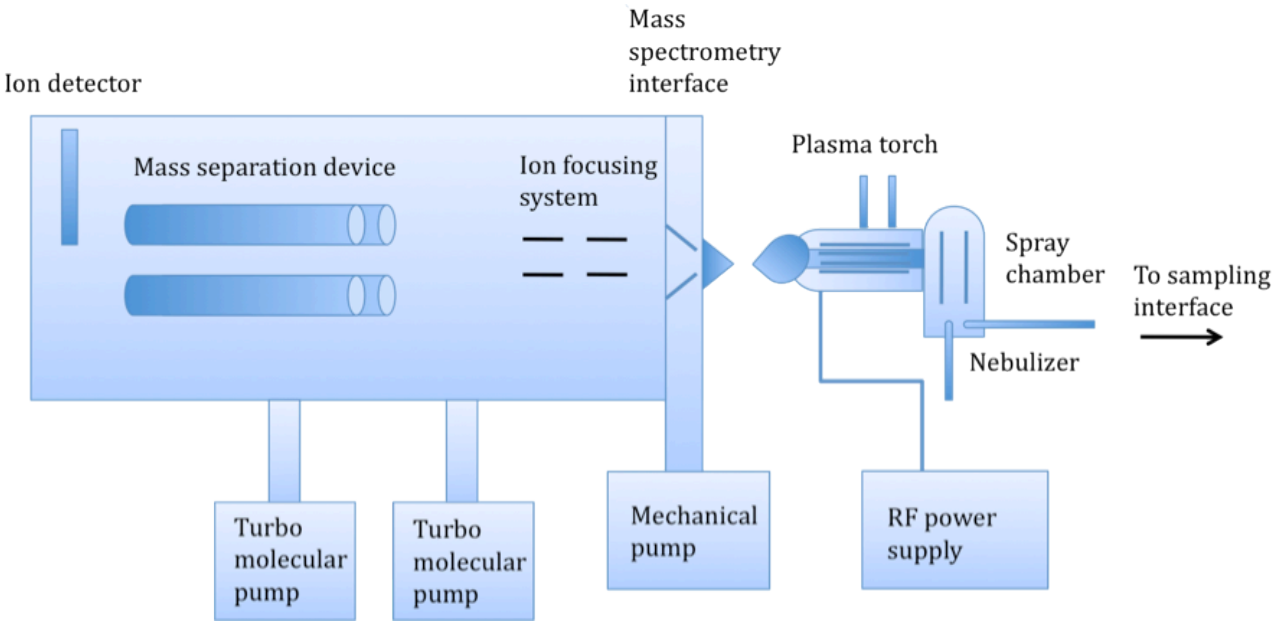

Figure 3. 2: ICP-MS schematic diagram

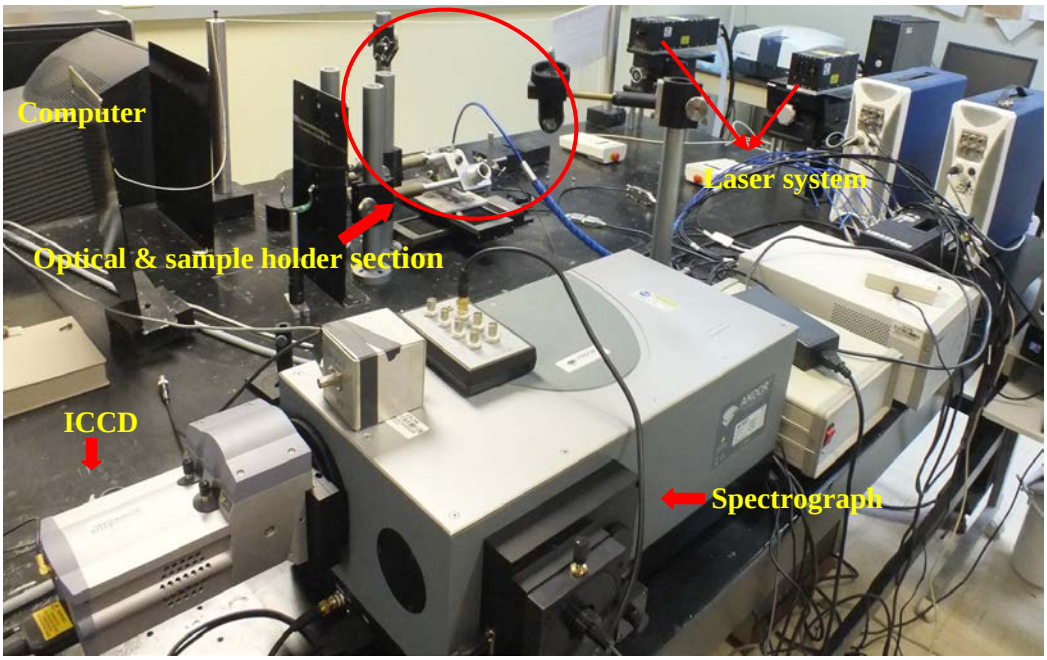

Figure 3. 3: LIBS set up

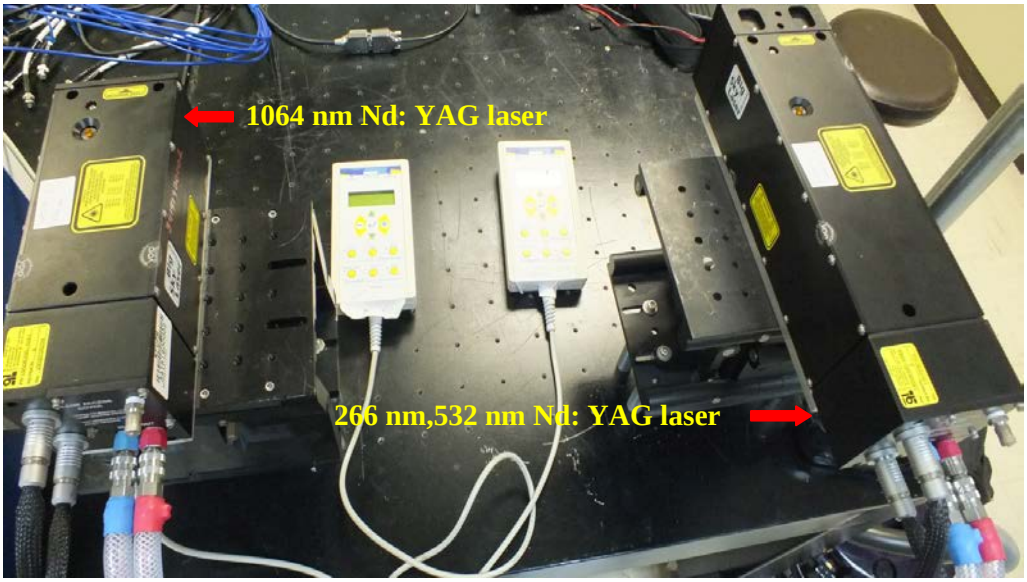

Figure 3. 4: Laser system

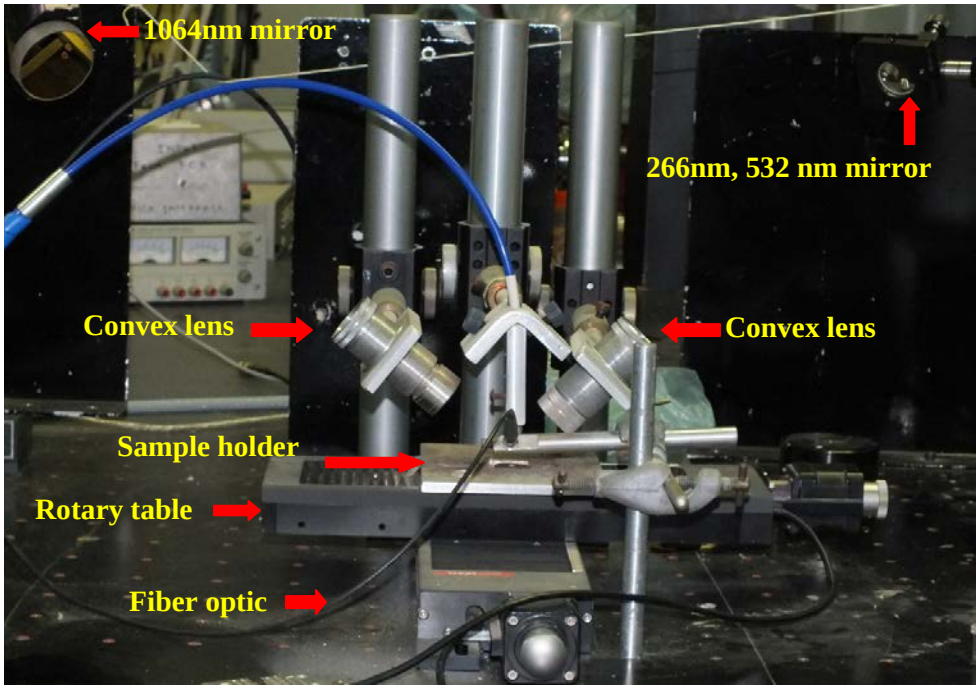

Figure 3. 5: Optical and sample holder section

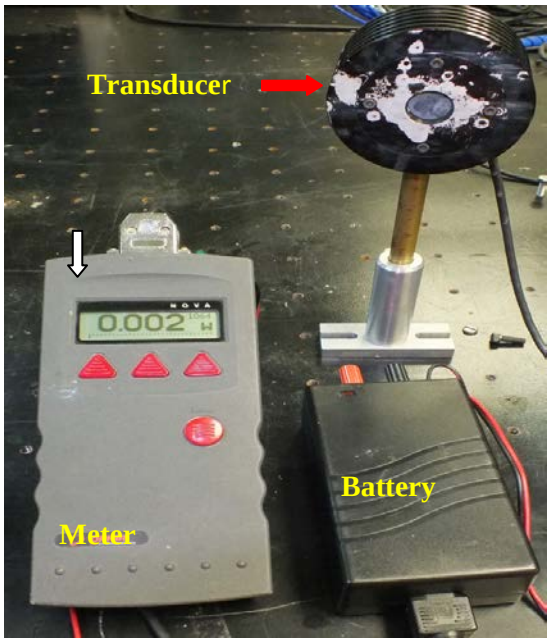

Figure 3. 6: Energy meter

Figure 3. 7: Oven

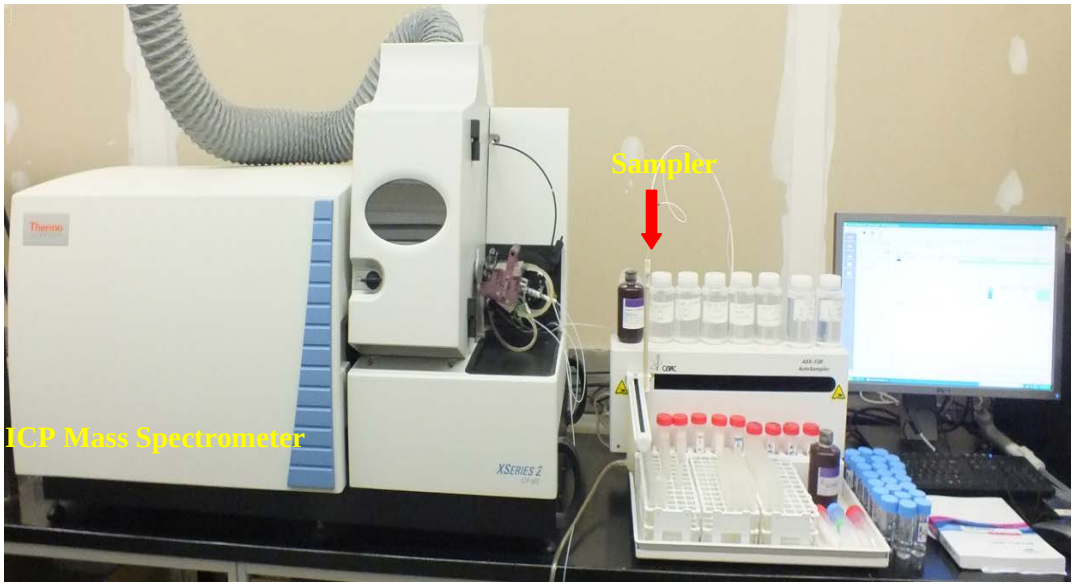

Figure 3. 8: Inductively Coupled Mass Spectrometer.

3.3 Sample preparation

The cosmetic products analyzed were toothpastes, synthetic hair dyes, kohl eyeliners and talcum powder. These products are not in solid form and therefore not trivial to analyze using Laser induced breakdown spectroscopy because during laser ablation the distance from the focusing lens to the sample surface will change due to excessive pitting. This can significantly affects the results of LIBS measurements. Hence a special pre - preparation method for each of the products is inevitable for an effective LIBS analysis as described below.

3.3.1 Target preparation for Plasma diagnostic studies

In this study, semi fluid samples of toothpaste were used and therefore the same sample preparation procedure as that used prior to the LIBS measurements to detect fluoride concentration levels in tooth paste samples as mentioned in the text below.

3.3.2 Toothpaste sample preparation for LIBS analysis

Semi fluid tooth paste samples of different brands were purchased from the local market. A cubical die of dimensions 2cm x 2cm x 1cm was filled with the paste and wrapped with an aluminum foil in order to prevent contamination. It was then allowed to settle for some time under ambient conditions so as to eliminate spaces within the bulk thus making it compact. The die filled with paste was then annealed in the oven at a temperature of 60 ^{0}C for 4 hours to make the sample hard in order to minimize pitting during laser ablation. The samples were then polished to achieve a smooth surface necessary for generation of uniform plasma sparks for LIBS analysis.

3.3.3 Synthetic hair dye sample preparation for LIBS and ICP analysis

Hair dye samples of different quality, brand and price range were procured from different cosmetic shops. These samples were in powder form which blows out of the sample holder when a high power pulsed laser beam is incident on it making LIBS analysis very complex. Hence a special form of preparation to transform the fine powder into solid compact pellets was devised for easy and effective analysis. The base matrix (fine powder) was mixed thoroughly with potassium bromide (KBr) as the binding material in appropriate ratios as per the standard procedure and grinded using agate pestle and motor to ensure homogeneity. The homogeneous mixture was then compacted using a 10 bar pellet press machine having a stainless steel cylindrical die with a diameter of 20 mm and thickness 2 mm. To avoid moisture, humidity effects and any form of contamination, the pellets were wrapped in a clean aluminum foil and safely stored in a desiccator ready for analysis. In order to validate the measurements obtained using our LIBS system, ICP spectrometry; a conventional technique was also used. In this case, each powder sample was digested by addition of nitric acid (HNO_3) and hydrogen peroxide (H_2O_2). The resultant solution was refluxed at 95 ^0C, for 5hrs and the exothermic reaction allowed to complete. The solution was then diluted to a desirable final volume which was analyzed using ICP-MS.

3.3.4 Kohl eyeliner sample preparation for LIBS and ICP analysis.

Kohl samples of different brands were bought from the local market. Some of them were in powder form and so not simple to analyze using a high power pulsed laser because the fine particles splash when the laser beam is incident on the sample, therefore pellets were prepared by mixing starch with the powder in appropriate proportions and a hydraulic press machine was used to compact the homogeneous mixture into solid palettes with dimensions 20 mm diameter and 2 mm thickness. In this case, starch was used as the binding material in order to avoid interference between the strong lead (Pb) line at 405.7 nm and potassium (K) line at 404.4 nm from the base matrix and KBr binder respectively. However, other kohl eye liners were in solid form and required little preparation to mould them into a shape that fits the dimensions of the sample holder of our LIBS system. To validate the LIBS measurements, ICP-MS a conventional technique was used. In this case kohl samples were digested in 5% nitric acid of 99% purity (Fisher scientific). 1 gram of each sample was digested by addition of nitric acid (HNO_3) and the resultant solution reduced in volume by heating at 95^0C continuously for 5 hrs. It was then diluted appropriately to a final desired volume and analyzed with ICP-MS calibrated system using reference standards.

3.3.5 Talcum powder sample preparation for LIBS analysis

Talcum powder samples of different brands were purchased from the local market. These samples were in powder form and hence not trivial to be analyzed using LIBS. A special method to convert the fine powder into pellets was used in order to effectively analyze the samples using LIBS. The base matrix (fine powder) was mixed thoroughly with starch as the binding material in appropriate ratios and grinded using agate pestle and motor to ensure homogeneity. The homogeneous mixture was then compacted using a 10 bar pellet press with a die of diameter 20

mm and thickness 2 mm. Here, the starch binder was also used in order to avoid interference between the strong lead (Pb) line at 405.7 nm and potassium (K) line at 404.4 nm from the base matrix and KBr binder respectively.

3.3.6 Standard materials

3.3.6.1 Standard materials for quantification of Fluoride (F) concentration levels in different toothpaste brands

In order to determine the fluoride concentration levels in the toothpaste samples(#1, #2 and #3) calibration standards of different fluoride concentrations that is (a) 439 ppm (b) 2195 ppm (c) 4390 ppm (d) 6585 ppm were prepared by mixing the sample matrix (sample #1) with very high purity sodium fluoride (99%) in the desired appropriate concentrations. Only sample #1 was used because basically, all the samples were ideally of the same matrix. A cubical die of dimensions 2cm x 2cm x 1cm was then filled with the homogeneous mixture and wrapped with an aluminum foil in order to prevent contamination. It was then allowed to settle for some time under ambient conditions in order for the bulk to become compact. The die filled with the mixture was heated in the oven at a temperature of 60 ^{0}C for 4 hours to make the target sample hard so as to minimize pitting during laser ablation. The samples were then polished to achieve a smooth surface necessary for generation of uniform plasma sparks for LIBS analysis.

3.3.6.2 Standard materials for quantification of Chromium (Cr) concentration levels in synthetic hair dye.

To estimate the concentration of chromium (Cr) in synthetic hair dye samples (#1, #2 and #3), standard samples with different concentrations of chromium (Cr) in parts per million (ppm) that is 40, 60, 80 and 100 ppm were prepared by homogeneously mixing chromium (II) sulphate with

the base matrix (synthetic hair dye powder) for sample# 1 and KBr (binding agent) in appropriate concentrations according to standard procedure. The resultant mixture was then compacted using a 10 bar pellet press having a dye with a diameter of 20 mm and thickness 2 mm. It is worth noting that only sample #1 was used to prepare the calibration standards because all the samples in our study had basically an identical matrix.

3.3.6.3 Standard materials for quantification of lead (Pb) and chromium (Cr) concentration levels in Kohl eyeliners.

For construction of calibration curves, standard pellets of different concentrations of lead (Pb) and chromium (Pb) were prepared appropriately using lead (II) sulphate and chromium (II) sulphate salts respectively. The matrices were blended with starch, a binding agent and grinded with an agate motor and pestle to ensure homogeneity. The resultant mixtures were compressed using a 10 bar pressure pellet press machine having a dye of diameter 20 mm and thickness 2 mm. It worth noting that only sample #1 was used because all the kohl samples in our study were of the same matrix. Calibration standards of 20 ppm, 40 ppm, 60 ppm, 80 ppm for both chromium (Cr) and lead (Pb) were prepared.

3.3.6.4 Standard materials for quantification of lead (Pb) and chromium (Cr) concentration levels in Talcum powder.

For Calibration of the LIBS system, standard pellets of different concentrations of Lead (Pb) and Chromium (Pb) were prepared appropriately using powdered lead (II) sulphate and chromium (II) sulphate salts respectively. The matrices were mixed with starch (binding agent) and grinded with an agate motor and pestle to ensure homogeneity. The resultant mixtures were then compressed using a 10 bar pressure pellet with a dye of diameter 20 mm and thickness 2 mm.

Sample #1 was used because all the talcum powder samples used in this study were of the same matrix. Calibration standards of 20 ppm, 40 ppm, 60 ppm, 80 ppm for both chromium (Cr) and lead (Pb) were prepared.

3.4 Precautions taken during preparation

1. The agate mortar and pestle should be clean to avoid contamination, and should be dry and all at the same temperature to minimize water absorbance. The dye must be cleaned after every single use.
2. Both KBr and the powder should be grinded in the mortar separately and thoroughly until there is no evidence of crystallinity, after that they should be well mixed to get a homogeneous mixture.
3. The amount of mixture compressed, pressure value and allowed pressing time had to be exactly the same for all standard pellets in order to get identical pellets.
4. All pellets were stored in desiccators to avoid moisture.

3.5 LIBS data accumulation and analysis

The LIBS spectra are recorded and displayed by the Andor i-star software application. All the files can be exported and processed by Origin 8.0 or Microsoft excel software programe. The Origin 8.0 software was used in identification of the peaks, curve fitting, and plotting calibration curves.

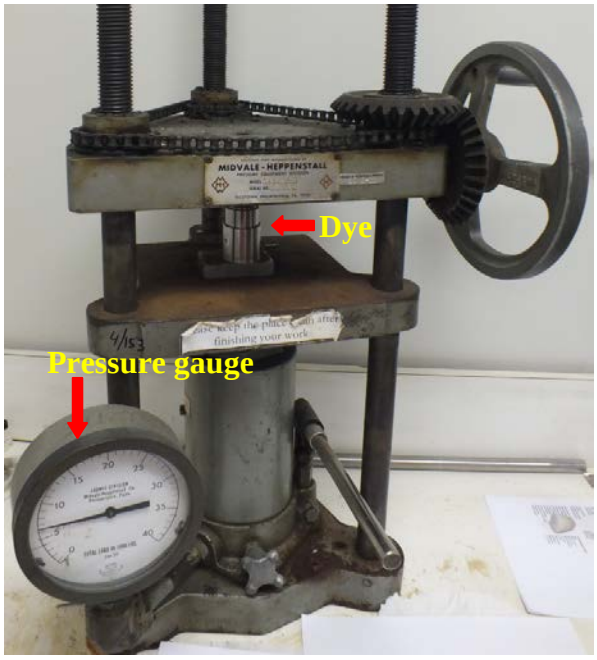

Figure 3. 9: Pellet press machine

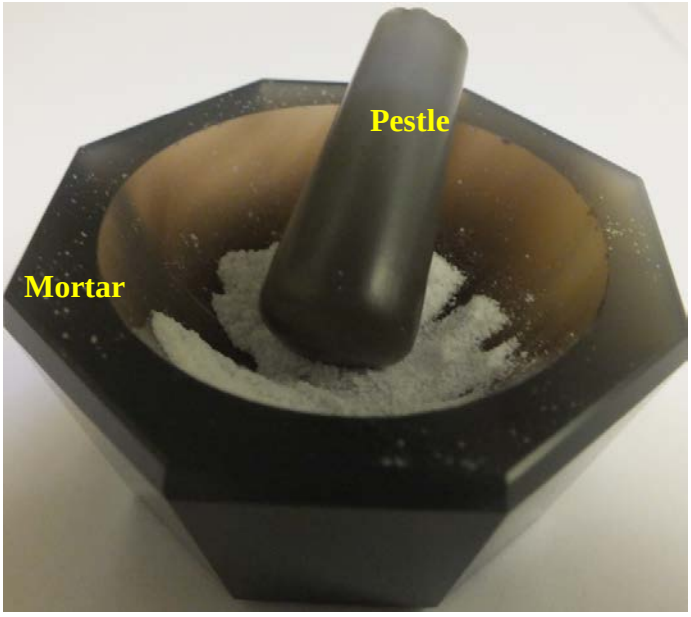

Figure 3. 10: Sample grinder

CHAPTER 4

RESULTS AND DISCUSSION

In this chapter, the experimental results obtained in our study are discussed in detail as below

4.1 Plasma parametric Dependence on Laser fluence, gate/time delay and excitation wavelength.

4.1.1 Introduction

Pulsed laser induced plasmas are of great importance because they have several applications such as elemental analysis. In Laser induced breakdown spectroscopy (LIBS) elemental analysis is based on the optical emission spectrum where by spectral analysis of light emitted from the plasma produced during laser ablation gives information about the composition of the plasma. This technique is a well known analytical technique to provide remote, in situ, rapid and multi-elemental analysis with no or minimum sample preparation [89, 90].

In order to evaluate the performance of the laser induced plasma and to further optimize the LIBS detection system. It's important to measure plasma parameters such as plasma temperature (T) and electron density (n_e) which are essential in understanding the physical and chemical processes such as excitations, ionizations and chemical reactions in these complex spectroscopic sources [91]. These plasma parameters are dependent on laser parameters, target material, and atmospheric conditions. For elemental analysis it is very important for the Laser Induced Plasma (LIP) to be optically thin and in Local Thermodynamic Equilibrium (LTE) whereby the excitation and ionization temperature governing the distribution of energy level excitation

through the Boltzmann equation and the ionization equilibrium through the Saha equation respectively are equal to the electronic temperature describing the Maxwellian distribution of electron velocities [49]. Hence plasma in LTE is defined by a common temperature T known as plasma temperature. The most widely used spectroscopic method for determination of plasma temperature is the Boltzmann plot method which employs intensities of spectral lines [49]. Currently typical methods used to measure electron density are Langmuir probes [92] Laser Thomson scattering [93] plasma radiation method [94] and stark broadening method [95]. However electrostatic Langmuir probe method is mostly used for low-pressure plasma and not well adapted to atmospheric plasma [92]. The laser Thompson scattering technique is complicated, expensive and has to be carefully implemented with many experimental difficulties mainly of optical nature [96]. Plasma radiation method calculates electron density from the ionization frequency after the turn off of the plasma and not during the process of plasma generation [94]. Comparatively, Stark broadening method is an effective method for measuring the electron density in LIPS due its simple equipment and reasonable approximation. It is based on stark effect and is caused by coulomb interaction of the emitting atoms with free electrons and ions which exist in the plasma. This implies that stark broadening of spectral lines emitted by particles in the plasma allows the determination of the electron density in a rapid and convenient way if the plasma temperature is known.

Most of the works focus mainly on identification of plasma species. However a few studies on the quantitative information on the fundamental plasma parameters such as plasma temperature, electron density have been done. In this section we have investigated the dependence of plasma temperature (T) and electron density (n_e) on gate/time delay, fluence and wavelength of the excitation source for plasma generated under ambient conditions by ablation of semi fluid

samples. Such data is required in order to develop test models of plasma processes that enable us evaluate energy transport in the plasma so as to be able to enhance the sensitivity of LIBS systems.

4.1.2 LIBS spectrum

Figure 4.1 shows a typical LIBS spectrum in the wavelength range of 700 - 800 nm recorded using a gate/time delay of 700 ns, laser fluence 23.5 Jcm^{-2} and other spectrometer parameters as mentioned earlier in the text. At this specific time/gate delay we have cooled plasma and hence most of the lines detected are from the neutral atomic species. It is observed clearly that the spectrum has neutral fluorine spectral lines at wavelengths 731.102 nm, 739.869 nm, 748.916 nm and 780.021 nm which are isolated and do not involve the ground state. Hence were used for plasma parametric studies.

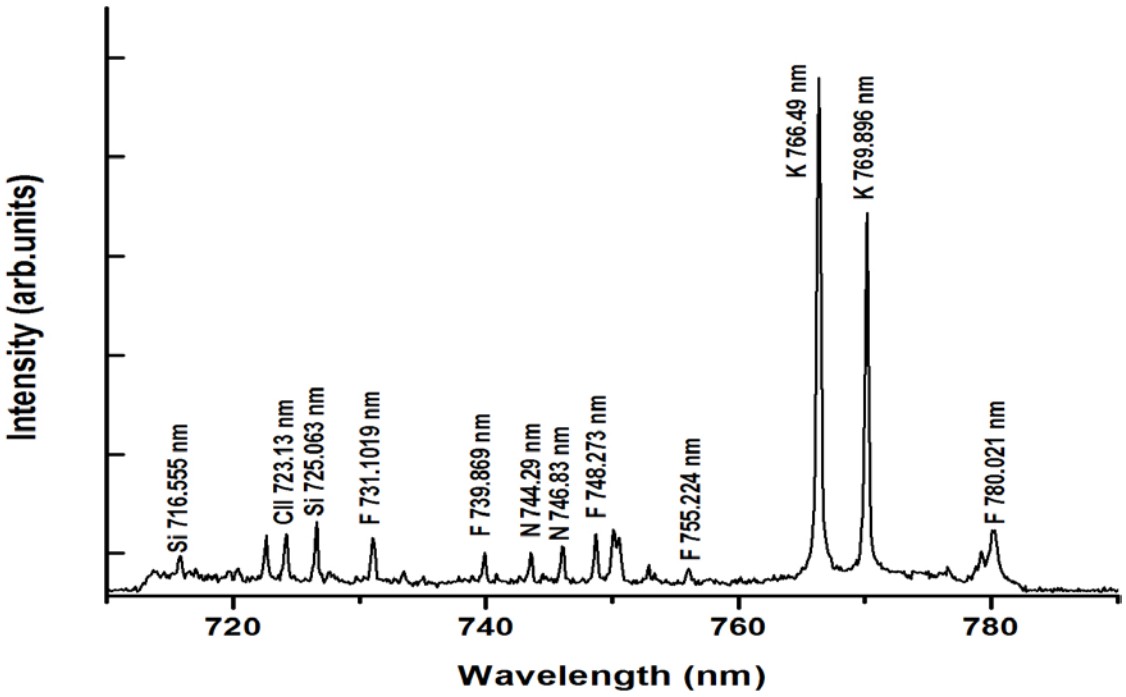

Figure 4. 1: Typical spectrum generated using gate/time delay and laser fluence of 700 ns and 23.5 Jcm^{-2} respectively for toothpaste sample #1

4.1.3 Plasma temperature and Electron density measurement

Determination of plasma temperature (T) and electron density (n_e) for laser induced plasmas is very vital in improving the sensitivity of a LIBS system. For optically thin plasma in LTE, re-absorption and absorption of the incident radiation by the plasma plume is negligible. In this case its temperature and electron density are obtained using the Boltzmann plot and Stark broadening respectively. From equation 11 plotting a graph of magnitude of the component on the left as a function of the energy for the upper levels of the species yields a linear plot referred to as the Boltzmann plot. Constants such as the transitional probabilities (A_{ik}), statistical weights (g) and upper energy levels (E_{ik}) of the selected spectral lines are obtained from the NIST data base as shown in Table 4-1 [18]. The value of T, the plasma temperature is then deduced from the slope of the plot. The electron density (n_e) of the plasma generated was determined using equation 13.

The selected lines used for plasma characterization do not interfere with other spectral lines in the spectrum, are not resonance lines and their shapes were well fitted by a lorentzian implying that self absorption is negligible. However, uncertainties in the plasma temperature (T) values determined remain, firstly, because the outer regions of the plasma plume can be at a lower temperature as compared to the interior of the plume and secondly because absorption of the emitted plasma radiation arising from the hotter regions of the plasma occurs at the periphery resulting into lower measured intensities of the emitted spectral lines. It is worth mentioning that only the hottest core regions of the plume contribute significantly to the measured signals and the temperature in the LIP is uniform since thermalization time is less than the expansion time. Thus the measured space averaged parameters that is plasma temperature and electron density retain their importance for the plasma characterization [97].

Differences in the radiation and kinetic properties of the plasma generated by all the Nd: YAG laser excitation sources of wavelengths 1064 nm, 532 nm and 266 nm are observed through comparison of electron density (n_e) and plasma temperature (T_e) estimates. It is very obvious that the excitation source wavelength ($\boldsymbol{\lambda}$) plays a crucial role in the properties of laser produced plasma. In order to estimate plasma temperature, spectral lines as indicated in Table 4-1 were used.

Table 4 - 1: Spectroscopic data of the fluorine spectral lines [18, 51]

Wavelength (nm)	g_k	A_{ik} (s^{-1})	E_k (eV)
731.102	2	2.7E+07	14.68
739.869	6	2.5E+07	14.37
748.916	2	1.3E+07	14.68
780.021	4	2.9E+07	14.61

Figure 4.2 shows the Boltzmann plot considering the data of all the observed neutral fluorine spectral lines in the 700 - 800 nm wavelength region for a gate/time delay and laser fluence of 700 ns and 23.5 Jcm^{-2} respectively using an excitation wavelength of 266 nm. The slope of the fitted line yields a plasma temperature value of 5324 K. Figures 4.2 and 4.3 are Boltzmann plots for plasma generated under the same conditions as in Figure 4.1 but for excitation wavelengths of 532 nm and 1064 nm. The slopes of these plots yield plasma temperatures of 3850 K and 2500 K respectively. The temperature of the plasma is observed to drop with increase in wavelength of the excitation source as expected.

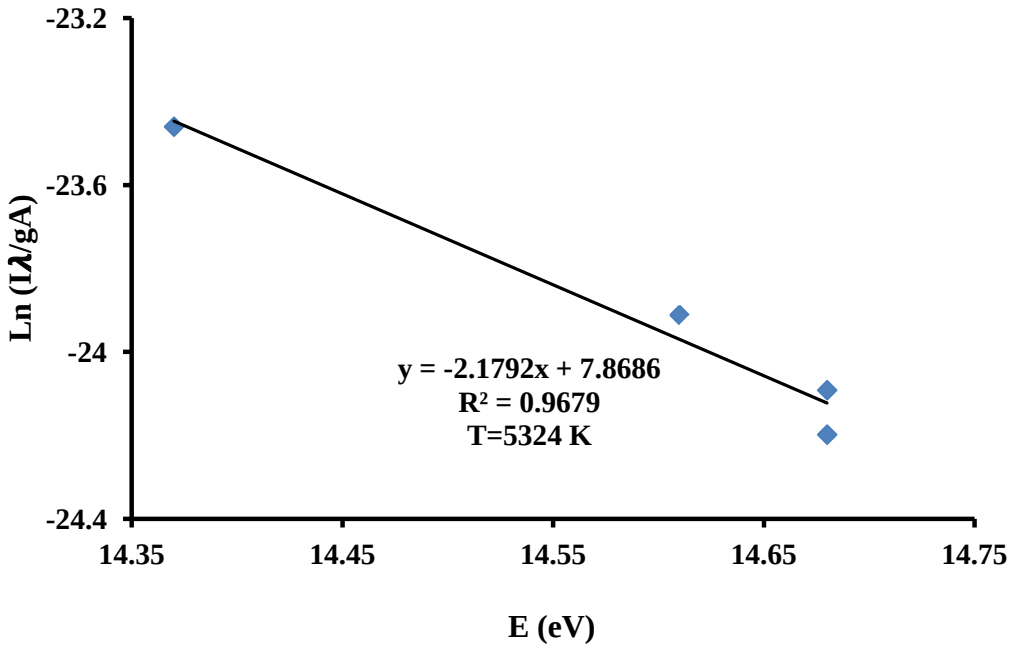

Figure 4. 2 Boltzmann plot for plasma generated using excitation wavelength of 266 nm, a time delay of 700 ns and a laser fluence of 23.5 Jcm^{-2}

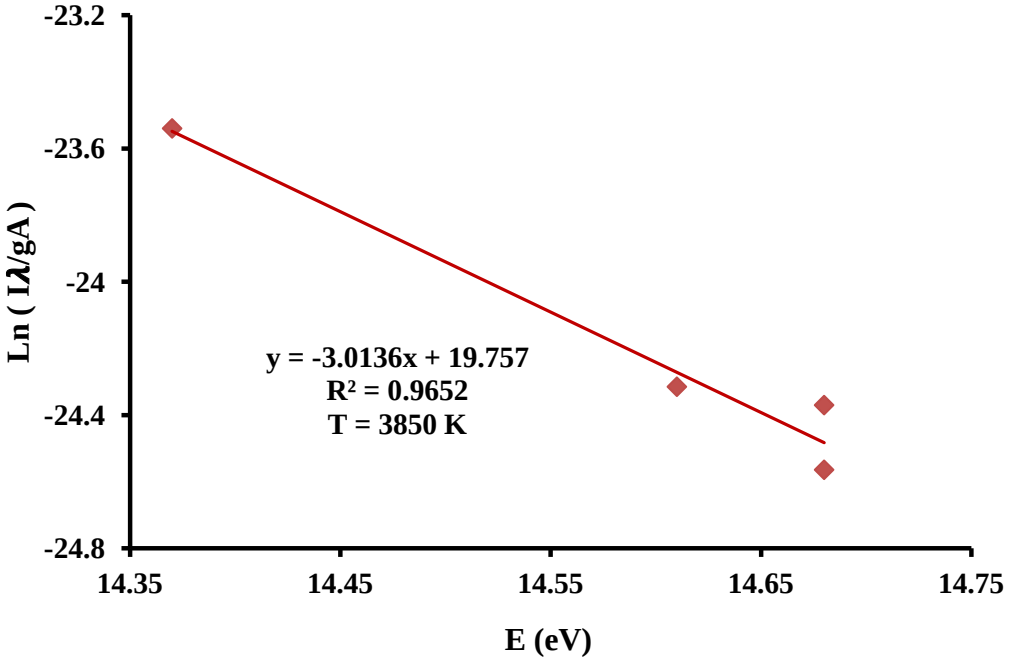

Figure 4. 3: Boltzmann plot for plasma generated using an excitation wavelength of 532 nm, a time delay of 700 ns and a laser fluence of 23.5 Jcm^{-2}

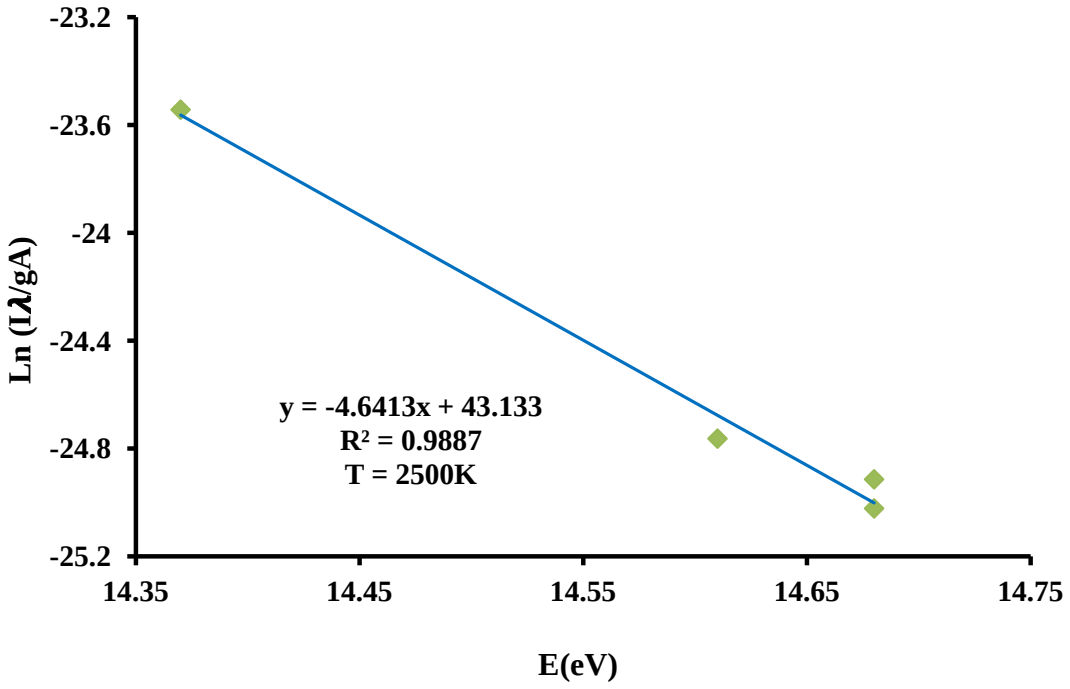

Figure 4. 4: Boltzmann plot for plasma generated using an excitation source of wavelength of 1064 nm, a time delay of 700 ns and a fluence of 23.5 Jcm^{-2}

Plasma temperatures for the laser induced plasma generated at a laser fluence of 23.5 Jcm^{-2} for gate/time delay in the range of 600 - 1500 ns using excitation sources of wavelength 266 nm, 532nm and 1064 nm were determined using the Boltzmann plot as depicted in Table 4-2. The plasma temperature values $T \sim 10^4$ K obtained almost under the same conditions have been reported [97]. From Figure 4.5, time resolved plasma temperature estimates showed similar trends for all the excitation wavelengths used with the 1064 nm and 266 nm consistently showing the lowest and highest values for the plasma temperatures respectively. In the initial stages of plasma evolution, the temperature is very high and changes rapidly. At longer times the plasma cools to much lower temperatures and then stabilizes. The temporal evolution of the

plasma temperature exhibits a t^{-2} dependence which is in accordance with the theoretical adiabatic model by Rumby and Paul [99].

Table 4 - 2: Calculated plasma temperature for Laser induced Plasma (LLP) generated at a laser fluence of 23.5 Jcm^{-2} and different gate/time delays for excitation source wavelengths of 266 nm, 532 nm and 1064 nm.

Time delay (ns)	Plasma Temperature (K)		
	266 nm	532 nm	1064 nm
700	5324	3850	2500
800	3877	2881	2100
900	3127	2550	1940
1100	2531	2252	1571
1300	2390	2216	1450
1500	2321	2159	1400

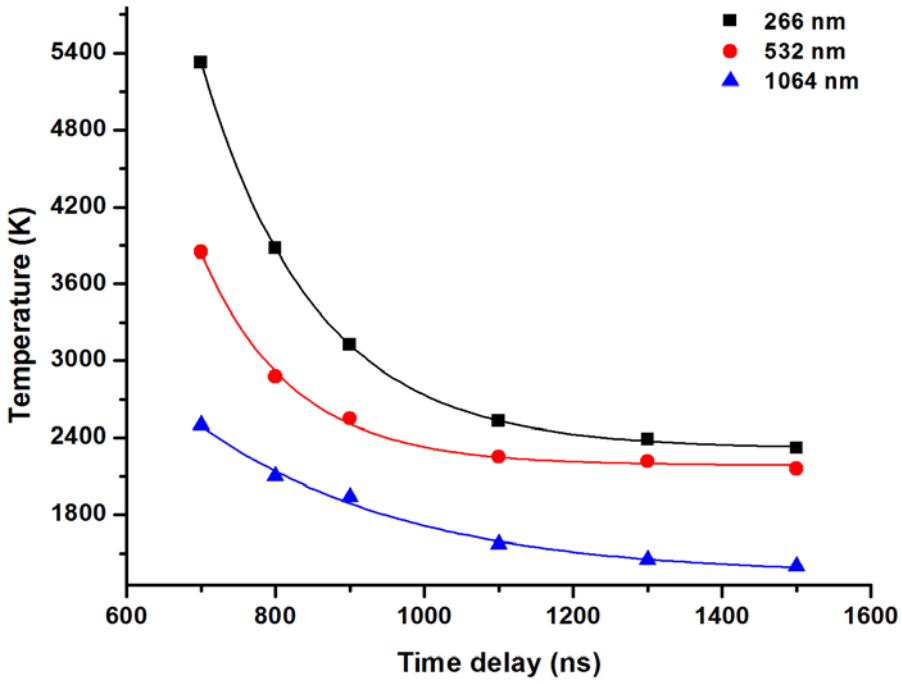

Figure 4. 5: Plasma temperature dependence on time delay in the range 700-1500 ns, for laser excitation sources of wavelengths 266, 532 and 1064 nm at a laser fluence of 23.5 Jcm^{-2} .

Plasma temperatures for the laser induced plasma generated at a gate/time delay of 700ns for laser fluencies in the range of 20.41 – 25.51 Jcm^{-2} using excitation sources of wavelength 266 nm, 532nm and 1064 nm were determined as clearly shown in Table 4-3. From Figure 4.6, all the trends are the same for all the excitation wavelengths. The plasma temperature increases steadily with increase in laser fluence and then saturates at higher laser fluencies. This saturation of the plasma temperature at higher laser fluencies is explained by the assumption of a self regulating regime. At higher laser fluencies a self regulating regime forms near the surface of the target material when the plasma absorbs an appreciable amount of laser energy. When the absorption of laser photons increases due to increase in the plasma density, evaporation of the species from the target surface decreases which in turn decreases the density of the charged species in the plasma. This consequently leads to absorption of laser photons by the surface of the target material and hence the increase in plasma temperature. Theoretically it has been proved that n_e and T adjust in such a way that the plasma absorbs the same amount of laser radiation in order to maintain a self regulating regime [100, 101].

Table 4 - 3: Calculated plasma temperature for spectral line FI (731.1 nm) generated at a gate/time delay of 700 ns and different laser fluencies for excitation source wavelengths of 266 nm, 532 nm and 1064 nm

Laser fluence (Jcm^{-2})	Plasma temperature (K)		
	266 nm	532 nm	1064 nm
20.41	4476	2995	2083
21.42	4658	3123	2210
22.45	4819	3304	2291
23.47	5136	3421	2395
24.49	5376	3598	2526
25.51	5360	2159	2521

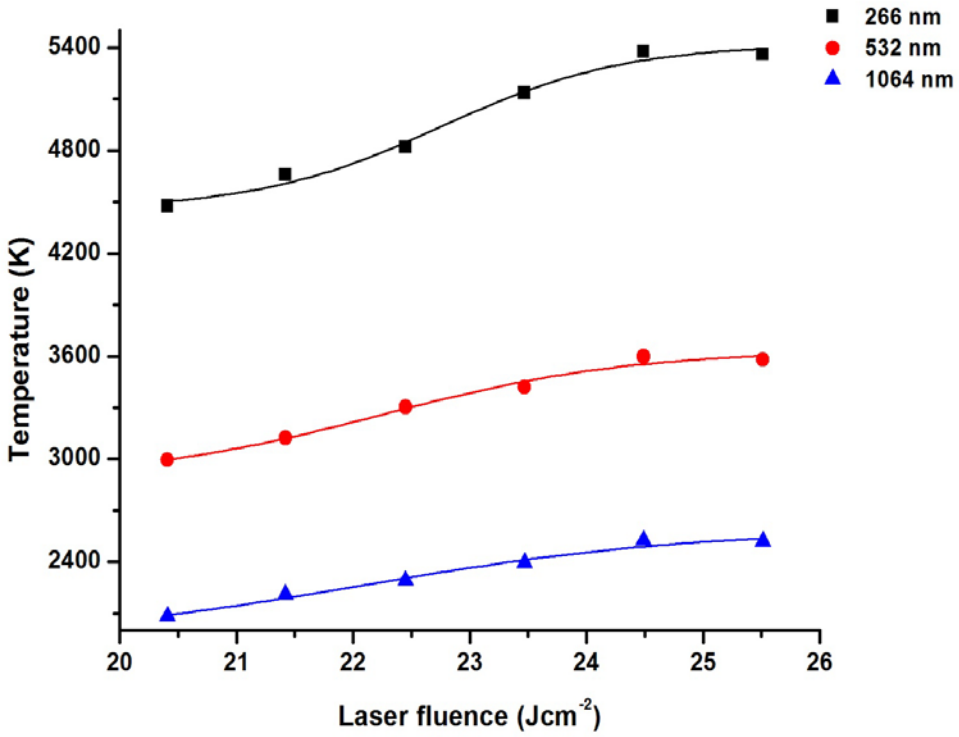

Figure 4. 6: Plasma temperature as a function of laser fluence in the range of 20.4 – 25.5 Jcm^{-2} for laser excitation sources of wavelengths 266, 532 and 1064 nm at a time delay of 700 ns

To estimate the electron density, data for a neutral spectral line of fluorine (FI 731.1 nm) was fitted using a lorentzian fit and its FWHM obtained using origin 8.0 software. Using the electron impact parameter *W* obtained from reference data [51], n_e is evaluated using equation 13. Figure 4.7, 4.8 and 4.9 depict lorentzian fits for a spectral line (FI 731.1 nm) in plasma obtained using a gate/time delay of 700 ns, laser fluence of 23.5 Jcm^{-2} for excitation sources of wavelengths 266 nm, 532 nm and 1064 nm. The electron densities obtained (6.5 x 10^{18} cm^{-3}, 6.12 x 10^{18} cm^{-3} and 5.3 x 10^{18} cm^{-3}) are observed to drop with increase in the wavelength of the excitation sources as expected. $n_e \sim 10^{18}$ cm^{-3} values have been reported for an 8 ns Laser produced plasma (LPP) under almost the same conditions as those obtained in this study [98].

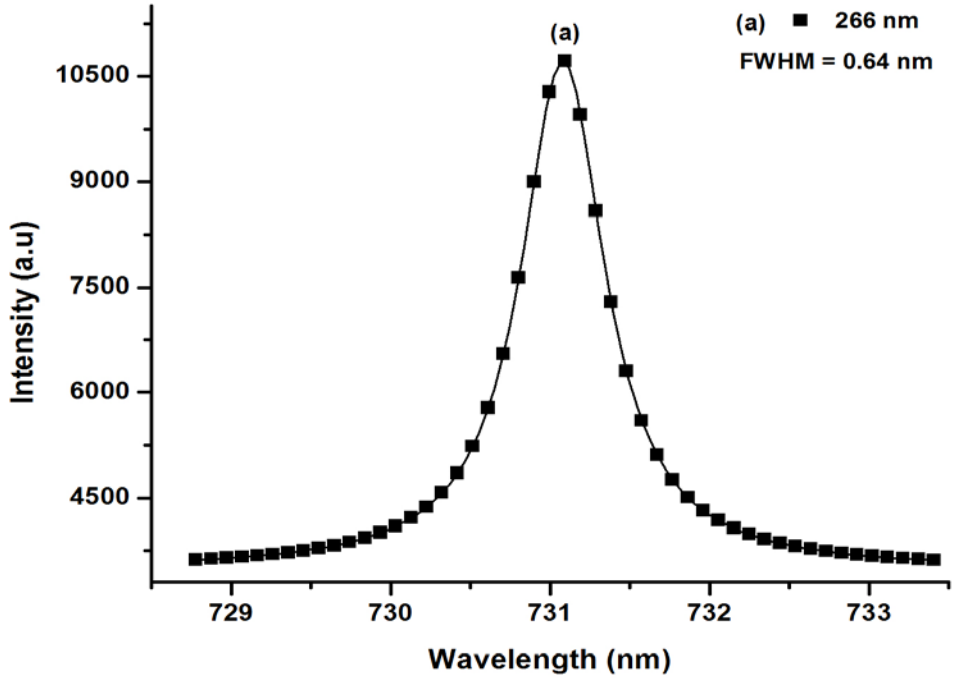

Figure 4. 7 Lorentzian fit for spectral line FI (731.1 nm) generated using a wavelength excitation source of 266 nm at a gate/time delay of 700ns and laser fluence of 23.5 Jcm^{-2}

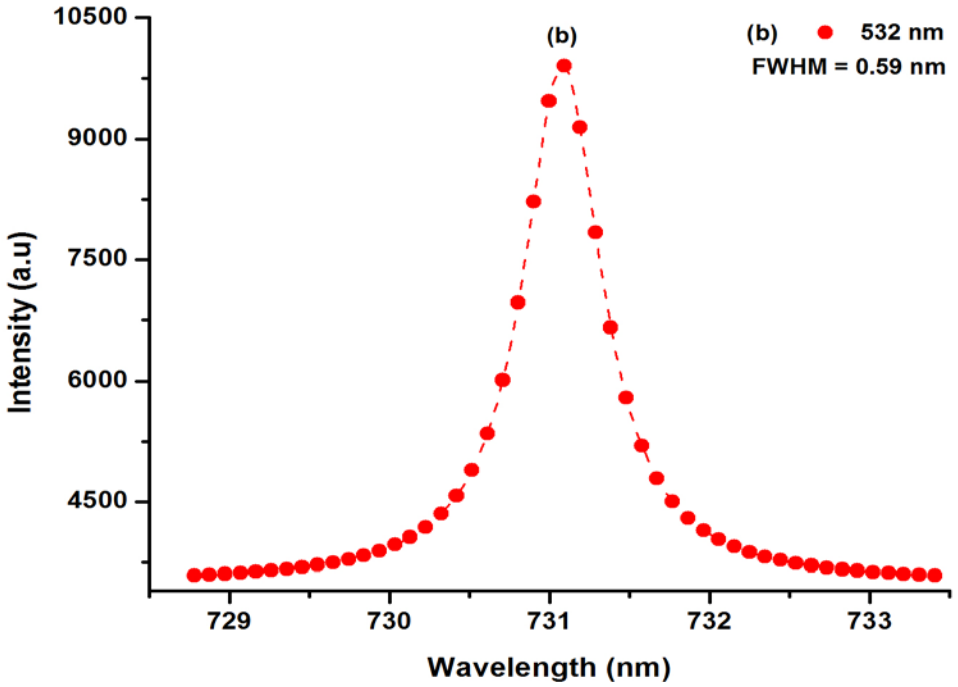

Figure 4. 8: Lorentzian fit for spectral line FI (731.1 nm) generated using a wavelength excitation source of 532 nm at a gate/time delay of 700 ns and laser fluence of 23.5 Jcm^{-2}

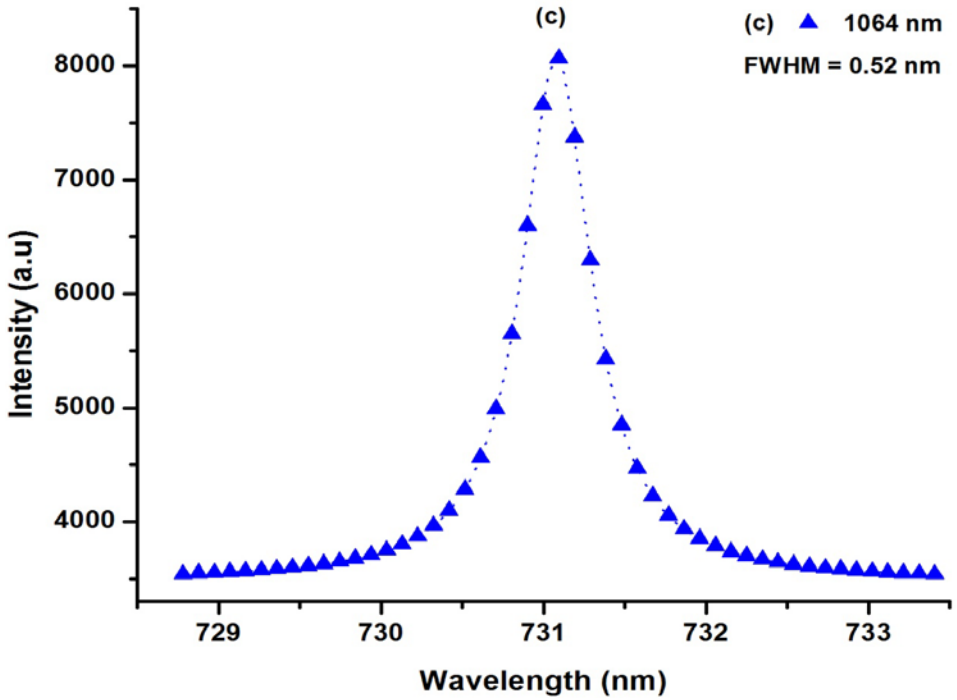

Figure 4. 9: Lorentzian fit for spectral line FI (731.1 nm) generated using a wavelength excitation source of 1064 nm at a gate/time delay of 700 ns and laser fluence of 23.5 Jcm^{-2}

The spectral line emission at t < 500 ns is masked by a continuum and therefore n_e cannot be determined using the stark broadening technique. This continuum is due to collisions of electrons with the ions and blackbody radiation of the plasma. However, the intensity of the continuum decreases with increase in the time/gate delay. Electron density (n_e) values for plasma generated at a laser fluence of 23.5 Jcm^{-2} for gate/time delays in the range of 700 – 1500 ns using wavelength excitation sources of 266 nm, 532 nm and 1064 nm were determined as clearly shown in Table 4-4. From Figure 4.10, time resolved electron density (n_e) estimates also showed similar trends for all the laser excitation sources used with 1064 nm and 266 nm yielding consistently the lowest and highest values respectively. The temporal evolution showed a rapid drop of n_e and then leveled off exhibiting t^{-2} dependence. The initial fast momentary decay is due to the expansion of the plasma in the ambient atmosphere and the leveling off is justified by the fact that the expanding plume equilibrates with the back ground pressure at later times and it's also partly attributed to the recombination processes[49].

Table 4 - 4: Calculated electron density values for spectral line FI (731.1 nm) generated at a laser fluence of 23.5 Jcm^{-2} for excitation source wavelengths of 266 nm, 532 nm and 1064 nm

Time delay(ns)	Electron density (x 10^{18} cm^{-3})		
	266 nm	532 nm	1064 nm
700	6.50	6.12	5.30
800	5.70	5.60	4.93
900	5.56	5.45	4.81
1100	5.43	5.35	4.73
1300	5.41	5.32	4.65
1500	5.40	5.31	4.61

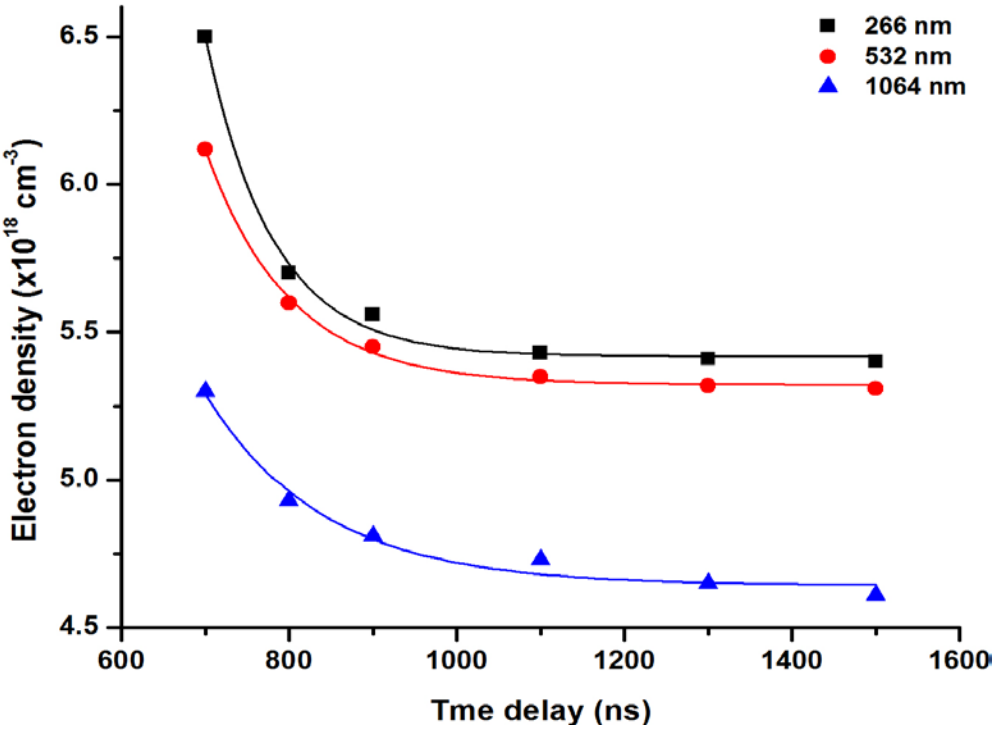

Figure 4. 10: Electron density dependence on time delay in the range of 700-1500 ns for excitation sources of wavelength 266, 532 and 1064 nm at a laser fluence of 23.5 Jcm^{-2}

Electron density (n_e) values for plasma generated at a gate/time delay of 700 ns for laser fluencies in the range of 20.41 – 25.51 Jcm^{-2} using excitation sources of wavelength 266 nm, 532nm and 1064 nm were determined as clearly shown in Table 4-4. .From Figure 4.11, n_e increases with increase in the laser fluence for all the wavelengths and then saturates but plasmas generated by the 1064 nm excitation source are least influenced by the increase in the laser fluence. The higher electron density for plasma generated using 266 nm excitation source is due to the enhanced ablation rate at shorter wavelength [195]. This explanation is consistent with a reported mass ablation rate which followed a $\boldsymbol{\lambda}^{-4/9}$ dependence on wavelength as well as the deep craters observed for the short wavelength excitation [196]. It's worth mentioning that enhanced plasma screening at longer wavelengths reduces the laser - target coupling leading to shallow craters for the IR wavelengths as compared to the UV radiation. Reflectivity of the target also affects the amount of laser energy absorbed by the target during ablation. Given that $E \sim I_0 (1-R) (1-A)$ where I_0 is the laser irradiance, R is the reflectivity, A is the percentage of absorption by the plasma reflectivity, it's clear that R affects effective laser-target coupling. Aluminum (Al) reflectivity for 266 nm, 532 nm and 1064 nm only differ slightly, 0.92, 0.92 and 0.95 respectively this implies that plasma absorption mechanisms are responsible for the different ablation rates [104]. Effects of 1064 nm, 532 nm and 266 nm were studied on copper in 1atm He gas using a comprehensive computational model. The model showed little differences between 266 nm and 532 nm crater depths. This is due to the balancing of target reflectivity and plasma shielding effects at 532 nm [105]. The observed saturation of n_e is due to plasma shielding that is absorption and reflection. The frequency (Vp) of the laser produced plasma $Vp = 8.9 \times 10^3 n^{0.5}$ is less than the frequencies of all the Nd: YAG laser excitation sources (V_l) for all estimated values of the electron density implying that the energy losses are negligible and thus reflection

can be neglected. The absorbing plasma created at the edge of the surface prevents light from reaching the surface of the target material. Consequently the surface is cutoff from the trailing edge of the incident laser pulse and therefore the amount of energy delivered at high power is less effective than that at low power in causing vaporization. Therefore the prominent mechanism responsible for absorption in laser induced plasmas is inverse bremsstralung.

Table 4 - 5: Calculated electron density values for spectral line FI (731.1 nm) generated at a gate/time delay of 700 ns for excitation source wavelengths of 266 nm, 532 nm and 1064 nm

Laser fluence (Jcm^{-2})	Electron density (x 10^{18} cm^{-3})		
	266 nm	532 nm	1064 nm
20.41	5.43	5.10	4.45
21.42	5.63	5.30	4.61
22.45	5.96	5.64	4.86
23.47	6.27	5.87	5.10
24.49	6.50	6.12	5.30
25.51	6.48	6.10	5.28

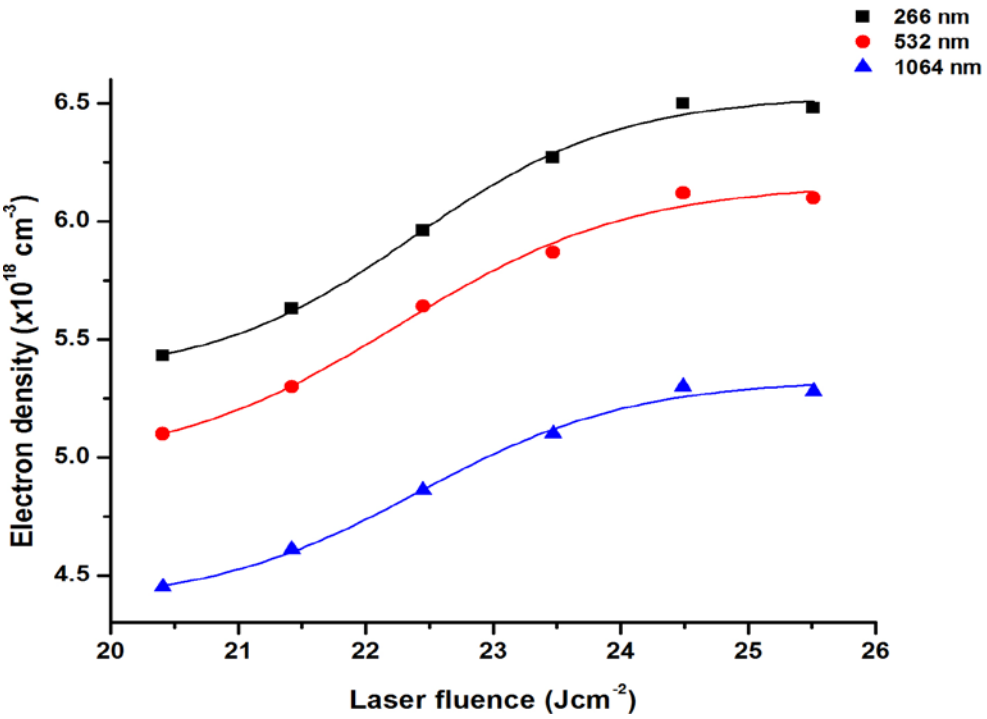

Figure 4. 11: Electron density dependence on time delay in the range of 700-1500 ns for excitation sources of wavelength 266, 532 and 1064 nm at a laser fluence of 23.5 Jcm^{-2}

4.2 Applications of the LIBS spectrometer

In this section, application of a self developed LIBS spectrometer to detect and quantify fluoride (F), lead (Pb) and chromium (Cr) in toothpaste, synthetic hair dyes, kohl eyeliners and talcum powder samples is discussed

4.2.1 Detection of fluoride (F) in Toothpaste Using a Maker line of 731.1 nm

4.2.1.1Introduction

Heavy metals and other toxic elements are present in the raw materials and byproducts pertained to various manufacturing industries [106, 107]. Sodium fluoride and sodium mono fluoro phosphate are chemical ingredients used for the manufacturing of toothpastes, gels and also in the foams used for the radiation therapy. Fluoride is one of the inevitable constituent of prescription and non prescription mouth washes available in the local market and therefore people are frequently exposed to it [108].

Several studies have confirmed that fluoride tooth pastes are risk factors for dental flourosis. Tooth paste is the main source of fluoride ingestion for 1-3yrs old children during the period of tooth development when their central incisors are most vulnerable to dental flourosis [109-114]. This is because more than 90% of the children start tooth brushing before the age of 2 yrs [109,115-117], a majority of them are not supervised while brushing their teeth [118,119], their swallowing reflex is not yet fully developed at this age [120-125] and most of the flavor used in the tooth paste brands encourages ingestion in children [126]. Fluoride intake of 0.05-0.07 mg/kg body weight/day is regarded as the optimum [127]. However another investigation reveals dental flourosis at concentrations as low as 0.04 mg/kg body weight/day [128]. Ingested tooth paste can

contribute up to 0.2-0.3 mg F per day to a child's fluoride intake [129- 131] which clearly increases the risk of flourosis. Fluoride causes neurotoxicity by targeting the hippocampal neurons. This causes learning disabilities and also negatively affects the memory [132, 133]. Fluoride also crosses the placenta [134] and thus exposing the developing brain of the unborn which is more vulnerable to intoxicants. This may possibly lead to permanent damage of the brain and the nervous system [135]. Increased Fluoride exposure in adults weakens the immune system, causes bone cancer and cell death [136-141].

To understand the highly reactive nature of fluoride and its adverse effect on human health, there has been many research works directed towards developing a reliable system to detect and quantify the fluoride levels in tooth paste and other supplements. The most popular in this respect is Fluoride Ion Selective Electrode (FISE) [142]. This device has a single LaF_3 membrane which has an enhanced selectivity for fluoride ion and a wide concentration range response for fluoride as well [143]. However, its response is Nernstian which yields a very large error in the analytical results due to the necessity of antilogarithmization. It also needs long times for obtaining the signal because it takes time for the establishment of equilibrium. To successfully apply the FISE technique, the sample under study has to be in the PH range of 5.2 - 5.5 to avoid interference from OH^- and conversion of F^- to HF and HF_2, the samples and the standards should have the same ionic strength and interference of ions that form complexes/ precipitates with fluoride should be avoided [144]. The addition of the total ionic strength adjustment buffer solution to a neutral tooth paste suspension, the last one is nearly impossible to implement because the main components of tooth paste are Si, Al, Ca and water soluble organic compounds that form complexes with fluorine [145]. Ion chromatography has also been widely used providing the possibility of determining several ions in the same sample but it has a lower

sampling rate as compared to the ISE and is expensive. Also the fluoride ion is weakly retained on the common columns of the ion chromatography system and this significantly affects the results [146, 147]. Other methods published recently are graphite furnace molecular absorption spectrometry [148], fluorescence [149], interdigitated microelectrode array [150], and colorimetry [151]. LIBS outsmarts the traditional techniques of elemental analysis like Atomic Emission Spectroscopy (AES), Induction Coupled Plasma (ICP), microwave induced plasma (MIP) etc. due to the fact that it requires no or minimum sample preparation, capable of multi elemental analysis, chances for contamination of the samples and necessity for chemicals is minimal [152-154].

LIBS has been increasingly used for the detection and analysis of halogens [155, 49]. The difficulty for halogen detection such as fluorine (F) using LIBS is due to the fact that its strong atomic emission lines are in the VUV region. This presents several limitations for the practicability of LIBS in this region such as strong absorption of the atmospheric oxygen and strong absorption of silica based light collection and imaging optics, optic fiber for signal transmission, thus necessitating the use of very expensive VUV optics based on MgF_2 and CaF_2 materials. However LIBS can be applied in the NIR region having atomic transition lines which are less strong than those in the VUV since no vacuum is required and imaging and fiber optics with good transmission in the NIR are cheap and readily available. Hence optimization of experimental parameters in order to improve on the signal response is very vital to achieve good analytical results.

In this chapter, LIBS has been used to detect fluoride concentration levels in toothpaste available in the local market. The objective of our study is to optimize experimental parameters in order to improve the signal to noise ratio, limit of detection and calibration curve linearity for the

detection of fluoride in toothpaste in the NIR spectral region. Gate/time delay and laser energy were optimized using a fluorine spectral marker line at 731.102 nm in order to produce the best signal response and optically thin plasma in local thermodynamic equilibrium. To verify the choice of the parameters that yielded the above mentioned plasma, the Mcwhirter criterion was used [49]. But prior to this, plasma temperature was determined using the Boltzmann plot and Stark broadening of the fluorine spectral line to estimate electron density.

4.2.1.2 LIBS spectra for toothpaste samples

Using the spectrometer parameters mentioned previously in the text, spectra were recorded in the wavelength range of 200 – 800 nm as shown in Figures 4.12 - 4.17. Spectral data published by the National Institute of Standards and Technology (NIST) was used to identify all the spectral lines in the spectra and elements such as nickel (Ni), iron (Fe), copper (Cu), sodium (Na), zinc (Zn), titanium (Ti), calcium (Ca), phosphorous (P), silicon (Si) potassium (K) and fluorine (F) were detected in the tooth paste samples by our LIBS detection system. In order to detect and quantify fluoride concentration levels in all the tooth paste samples, fluorine neutral atomic transition (FI) at a wavelength of 731.1 nm was selected as the spectral marker line since it is isolated, strongly intense and doesn't involve the ground state.

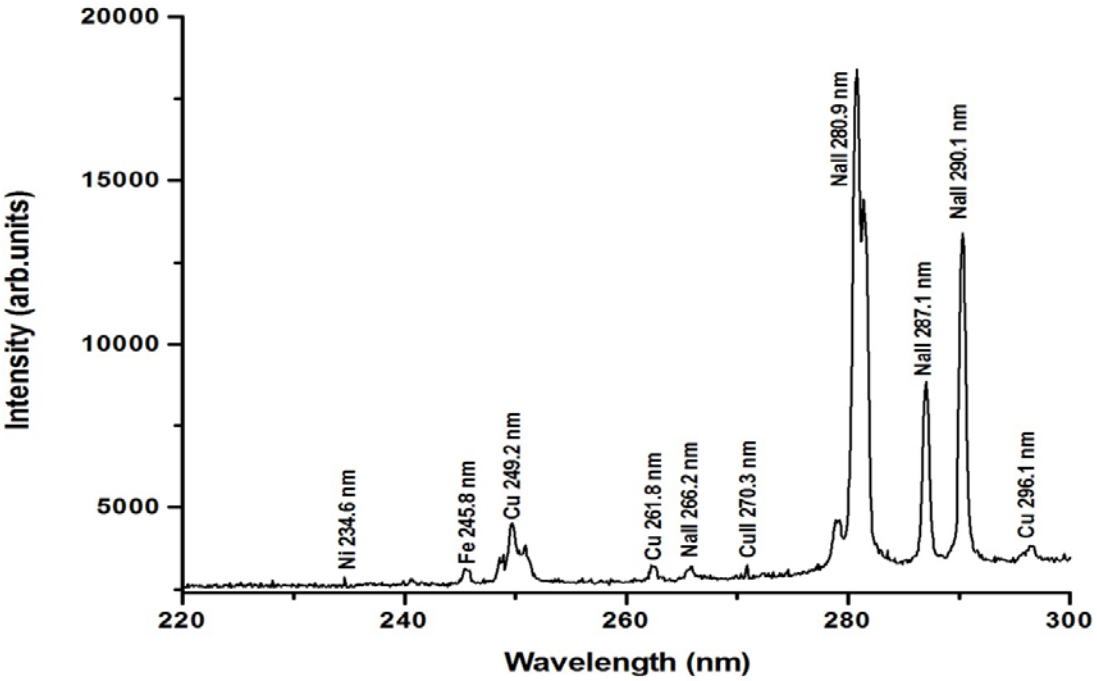

Figure 4. 12: Typical LIBS spectrum in the 200 - 300 nm wavelength range for sample#1.

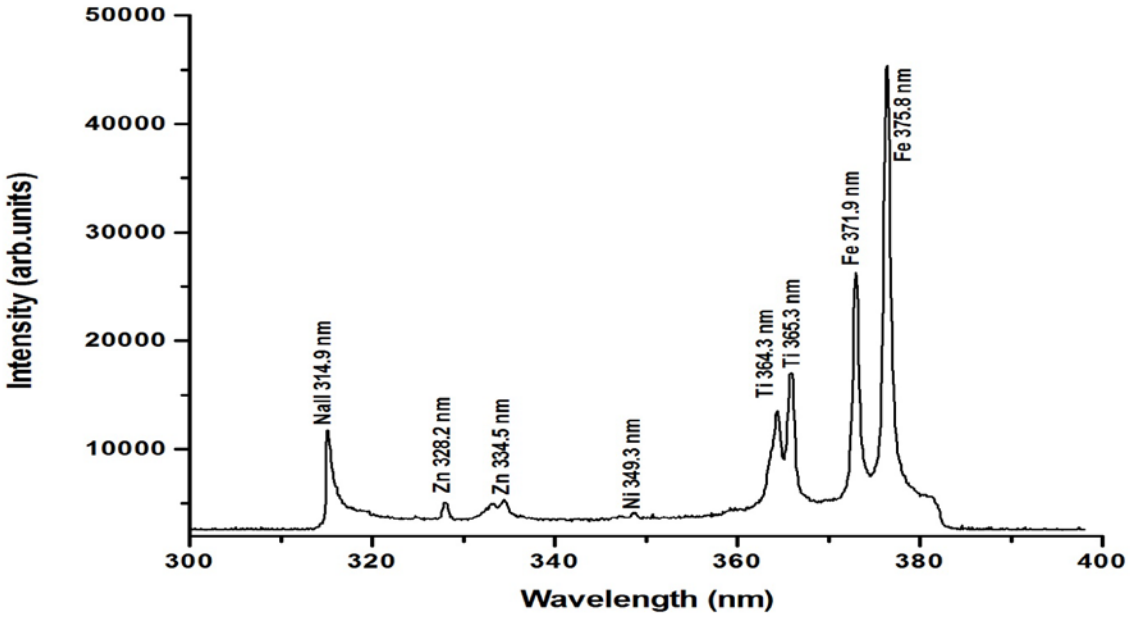

Figure 4. 13: Typical LIBS spectrum in 300 - 400 nm wavelength range for sample #1.

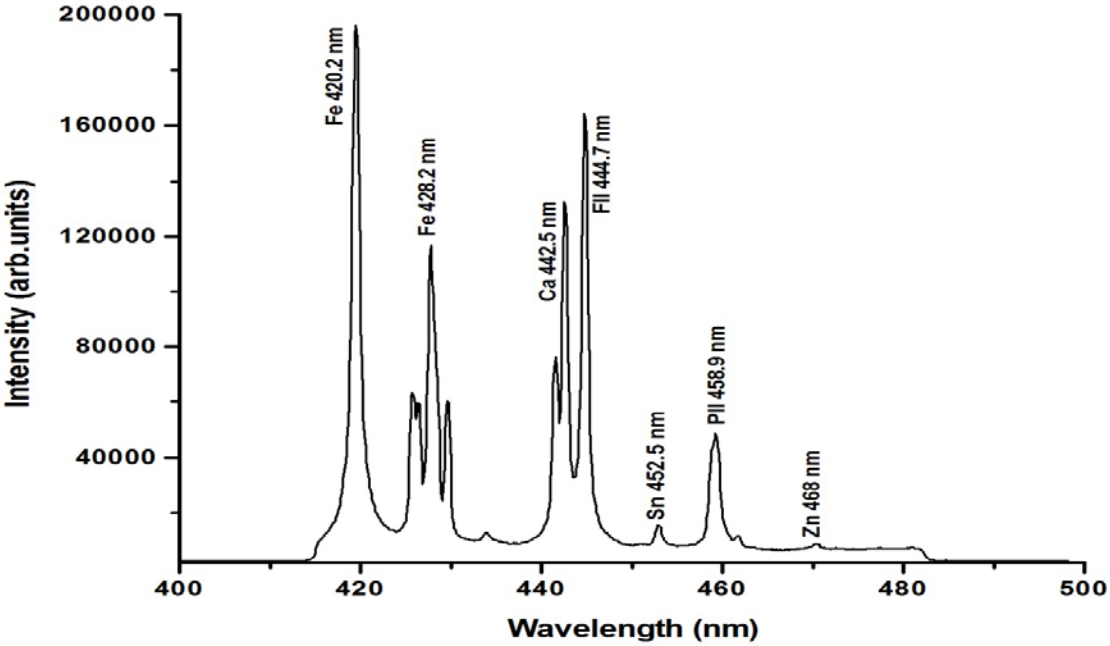

Figure 4.14: Typical LIBS spectrum in 400nm -500 nm wavelength range for tooth sample #1.

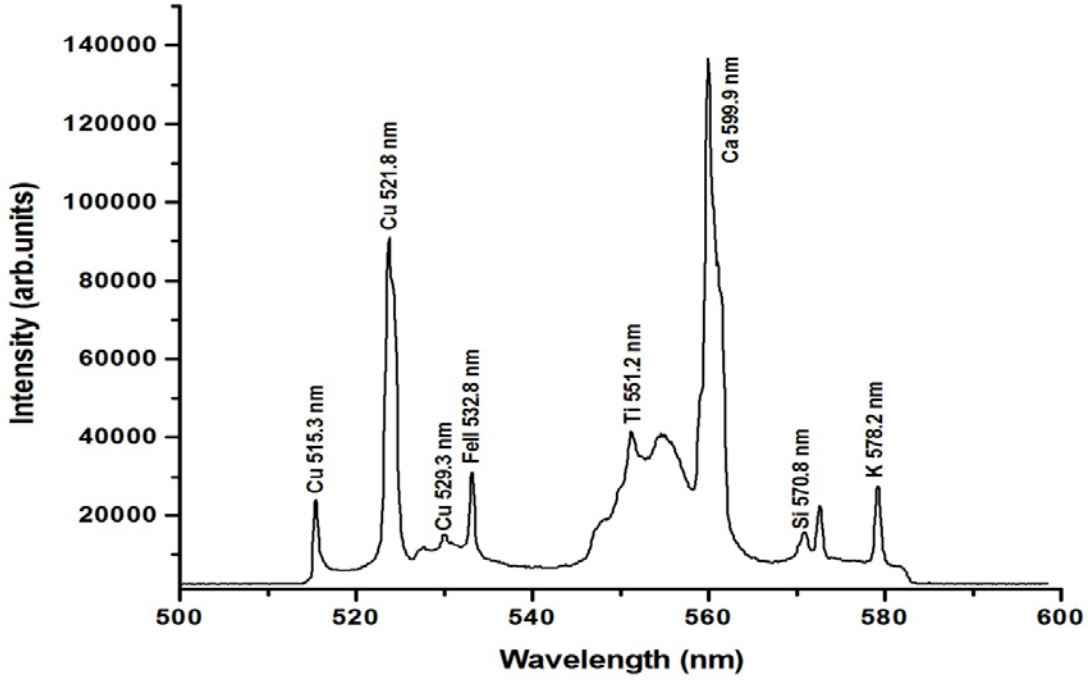

Figure 4.15: Typical LIBS spectrum in 500nm -600 nm wavelength range for tooth sample # 1.

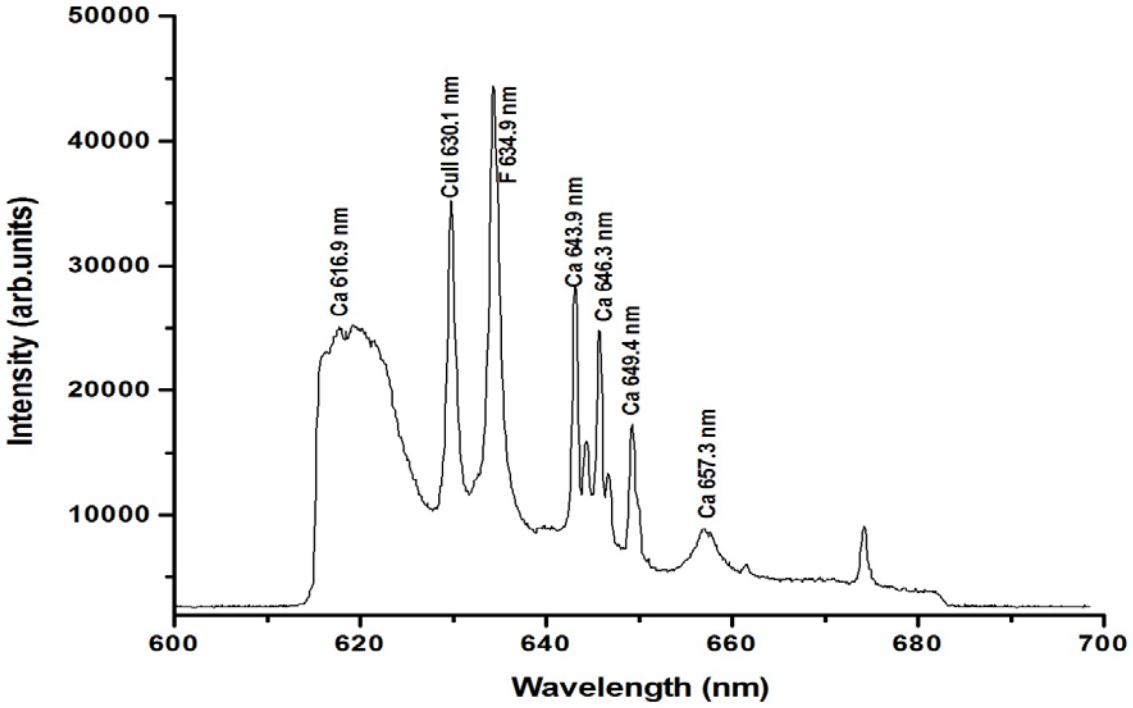

Figure 4. 16: Typical LIBS spectrum in 600 - 700 nm wavelength range for tooth sample # 1.

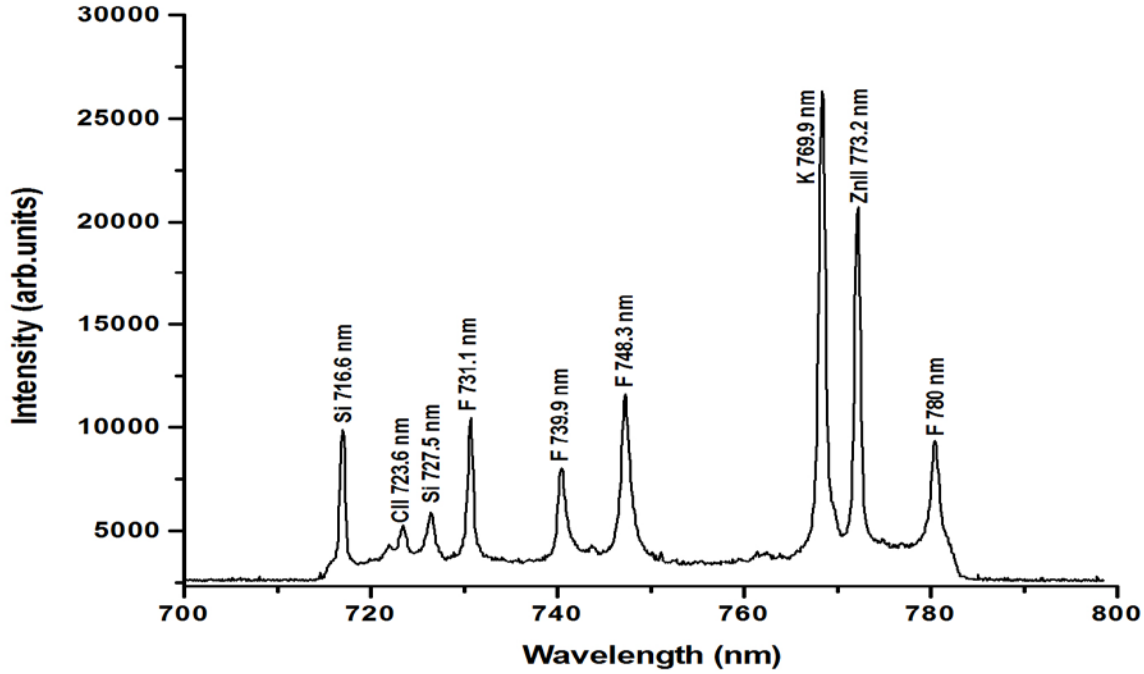

Figure 4. 17: Typical LIBS spectrum in 700 - 800 nm wavelength range for tooth sample #1.

4.2.1.3 Time/gate delay optimization for tooth paste samples

In the case of LIBS, the gate width of acquisition and the gate/time delay between the laser excitation and data acquisition are important factors, because they not only alter the level of the LIBS signal but also the type of atomic specie detected. After the excitation, due to the high plasma temperature all kind of excited atomic, ionic and molecular species are present and this gives rise to an unstructured broad continuum in the LIBS spectrum. In order to avoid this broadening, the acquisition time window was delayed to a certain value ranging from hundreds of nanoseconds to a few microsecond. In the LIBS analysis both the neutral and singly ionized atomic species are of interest and when the time delay is below 200 ns most of the atomic transitions recorded are from the singly ionized atoms and in the subsequent time, the transitions from the neutral atoms are recorded [1]. From Figure 4.18, the Relative Standard Deviation (R.S.D) decreases with increase in the number of accumulations but no change is observed beyond 20 accumulations, this makes it the optimum number of accumulations. In our study the LIBS signal was optimized for the strong fluorine atomic emission line at 731.1 nm (FI) as the marker wavelength with respect to the time/gate delay between the excitation and data acquisition as depicted in Figure 4.19, It is clear from figure 4.21 that 700 ns is the optimum time/gate delay for the detection of fluoride and this particular delay was used for this study.

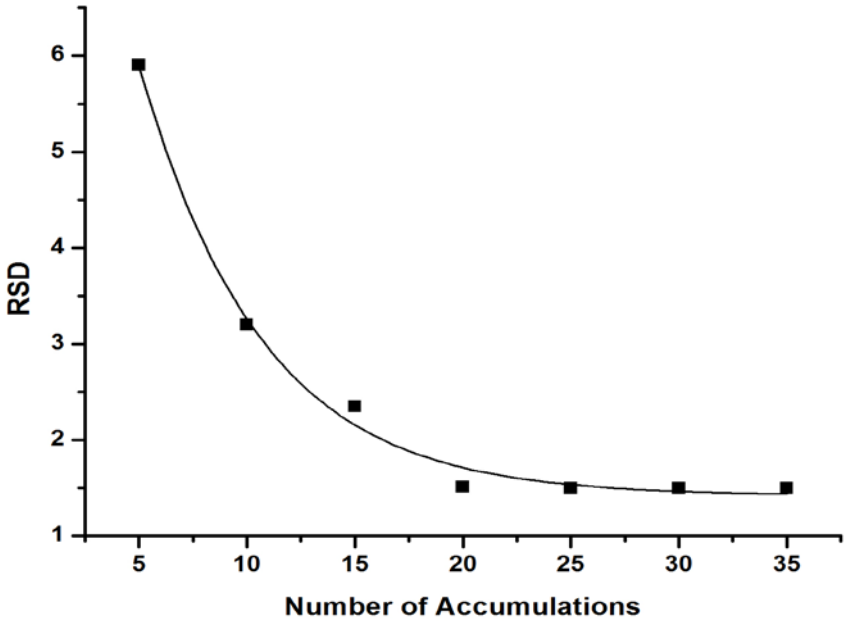

Figure 4. 18: Relative Standard Deviation (RSD) as a function of the number of accumulations.

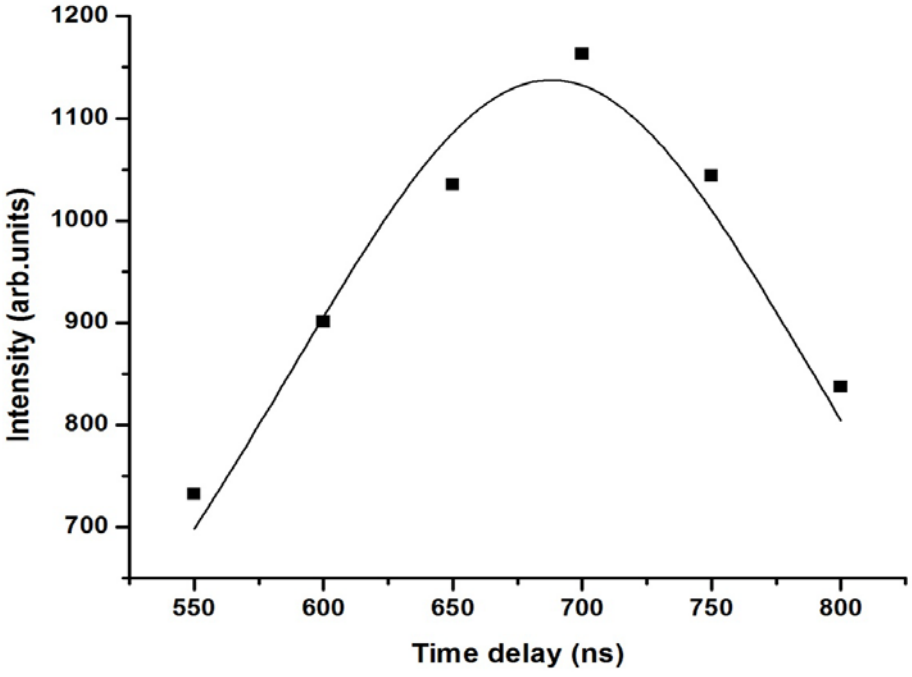

Figure 4. 19: LIBS signal intensity dependence on time delay between laser excitation and gate opening of the detection system for FI at 731.1 nm.

4.2.1.4 Laser energy optimization for tooth paste samples

Figure 4.20 depicts LIBS signal intensity dependence on the laser fluence for the same spectral line (731.1 nm) and at the other optimum experimental conditions (700 ns time delay) reached in the previous discussion. It was observed that the trend of LIBS signal as a function of laser fluence showed a linear dependence at the beginning and started to flatten when the fluence reached 23.5 J/cm^2. When the laser fluence was increased beyond 23.5 J/cm^2, the increment factor of the LIBS signal intensity reduced significantly due to self absorption making 23.5 J/cm^2 the optimum laser fluence. Self absorption is due to the fact that atoms inside the plasma have higher energies in comparison with atoms on its surface. Therefore when atoms producing resonance lines inside the plasma de-excite, atoms on its surface absorb the energy resulting into a less intense spectral line.

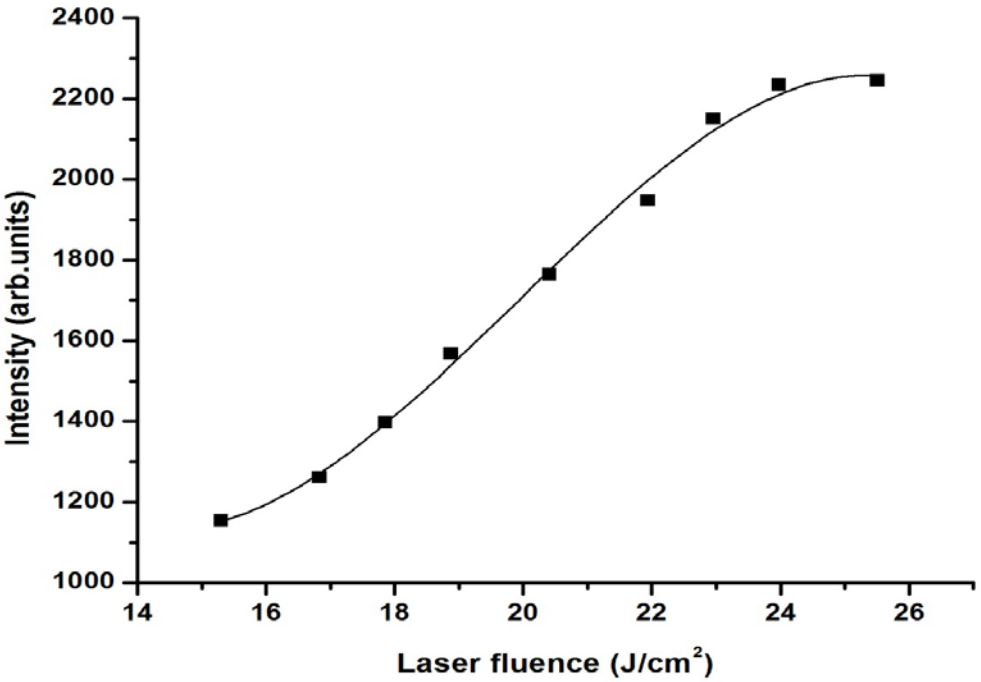

Figure 4. 20: LIBS signal intensity dependence on laser fluence imparted on the surface of sample #1 for FI at 731.1 nm.

4.2.1.5 Local thermodynamic equilibrium (LTE) condition for toothpaste samples.

To Detect and quantify elements using spectral line intensities in LIBS, the laser induced plasma should be optically thin and in local thermodynamic equilibrium (L.T.E). In a transient system like plasma formed by a pulsed laser ablation, LTE is achieved if the electron-atom and electron-ion collision processes are extremely rapid and dominate the radiative processes. The plasma generated during ablation is complex and is understood by the following different physical laws: The constituent particles in the plasma obey Maxwellian velocity distributions, populations in the energy levels follow Boltzmann's statistics and ionization processes are described by Saha equation [153]. In our study plasma was generated using all the optimum parameters achieved and in order ascertain that such plasma was optically thin and in local thermodynamic equilibrium, the Mcwhirter criterion of minimum density condition for plasma to be optically thin and in Local thermodynamic equilibrium was used as given in equation 7 [156,157].

In this case temperature and electron density of the plasma were evaluated using a Boltzmann plot method and Stark broadening respectively. Plotting a graph of magnitude of the component on the left hand side of the equation 11, as a function of the energy for the upper level of the species in ionization stage *z* yields a Boltzmann plot. The value of plasma temperature *(T)* is then deduced from the slope of the plot. A spectrum for a wavelength range of 700 nm – 800 nm was obtained using the optimal conditions and spectrally isolated characteristic atomic transition lines of neutral fluorine (F I) are identified as 731.102 nm, 739.869 nm, 748.916 nm and 780.021 nm. These atomic transition lines are used to determine the plasma temperature which is $T = 4953 \pm 650K$ as deduced from Figure 4.21. Transitional probabilities (A_{ik}), statistical weights (g) and upper energy levels (E_{ik}) are obtained from the NIST data base as shown in Table 4-1 [18]. We believe that the plasma temperature obtained in the present work is accurate because a

sufficient number of strong spectral lines have been accounted for. The quoted uncertainty in the plasma temperature is mainly due to errors in the reported transition probabilities and the measurements of the integrated intensity ratios of the spectral lines.

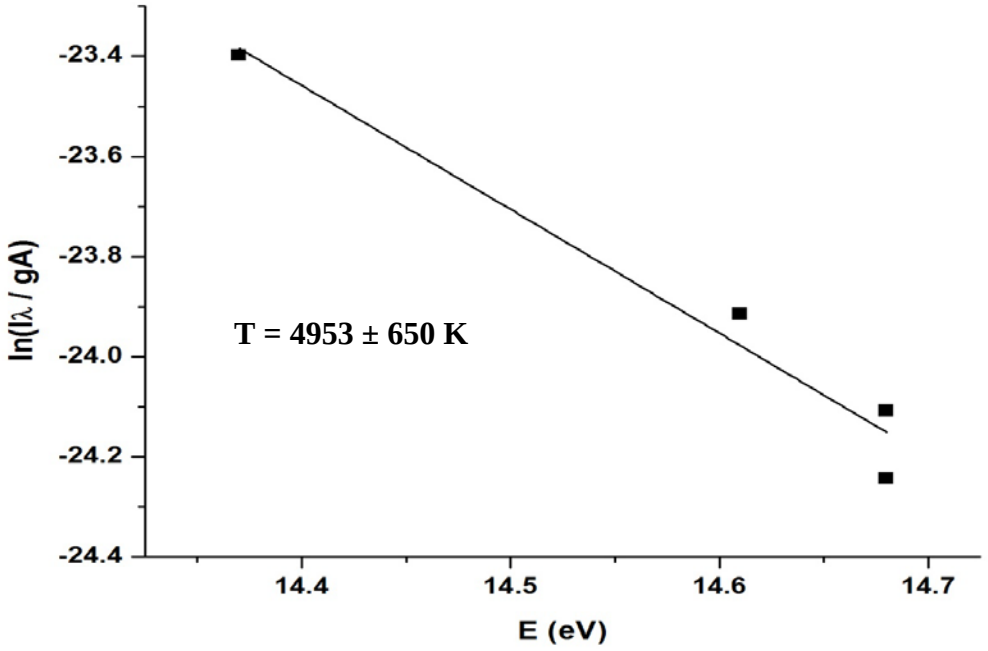

Figure 4. 21: Boltzmann plot to estimate temperature of plasma of tooth paste sample #1.

In an optical spectrum, a spectral line has a nonzero line width and its center may be shifted from its nominal central wavelength. This broadening and shift is due to instrumental, Doppler, natural and Stark broadening [157- 160]. In our study, instrumental broadening was minimized by adjusting the spectrograph to its maximum resolution. It's worth mentioning that in highly dense plasmas generated under atmospheric pressure, Stark broadening is the only dominant form of broadening therefore was used to determine electron density of the plasma [51]. Stark broadening of spectral lines in plasma is due to collisions of electrons and atoms with charged

species resulting into broadening and corresponding shift in the peak wavelength of the line. The line profile for Stark broadening is described by a Lorentzian function [157-160] and has a full width at half maximum as shown in equation 13.

From Figure 4.22, electron density was calculated from the Stark broadened profile of singly ionized atomic transition line of fluorine (F I) at 731.1nm because it is isolated, free from interference with other spectral lines in the spectrum and doesn't involve the ground state. The Full Width at Half Maximum (FWHM) of 0.637 nm was obtained from a fitted Lorentzian curve. Using the electron impact parameter W from reference data [51], electron density (n_e) is evaluated *as* 2.86 x 10^{18} cm^{-3}. The critical value of the plasma density determined using the plasma temperature and energy gap (1.695 eV) is 4.79 x 10^{16} cm^{-3}. It is clearly seen that the measured electron density is higher than the critical value; hence the plasma obtained in our study is in LTE. Therefore the emissions produced by the plasma are fully radiated without any self absorption and also the plasma is transparent to the laser beam. This consequently maximizes the emission intensities and the laser induced plasma can be described using thermodynamic parameters.

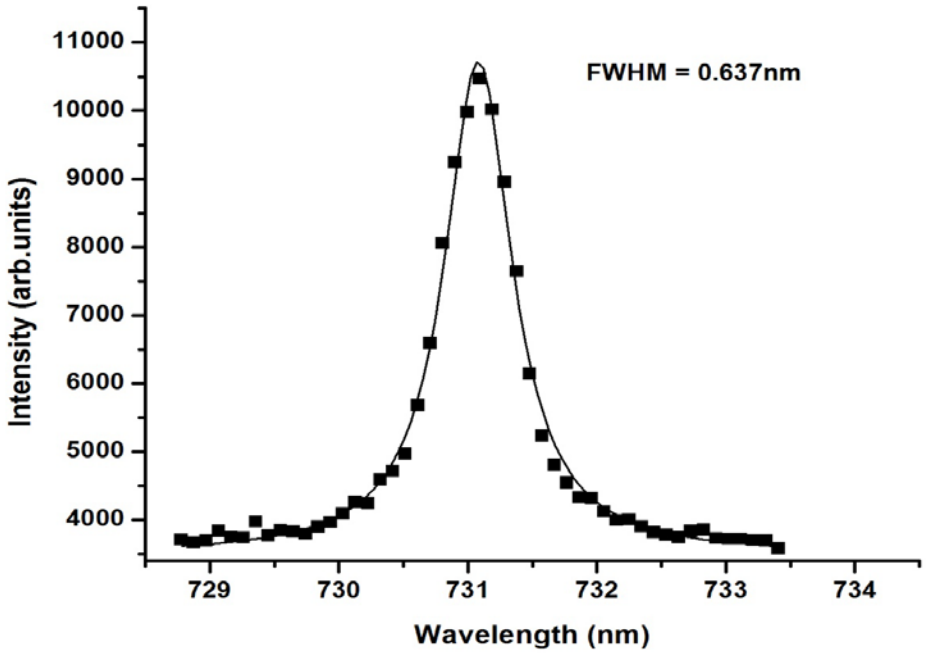

Figure 4. 22: Stark broadening profile of the atomic transition line of FI at 731.102 nm used to estimate the electron density.

4.2.1.6 Detection of fluoride levels in toothpaste

In this case, the optimum experimental parameters obtained previously in the text were used and spectra for the samples #1, #2 and #3 were taken in the wavelength range between 700 and 800 nm for qualitative analysis as observed in Figure 4.23. Several strong spectral lines of Fluorine were detected in this wavelength range for all the samples based on the NIST spectral data. Although several fluorine lines are present in the spectrum in Figure 4.23, we chose the atomic transition line of neutral fluorine at 731.102 nm as the marker wavelength. This marker line at 731.1 nm is due to atomic transition between $2s^2 2p^4$ (^3P) 3s and $2s^2 2p^4$ (^3P) 3p and it is of a moderate intensity. There are many other atomic transition lines of neutral fluorine with higher intensities within our experimental range but these lines show weak signal due to the self absorption by the LIBS plasma. However the atomic transition line at 731.1 nm not only appears

with the measurable signal intensity but also showed a systematic linear growth of the LIBS signal with the increasing concentration of fluoride in the samples. The presence of fluoride in the toothpaste sample is confirmed by externally adding different concentrations of fluoride in the tooth paste sample (sample #1) and monitoring the LIBS signal intensity of the spectral line at 731.1 nm and the increased LIBS signal with the increased concentration of fluorine in the tooth paste sample is evident from Figure 4.24 (a) 439 ppm (b) 2195 ppm (c) 4390 ppm (d) 6585 ppm. The appearance of 731.1nm atomic transition line and its growth with increasing concentration at the same wavelength strongly confirms the presence of fluorine in the tooth paste.

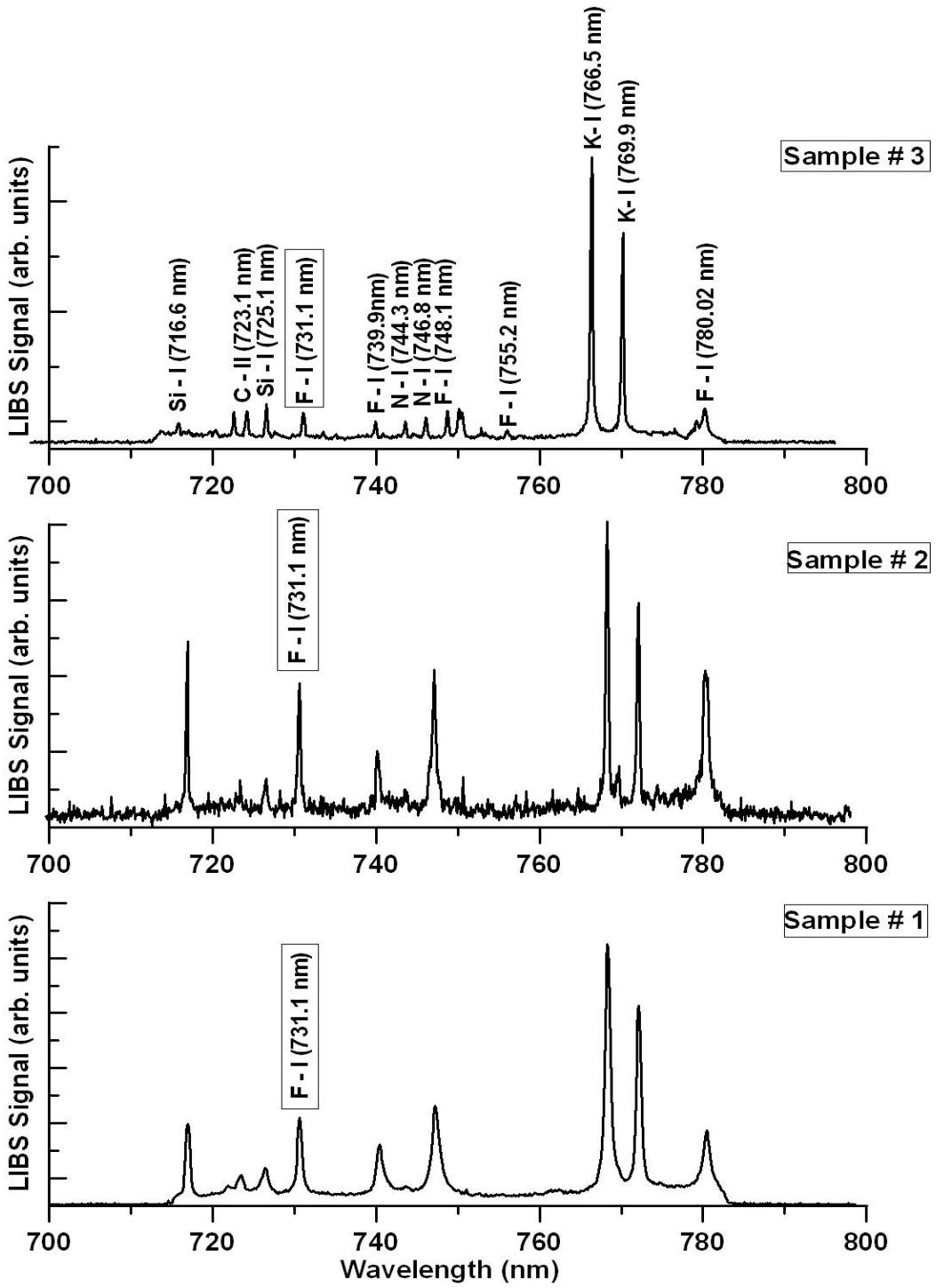

Figure 4. 23: A representative LIBS spectrum for tooth paste (samples 1, 2 and 3) in the wavelength of 700 nm - 800 nm. The identified atomic transition lines are marked on the spectrum.

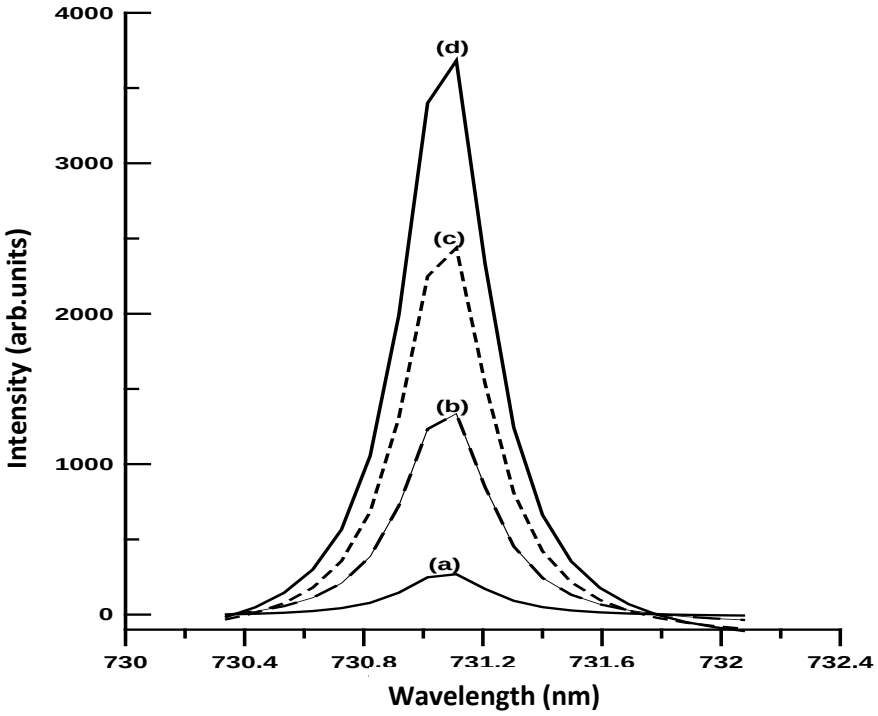

Figure 4. 24: The growth of the LIBS intensity of FI (731.102 nm) marker line with increased concentration of added fluoride. (a) 439 ppm (b) 2195 ppm (c) 4390 ppm (d) 6585 ppm.

In LIBS, atomic emission intensity is used for analysis and quantification. From equation 10 a plot of Intensity as a function of the concentration yields a calibration curve. If the dependence on the LIBS signal intensity is linear, then one can determine an unknown concentration within the linear region of the calibration curve at any LIBS signal if the same experimental conditions (time delay, laser energy, collecting fiber optics and incidence focusing distance, target rotation speed, atmospheric pressure) are maintained and the unknown concentration is within the dynamic range of the curve. To Quantity the fluoride concentration levels in the toothpaste samples, the spectrometer was adjusted to a center wavelength of 731.1 nm, and spectra recorded for all the calibration standards. The intensities corresponding to each calibration standard were measured using origin 8.0 software and calibration curve was established by plotting Intensity

(arb.units) as a function of the concentration of fluoride in the units of parts per million (ppm). The intensity of the spectral line FI 731.1 nm was observed to increase linearly with increasing fluoride concentration (ppm) and the linear concentration plot is depicted in Figure 4.25.

To evaluate the sensitivity of our detection system a limit of detection (LOD) was estimated using the calibration data [161] and equation 14. The LOD for our LIBS system is 156 ppm as shown clearly in Table 4 – 6.

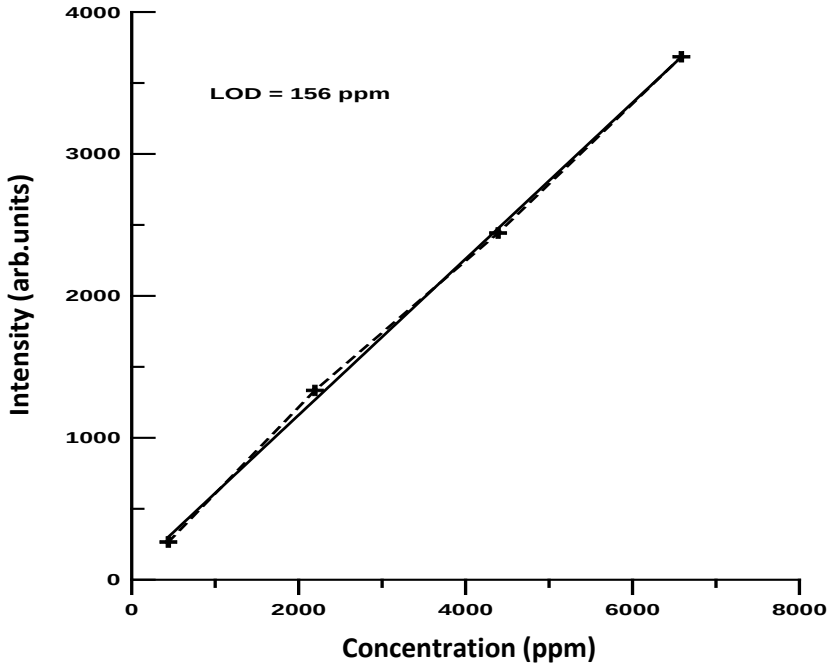

Figure 4. 25: Calibration curve with intensities of LIBS signal of FI (731.102 nm) vs fluoride concentration sample #1.

Table 4 - 6 Concentration levels of fluoride present in the tooth paste samples.

Element	Wavelength (nm)	Transition	Concentration (ppm)			LOD (ppm)
			Sample #1	Sample #2	Sample #3	
Fluorine	731.102	$2s^2 2p^4$ (^{3}P) 3s to $2s^2 2p^4$ (^{3}P) 3p	1723	1472	1315	156

4.2.2 Detection of carcinogenic chromium (Cr) in Synthetic Hair dyes using a Marker line of 427.5 nm

4.2.2.1 Introduction

Hair dyes are widely used as cosmetics to change hair color and improve appearance mostly by women all over world, therefore play an important role in the quality of our lives [162]. However, heavy metals such as chromium, cadmium and arsenic are common contaminants in synthetic hair dyes as color additives [163, 164].These toxic metals damage body organs, disrupt the nervous system and have adverse negative effects on metabolism. [165]. Chromium enters the body through dermal, gastrointestinal and inhalation exposure. Toxicity of chromium causes mutations and chromosomal damage in human cells [164, 166]. Due to its corrosive and reactive nature, it causes lung, nasal and gastrointestinal cancer in addition to allergic eczematous dermatitis. Prolonged exposure to chromium has adverse systemic effects such as damaging the kidney, liver and blood forming organs [167-172]. Considering the extent and frequency of contact of the dyes with the permeable human skin, hair dyes and their ingredients penetrate into the body and therefore are deemed hazardous to humans' health. The safe maximum permissible limit for chromium is 1ppm [173-174]. Hence control and easy detection of toxic metals in hair dyes is of practical significance.

To detect toxic metals in various cosmetic products, methods such as Hg-based stripping voltammetric analysis, Screen printed silver electrode technique, chromatography methods and atomic absorption spectrometry which are time consuming, expensive, laborious and require a lot of sample preparations have been extensively used by researchers [175-179]. On the contrary, Laser Induced Breakdown Spectroscopy (LIBS) is a far superior technique as compared to the

conventional methods in that it is cheap, little or no sample preparation is required, enables fast and rapid analysis.

In this chapter, we have developed a laser induced breakdown spectrometer for detection and quantification of chromium concentration levels in synthetic hair dyes available on the local market. In order to achieve the best limit of detection by maximizing signal intensity and at the same time reducing the signal to noise ratio of the LIBS system, vital parameters that affect the sensitivity of the LIBS system such as time/gate delay, laser fluence and sampling geometry were optimized. The choice of these parameters was validated using the Mcwhirter criterion which proved that the laser induced plasma (LIP) generated by our LIBS system was optically thin and in local thermodynamic equilibrium (LTE) a condition which is very fundamental and must be satisfied in (LIBS) applications. Prior to this temperature of the plasma (T) and electron density (n_e) were obtained using the Boltzmann plot and Stark broadening respectively. This study will be important to provide baseline data that will help to determine the levels of chromium toxicity of hair dyes and other related cosmetic products.

4.2.2.2 LIBS spectra for synthetic hair dye samples

Considering the spectrometer parameters mentioned earlier in the text, spectra were recorded in the wavelength range of 200 – 600 nm as shown in Figures 4.28 – 4.31. NIST data base was used to identify all the spectral lines in the spectra and elements such as iron (Fe), copper (Cu), sodium (Na), zinc (Zn), titanium (Ti), calcium (Ca), silicon (Si), potassium (K) and chromium (Cr) were detected by our LIBS system. Four strongly intense and persistent atomic transitions of chromium (Cr) were identified in the spectrum which indicates the presence of chromium in the synthetic hair dye as shown clearly in Figure 4.30. However, the chromium (Cr) atomic transition at wavelength 425.7 nm was selected as the spectral marker line for detection and quantification of Chromium (Cr) in all the synthetic hair dye samples because it is isolated, free from interference with other spectral lines in the spectra and it does not involve the ground state that is, it is not a resonance line and therefore free from self absorption.

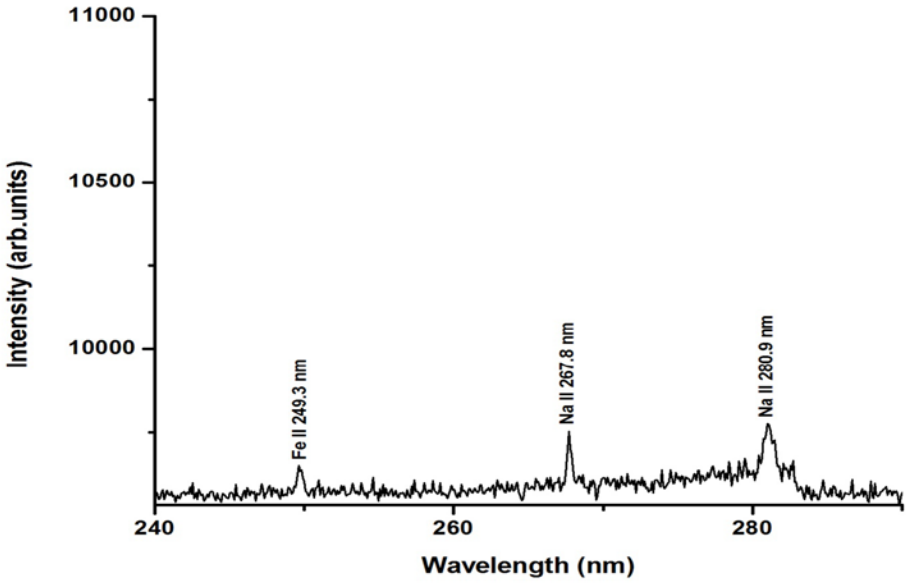

Figure 4. 26: Typical LIBS spectrum in 300- 400 nm wavelength range for sample #1.

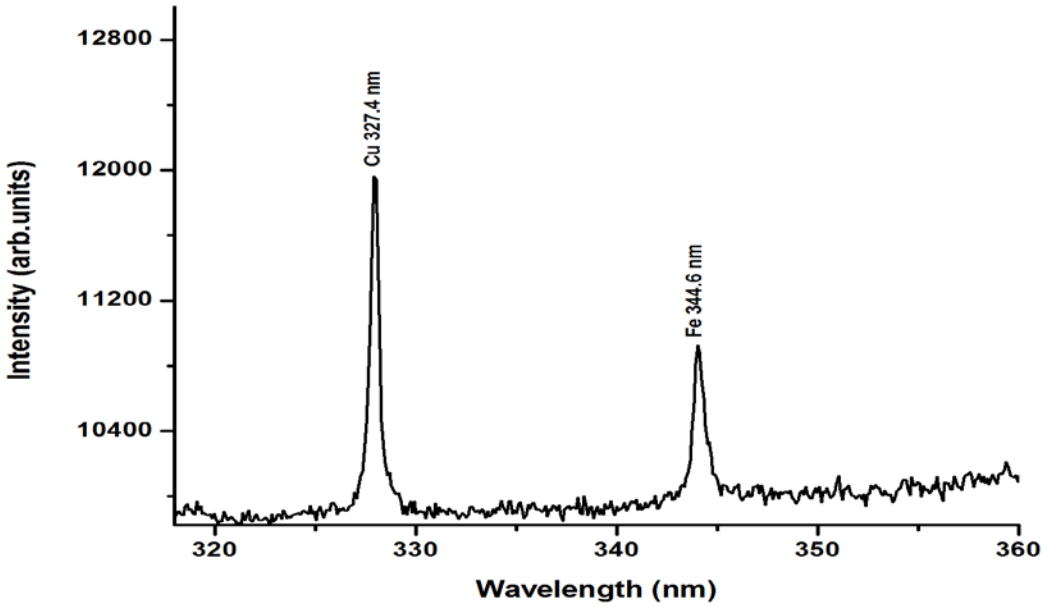

Figure 4. 27: Typical LIBS spectrum in 300- 400 nm wavelength range for synthetic hair dye sample #1.

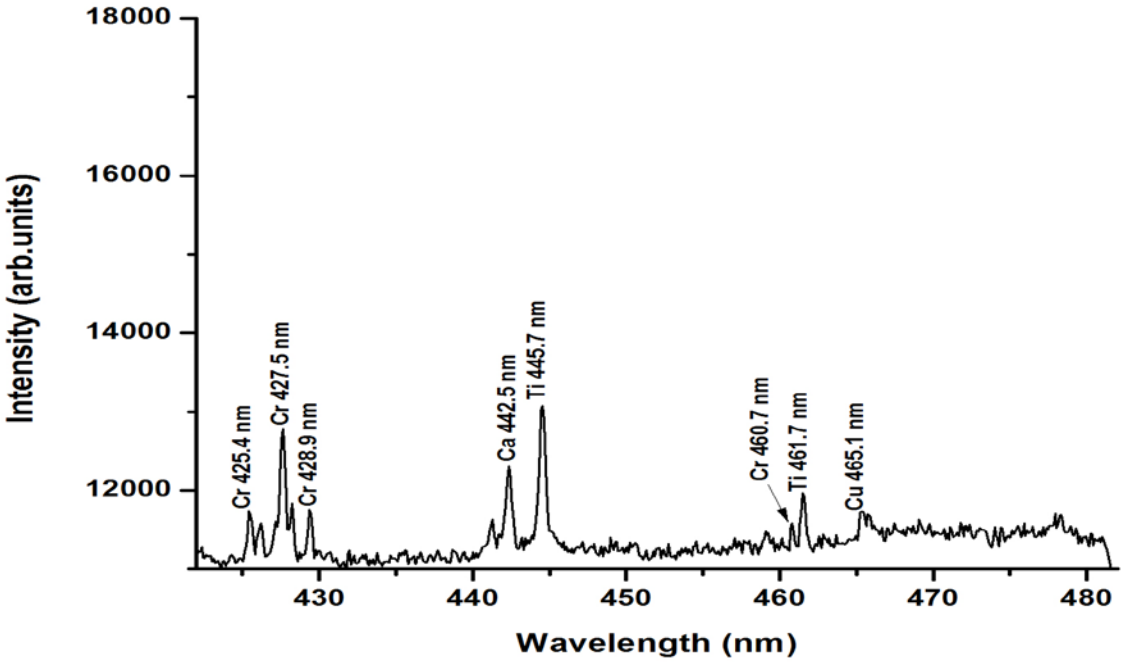

Figure 4. 28: Typical LIBS spectrum in 400- 500 nm wavelength range for synthetic hair dye sample #1.

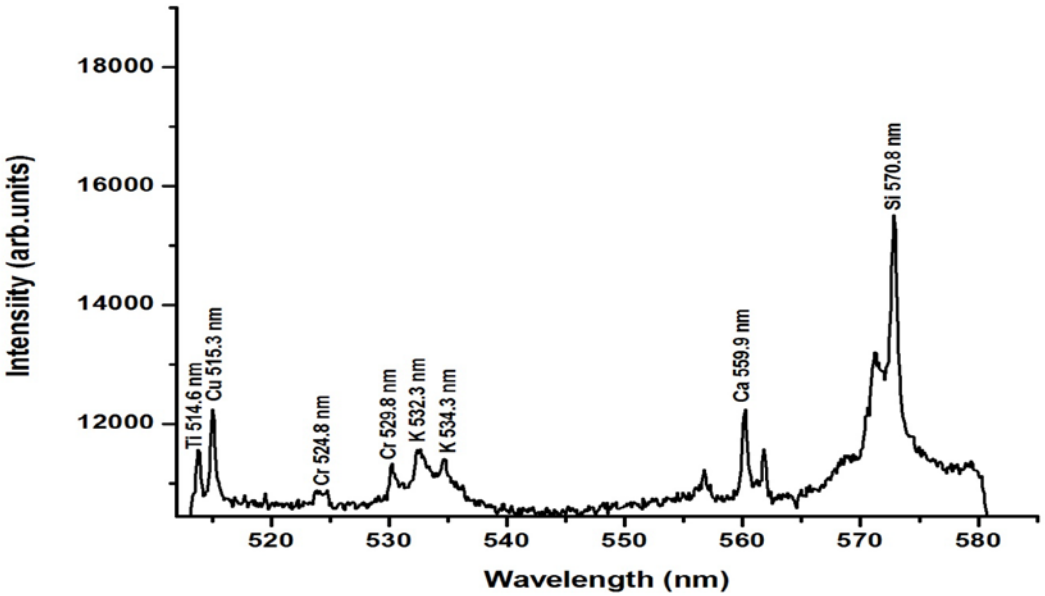

Figure 4. 29: Typical LIBS spectrum in 500- 600 nm wavelength range for synthetic hair dye sample #1.

4.2.2.3 Time/gate delay optimization for synthetic hair dye samples

At the early stages of plasma formation that's for time delay < 400 ns, the typical LIBS spectrum consists of basically a continuum (background noise) which is due to blackbody radiation of the plasma and elastic collisions of electrons with the ionic species (Bremsstralung). Concurrently, broadened ionic and weak atomic lines are superimposed on the continuum and often overlap. After some appropriate time the plasma expands and cools down. As a consequence, the atomic lines used for spectroscopy become stronger and dominant [49]. Hence the delay between the laser pulse trigger and acquisition of the spectrum has to be optimized in order to minimize the background noise and maximize the intensity of the emission line of interest. Spectrometer parameters mentioned earlier in the text were used to obtain intensities of the spectral marker line (Cr 427.5 nm) for different time/gate delays in the range of 600 – 1000 ns. From Figure 4.30, the intensity increases, reaches a maximum of 800 ns and then drops. Hence 800 ns was selected as the optimum time/gate delay. It's worth noting that optimum time/gate delay depends

on the transitional probability and the energy of the upper level of the analytical spectral line. Therefore different elements have different and unique intensity temporal evolutions.

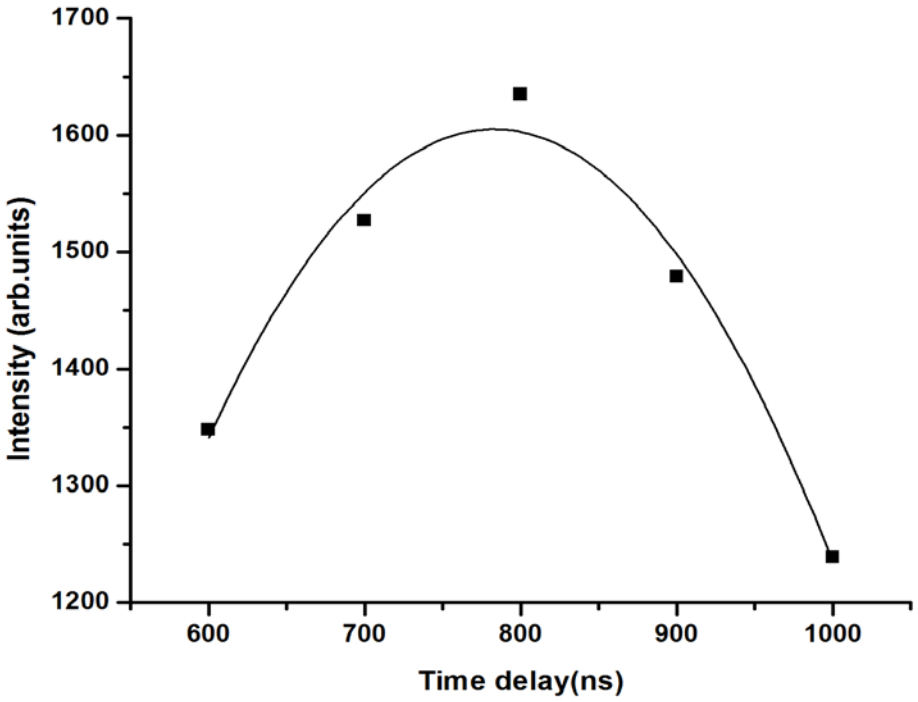

Figure 4. 30: Emission intensity of spectral line CrI at 427.5 nm as a function of gate/time delay for synthetic hair dye sample #1.

4.2.2.4 Laser energy optimization for synthetic hair dye samples

The incident laser fluence is an important parameter in plasma generation and plays a vital role in the sensitivity of the LIBS system due to the fact that it is proportional to the emission intensity of an analyte when the plasma is optically thin. The emission intensity as a function of laser fluence for the spectral marker line (Cr 427.5 nm) using the optimal time/gate delay (time between the laser trigger and acquisition of the spectrum) of 800 ns was studied in order to optimize the LIBS signal intensity. From Figure 4.31, the intensity initially increases linearly with the incident laser fluence. This phenomenon is attributed to the increase in the amount of ablated material and to the increase in the electron temperature. For laser fluence values higher

than 24 Jcm^{-2}, the emission intensity reaches saturation, mainly due to the absorption of the laser beam by the plasma formed in front of the target of the sample a process known as plasma shielding. Also self absorption can be used to account for this effect. Hence 24 Jcm^{-2} is the optimum laser fluence for our LIBS system. It's worth noting that the most prominent mechanism responsible for the plasma absorption at such high laser fluence is inverse bremsstralung whereby a free electron absorbs a laser photon. However the saturation can also be explained by assuming the formation of a self regulating regime near the target surface at such higher laser fluence levels [180]. In this case laser photon absorption by the plasma becomes higher when its temperature decreases and therefore, evaporation of the species from the surface of the material becomes less which in turn decreases the density of the ionic species. This behavior as a result increases the absorption of the laser photons by the plasma hence increasing the temperature of the plasma. On the other hand, when the absorption of the laser energy is less, the process is reversed. It has also been theoretically proved that the density and temperature of the plume adjust in such a manner that the plasma absorbs the same amount of laser radiation to maintain a self regulating regime [49].

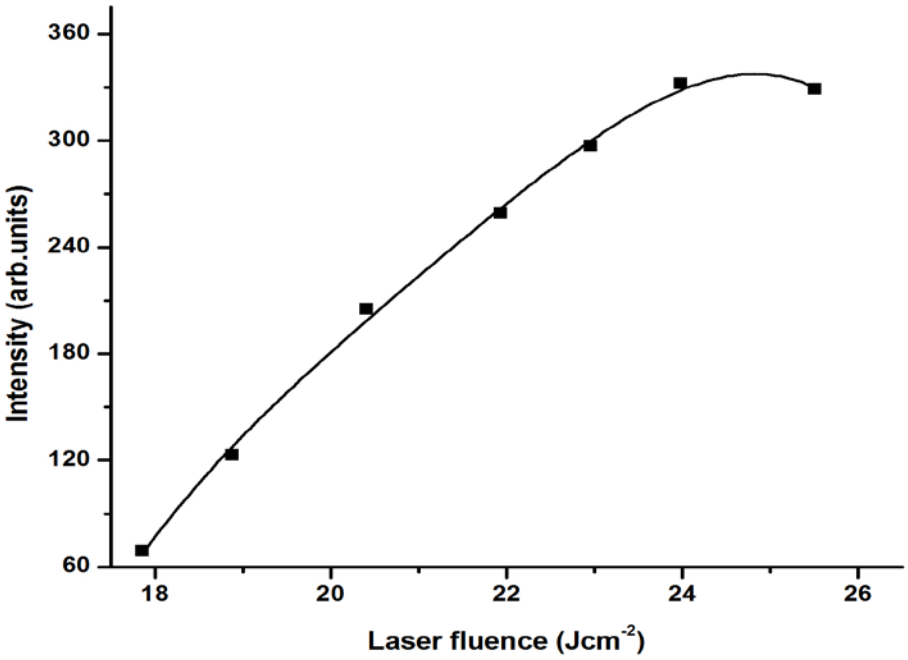

Figure 4. 31: Emission intensity of spectral line CrI at 427.5 nm as a function of laser fluence for synthetic hair dye sample #1

4.2.2.5 Local Thermodynamic Equilibrium Condition for synthetic hair dye samples

In order to calibrate a LIBS system using spectral line intensities, the laser Induced Plasma (LIP) should be optically thin (re-absorption and absorption of the incident radiation by the plasma is negligible) and in local thermodynamic equilibrium (LTE). In a transient system such as plasma produced in LIBS, the LTE condition holds if the free electrons in the plasma have a Maxwellian distribution. It's worth mentioning that the electron velocity distribution for a relatively dense plasma with a low temperature ($n_e > 10^{16}$ cm^{-3}, $kT < 5$ eV), is nearly always Maxwellian [160]. Also, collision, excitation and de-excitation processes should dominate over the radiative processes for the LTE condition to be valid. In our study plasma was generated using all the optimum parameters achieved and in order ascertain that such plasma was optically thin and in local thermodynamic equilibrium, the Mcwhirter criterion of minimum density condition for

plasma to be optically thin and in Local thermodynamic equilibrium was used as given in equation 7.

In this case plasma temperature (T) and electron density (n_e) were explicitly determined using the Boltzmann plot and Stark broadening respectively. For optically thin plasma in LTE, its temperature is obtained using equation 11.

A plot of magnitude of the component on the left of equation 11 as a function of the value for the upper energy levels (E_k) for the spectral lines under consideration yields a Boltzmann plot which is used to determine the temperature of the plasma. The main sources of error when using equation 11 arise from using inaccurate values of $A_{ki,}$ imprecision in the recorded intensities or choosing transitions having upper levels with a small energy difference [181, 51]. However the use of logarithmic relations significantly reduces the error. In our experiment the plasma temperature was estimated using the atomic emission line intensities of chromium (Cr) observed in the laser induced plasma. It is worth noting that the spectral lines selected were in close spectral proximity, well resolved, strongly intense, with well known transitional probabilities and upper energy levels. The required parameters for the Boltzmann plot as obtained from NIST data base and Griem [18, 51] are summarized in Table 4-7. Figure 4.34 shows the Boltzmann plot on which data was fitted with the least-square approximation and the slope of the plotted curve yielded a plasma temperature *(T)* of 5286 ± 850 K.

Table 4 - 7: Spectroscopic data for chromium spectral lines [18, 51]

Wavelength (nm)	g_k	A_{ik} (s^{-1})	E_k (eV)
425.433	9	3.15E+07	2.913
427.481	7	3.07E+06	2.899
428.973	5	3.16E+07	2.889
460.742	7	2.5E+06	3.698

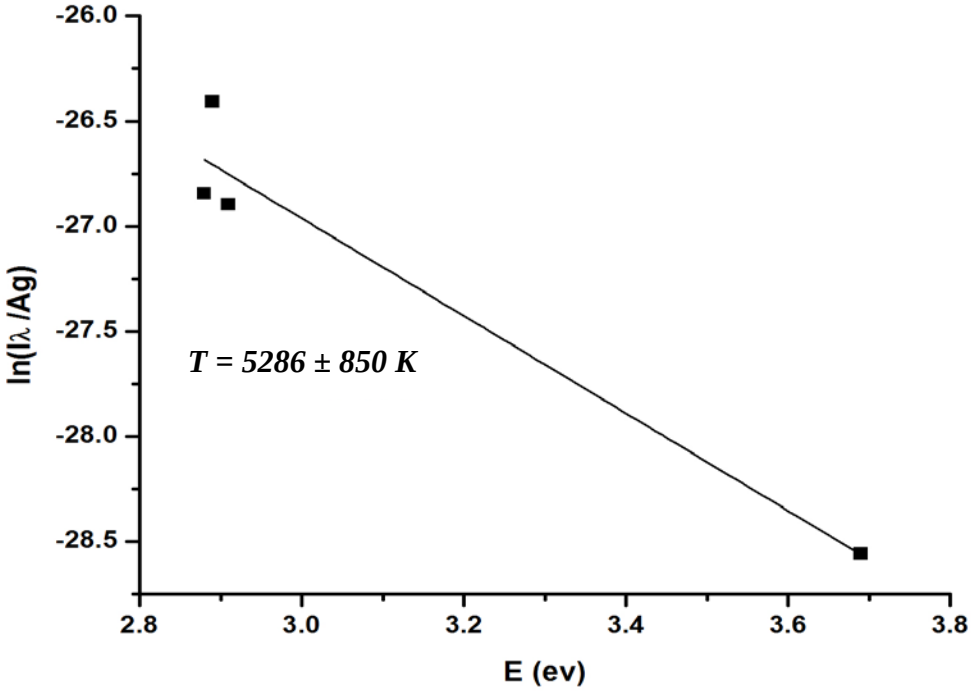

Figure 4. 32: Boltzmann plot for plasma temperature determination of the synthetic hair dye plasma using sample # 1.

In a laser induced plasma, a spectral line is broadened due to Stark, Doppler, Instrumental and Natural broadening mechanisms. In our case instrumental broadening was minimized by setting the detection system at its maximum resolution. It's worth mentioning that in a low temperature, high density plasma generated in our study, stark broadening is dominant therefore was used to estimate the electron density by determining the full width at half maximum (FWHM) of the broadened profile for the chromium atomic transition spectral line at a wavelength of 427.5 nm. Stark broadening is due to collisions of the electrons with charged species resulting in both broadening of the line and shifting in the peak wavelength [141- 144]. A stark broadened profile is described by a Lorentzian function and equation 13 relates its FWHM with the electron density. To estimate the electron density of the plasma, the line profile for chromium atomic spectral transition at 427.5 nm was used as shown in Figure 4.35.The data points were fitted with a lorentzian fit using origin 8.0 software to yield a profile with a FWHM of 0.412 nm. The electron impact parameter *w* is obtained from Griem [51] and therefore electron density is 1.68 X 10^{18} cm^{-3}.

In our case the electron density determined using a gate/time delay and laser fluence of 800 ns and 24 Jcm^{-2} respectively as the optimal values is 1.68 X 10^{18} $cm^{-3.}$ Implying that $n_e \sim 10^{18}$ cm^{-3} and $kT \sim 0.56$ eV which explicitly justifies that the free electron velocity is Maxwellian. Also the estimated minimum electron density is 1.98 X 10^{17} cm^{-3} which is lower than the actual electron density, hence the plasma generated by our LIBS system is optically thin and in LTE.

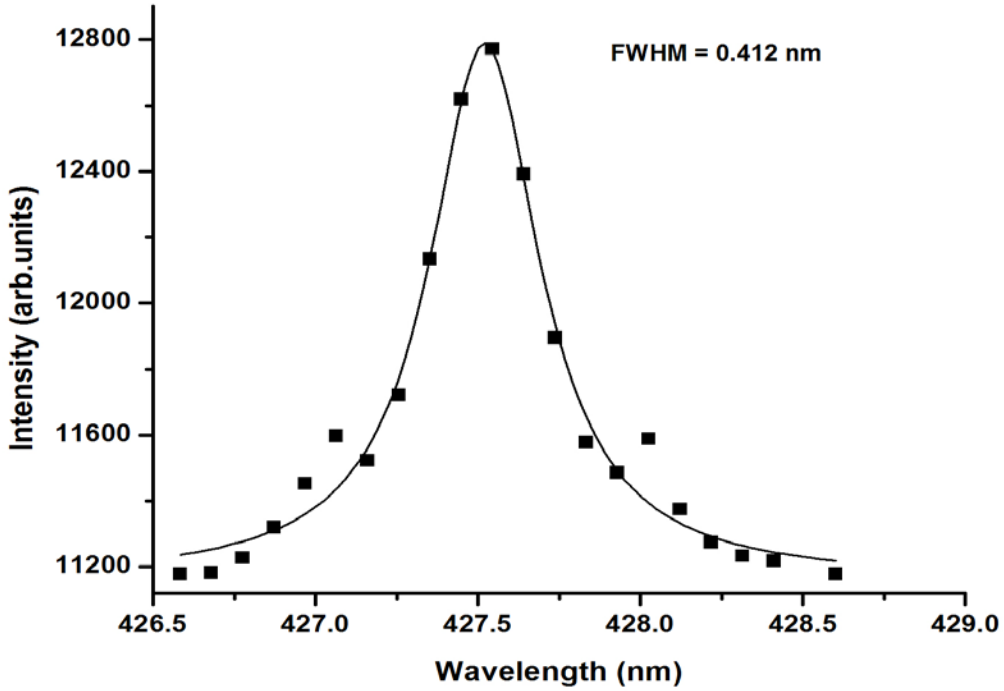

Figure 4. 33: Lorenztian fit for CrI at 427.5 nm for time/gate delay and laser fluence of 800 ns and 24 Jcm^{-2} respectively using synthetic hair dye sample #1.

4.2.2.6 Detection of chromium levels in synthetic hair dyes

In this case, the optimum experimental parameters discussed previously which yield maximum LIBS signal intensity and a good signal to noise ratio were used. To further consolidate on the presence of chromium in the synthetic hair dye, pellets of different chromium concentrations in parts per million (ppm) were prepared by mixing the base matrix with chromium (II) sulphate and analyzed using our LIBS system. The spectrometer was adjusted to a center wavelength of 427.5 nm and spectra recorded for the different chromium concentrations. It was observed that the intensity of the neutral atomic spectral line for chromium (CrI) at a wavelength of 427.5 nm grows consistently at the same spectral position with increase in the concentration of chromium as depicted in Figure 4.36. This strongly confirms the presence of chromium (Cr) in the synthetic hair dye.

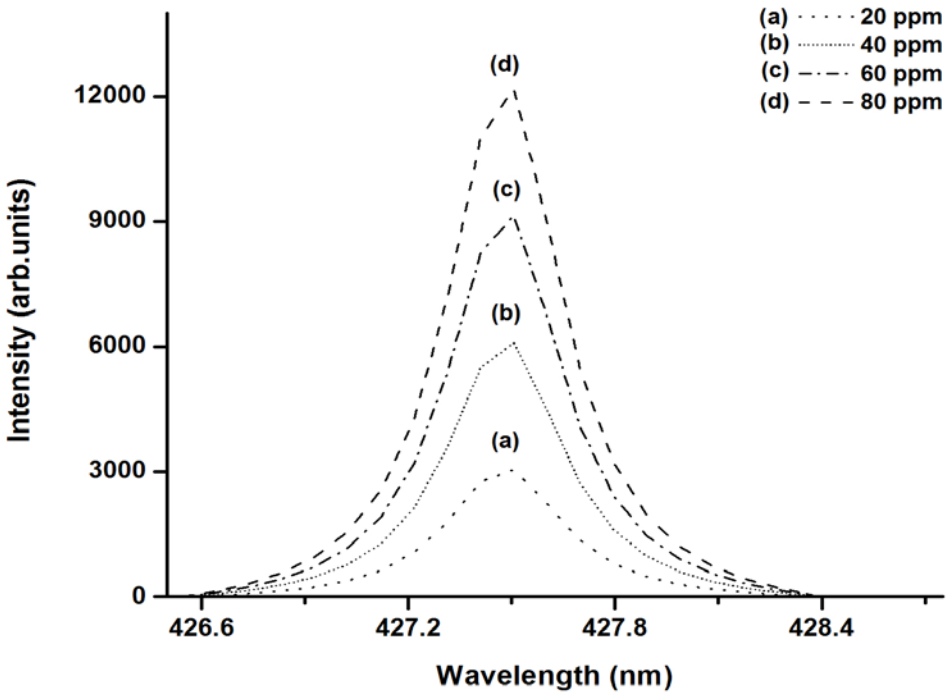

Figure 4. 34: Intensities of the spectral line (Cr 427.5 nm) for different chromium concentrations in synthetic hair dye sample #1.

In LIBS, atomic emission intensity of a spectral line is used for analysis and quantification of a particular element in any given sample. From equation 10 a plot of Intensity as a function of concentration of chromium (Cr) yields a calibration curve. If the curve is linear then one can determine an unknown concentration of an analyte at any intensity provided the analyte concentration exists within the dynamic range of the curve and the same experimental conditions are observed. The LIBS detection system was calibrated in order to quantify the concentration of chromium present in the synthetic hair dye samples using the chromium calibration standards. To validate the homogeneity of the stoichiometric samples, measurements were made at several different points on the surface of the samples. To further enhance the precision, a few laser shots

were applied on the surface of the sample prior to the actual measurements and to eliminate the effect of laser pulse fluctuation during the analysis, the laser was allowed sufficient time to stabilize. The spectrometer was then adjusted to a center wavelength of 427.5 nm and the LIBS spectra for all the stoichiometric samples were obtained. Intensities corresponding to the atomic transition line 427.5 nm for each sample were recorded and a linear calibration curve established by plotting the Intensity (arb.units) as a function of concentration (ppm) as illustrated in Figure 4.37. Considering the experimental optimal conditions as mentioned before in the text, typical LIBS spectra for all the synthetic hair dye samples were recorded in the wavelength range of 426 - 444 nm as depicted in Figure 4.38 and the intensities corresponding to the chromium (Cr) atomic transition spectral marker line of wavelength 427.5 nm recorded which were used to estimate the chromium concentration levels in the synthetic hair dye samples. The concentrations measured by our LIBS system are in the range of 5-11 ppm which is above 1 ppm set by the Environmental agency and other regulatory authorities [182].

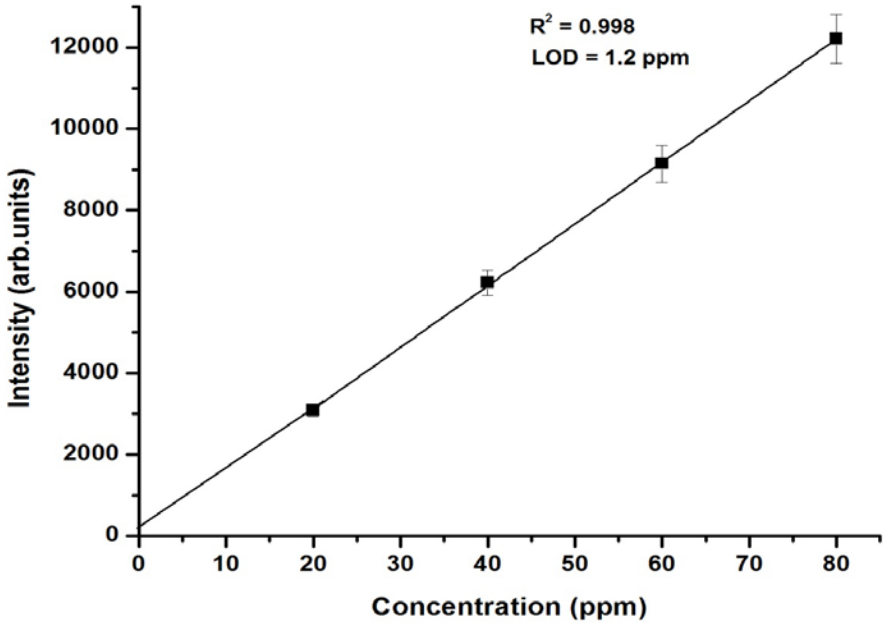

Figure 4. 35: Calibration curve for chromium (Cr) in the synthetic hair dye with intensities (arb.units) vs. Concentration of chromium (ppm).

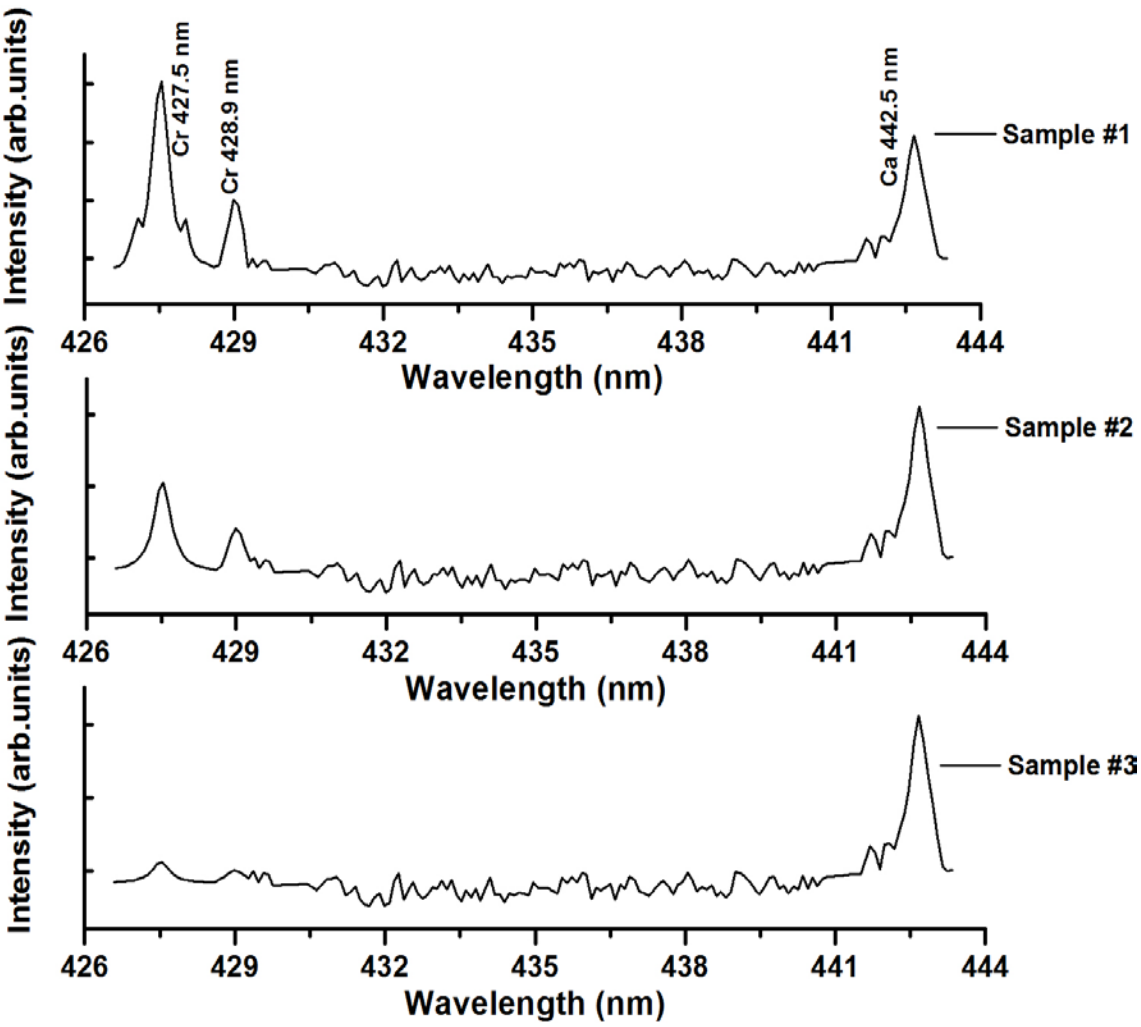

Figure 4. 36: Typical spectra showing chromium levels in all synthetic hair dye samples analyzed using LIBS

These LIBS results were counter verified using ICP spectrometry and both measurements were in agreement as shown in Table 4- 8. This work clearly demonstrates that LIBS can be applied for online rapid analysis of toxic elements in cosmetic products.

To evaluate the sensitivity of the LIBS detection system, the limit of detection (LOD) was determined. It is the lowest amount of concentration of chromium (Cr) that can be reliably detected by our LIBS system. The LOD was estimated using the calibration data and equation 14 and it is 1.2 ppm.

The R.S.D value of the measurements obtained by our LIBS system was estimated using equation 16 and it decreased with respect to the number of accumulations but no improvement was observed after 20 accumulations. It is worth mentioning that typical values of R.S.D for LIBS are in the range of (1-10%) [183] and in our case the R.S.D value was 1.6 % hence highly repeatable and reproducible results were obtained.

Accuracy of the LIBS system was evaluated using equation 17. The residual error was calculated between the values obtained using the LIBS system and ICP spectrometry. Both values are comparable yielding a residual error in the range of 0.12 – 0.40 which is acceptable for any good analytical system.

Table 4 - 8: Concentrations levels of chromium present in the synthetic hair dye samples

Element	Wavelength (nm)	Transition	Concentration (ppm)						LOD (ppm) for LIBS
			Sample #1		Sample #2		Sample #3		
			LIBS	ICP	LIBS	ICP	LIBS	ICP	
Chromium	427.4	$3d^5(^6S)4s$ to $3d^5(^6S)4p$	11	9.8	9	8.1	5	4.6	1.2

4.2.3 Detection of Lead (Pb) and Chromium (Cr) in commercially available Kohl

4.2.3.1 Introduction

Kohl is widely used in the Middle East, Asia and North Africa for cosmetic and medicinal purposes. It is applied on the conjunctive eyelid surface for beautification and most notably by the Bedouins from the remote areas in the Arab peninsula to make permanent signs on their faces [184]. On the other hand it is as an umbilical stump remedy and also used after circumcision to stop bleeding as a hygienic precaution. Traditionally it is used to relieve eyestrain, pain, soreness and prevention of sun glare. Also kohl is regarded as a very precious gift during the pilgrimage season hence widely used [185].

Previous studies have revealed that kohl contains toxic metals [186-188]. Chemical analysis show that the main component of kohl stone is galena (PbS) having lead a toxic metal as one of its constituents [189]. Other toxic metals such as chromium are used in cosmetic products as color pigments due to their inherent color properties [189]. These hazardous metals enter the body through inhalation, ingestion and skin exposure [190]. Infants under the age of six may be exposed due to their usual mouth-hand activity and high efficiency of lead absorption by gastrointestinal tracts [191]. Chronic low dose of lead leads to renal tubular injury in children, hypertension in adults, is hazardous to women in the first trimester of their pregnancies and causes undesirable changes in the development of the retina of unborn babies resulting into visual system defects in the future [192-194]. Lead exposure affects a developing brain and the nervous system, results into behavioral disorders, impaired hearings and stunted growth [195]. Exposure to chromium causes respiratory irritation, cancer, liver damage and pulmonary congestion [161]. It is worth mentioning that the safe maximum permissible limits for lead and chromium are 0.5ppm and 1ppm respectively [196].

Several techniques have been used to study the chemical composition of cosmetic products recently. Energy dispersive X-ray fluorescence spectrometer which is basically capable of only qualitative analysis [189], Atomic absorption spectrometer that is time consuming and contamination of the samples is highly probable [185]. Neutron Activation Analysis is a widely used non destructive technique to detect trace elements in samples but restricted by half lives and cross sections of the isotopes. For that reason lead is not detected in a galena sample which contains more than 80% of this element [185].

LIBS has been used to determine elemental composition and lead levels of different kinds of kohl stones [197]. However no studies have been done on the already made cosmetic eyeliners which have a lot of elements concocted with galena (base material) as supplements during the manufacturing processes which can be hazardous to human. Due to the afore suggested potential health effects of toxic metals on human health, in this section LIBS has been used to detect and quantify levels of lead and chromium in commercially available kohl eyeliners which are frequently used by people across the entire globe. Vital parameters such as gate/time delay and laser fluence have been optimized in order to improve on the signal to noise ratio and at the same time obtain the maximum LIBS signal possible so as to achieve the best Limit of detection.

4.2.3.2 LIBS Spectra for kohl samples

Considering the spectrometer parameters mentioned previously in the text, typical LIBS spectra were recorded in the wavelength range of 200 – 800 nm as clearly depicted in Figures 4.37 – 4.42. Spectral data published by NIST was used to identify all the spectral lines in the spectra and elements such as iron (Fe), copper (Cu), sodium (Na) ,zinc (Zn), titanium (Ti), calcium (Ca), phosphorous (P), silicon (Si) potassium (K), chromium(Cr), lead (Pb) were detected by the LIBS system. To detect and estimate the concentration levels of lead (Pb) and chromium (Cr), neutral atomic transitions at wave lengths 405.7 nm and 425.4 nm were selected as the spectral marker lines respectively due to the fact that they were strongly intense, isolated and do not involve the ground state.

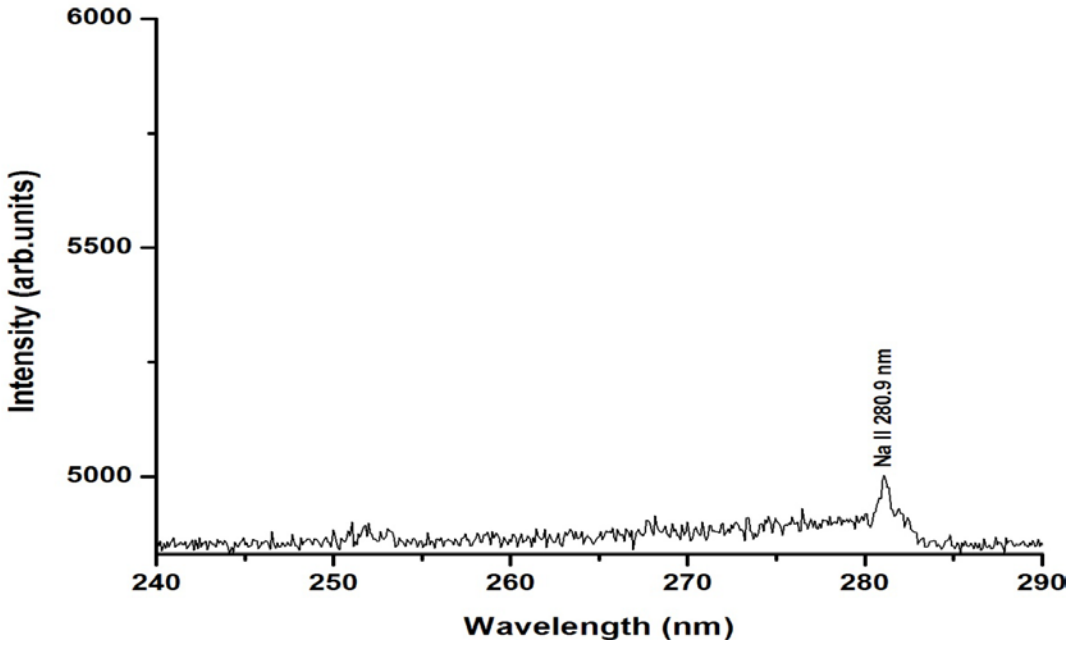

Figure 4. 37: Typical LIBS spectrum in the wavelength region of 200 – 300 nm for sample #1.

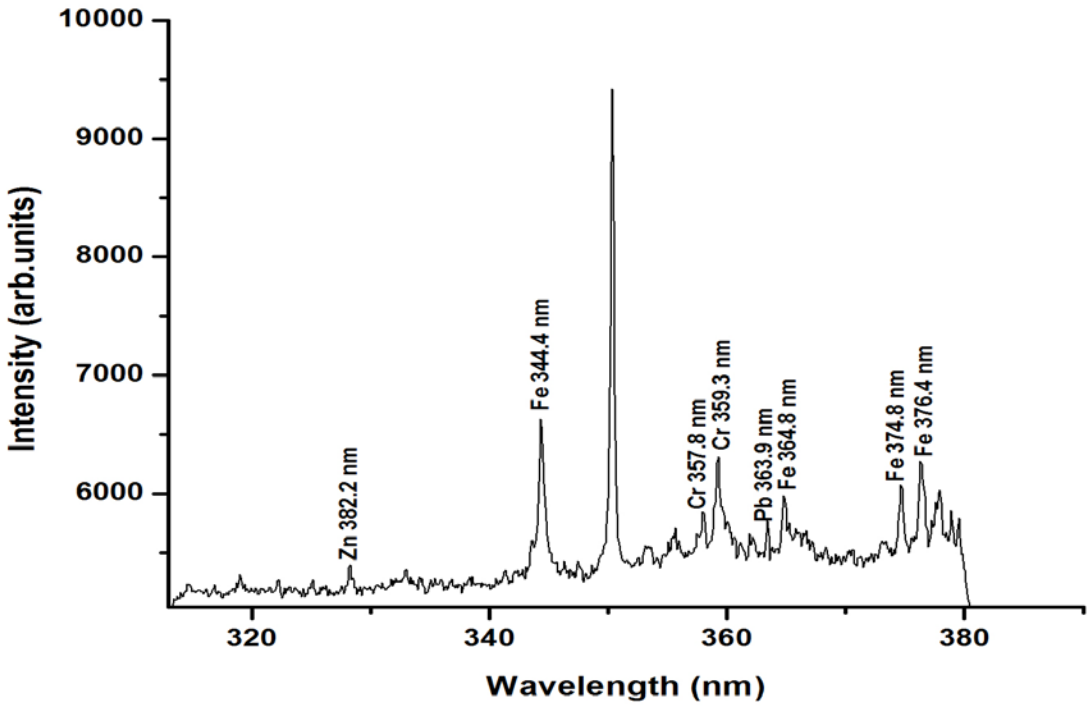

Figure 4. 38: Typical LIBS spectrum in the wavelength region of 300 – 400 nm for kohl sample #1.

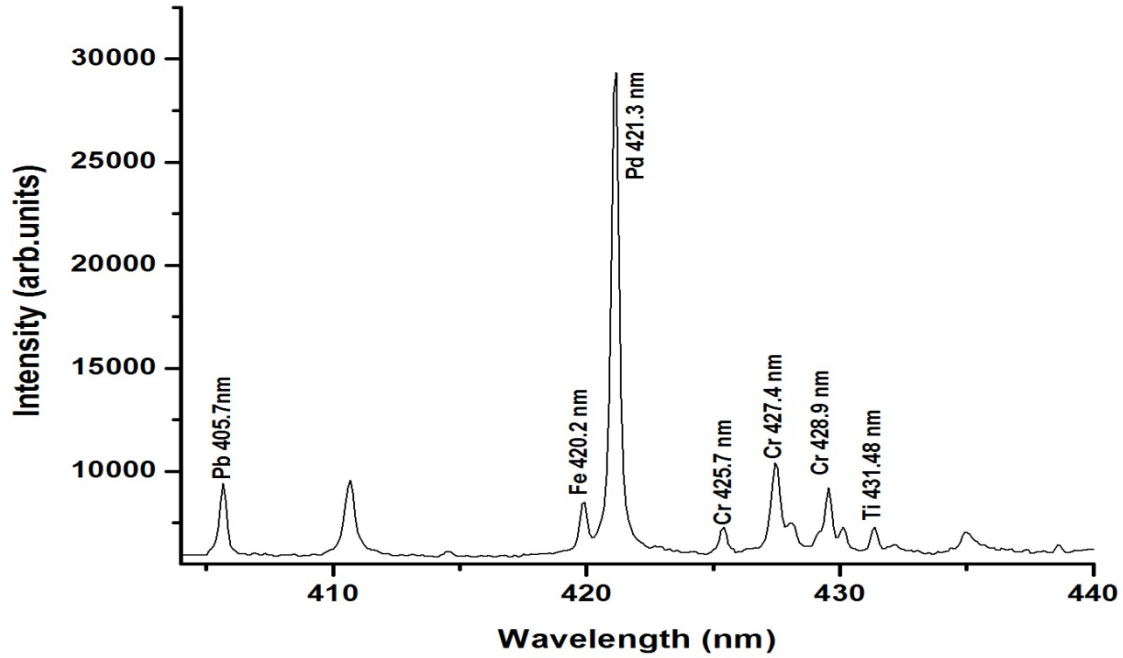

Figure 4. 39: Typical LIBS spectrum in the wavelength region of 400 – 500 nm for kohl sample # 1.

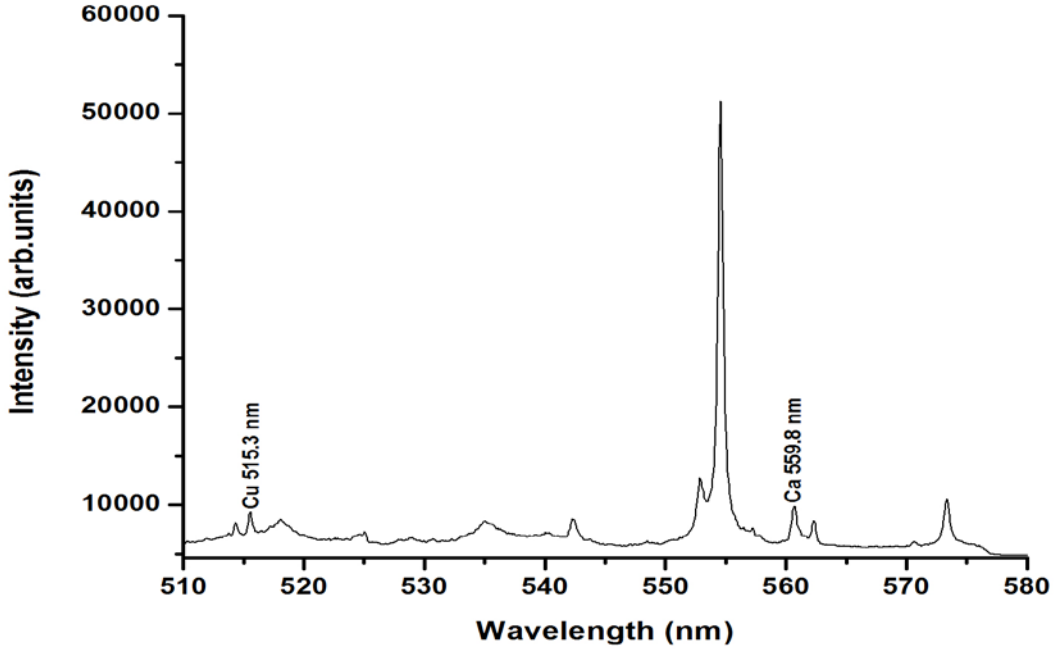

Figure 4. 40: Typical LIBS spectrum in the wavelength region of 500 – 600 nm for kohl sample # 1.

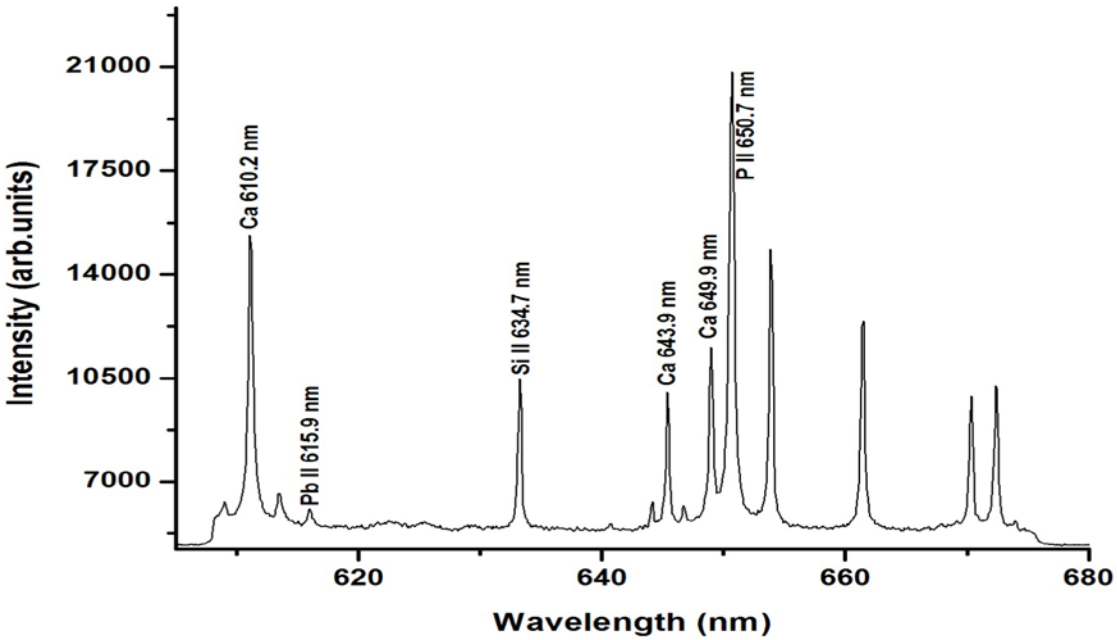

Figure 4. 41: Typical LIBS spectrum in the wavelength region of 600 – 700 nm for kohl sample # 1.

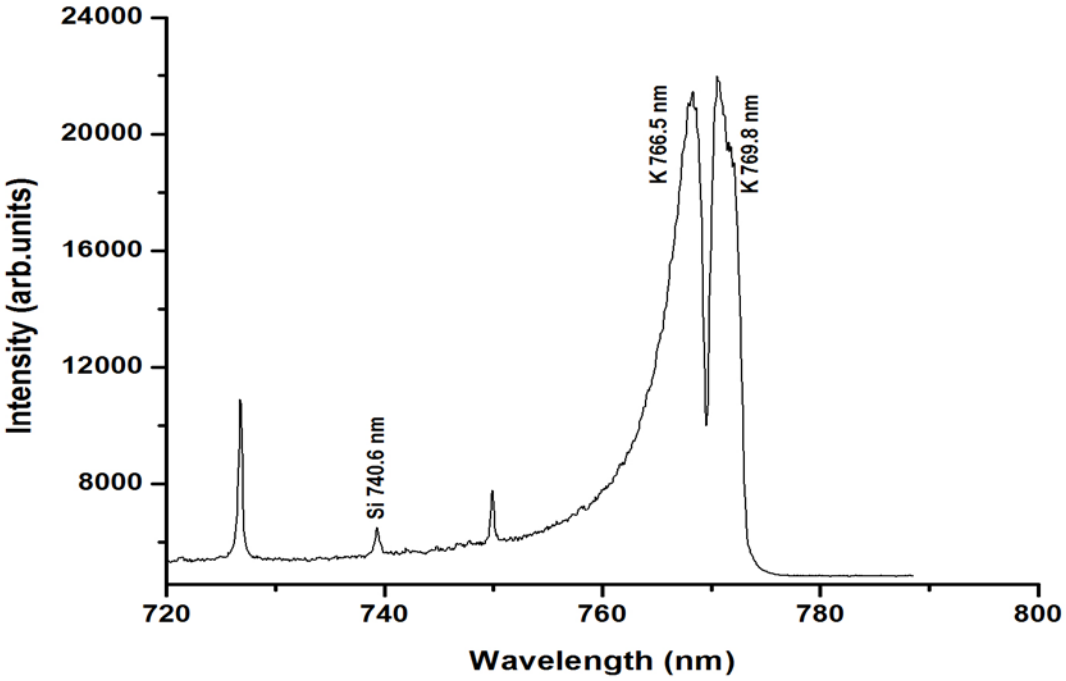

Figure 4. 42: Typical LIBS spectrum in the wavelength region of 700 – 800 nm for kohl sample # 1.

4.2.3.3 Time delay optimization for kohl samples

During the early stages of plasma formation, the emitted spectrum is dominated by an intense continuum which is due to collisions of electrons with atoms and ions (free-free emission) and recombination of electrons with ions (free-bond emission). At the same time relatively weak atomic spectral lines are superimposed on the continuum and often overlap with the ionic lines hence cannot be isolated and measured effectively [198]. In this case time delay optimization becomes very necessary in order to achieve a good signal to noise ratio. However, each spectral line exhibits a different temporal evolution dependent on the element and the atomic energy level. Therefore it's imperative to determine the optimum time delay for each element under consideration. In order to optimize the time/gate delay for detection of lead (Pb), the grating of the spectrometer was centered at a wavelength of 405.7 nm corresponding to the wavelength of

the spectral marker line. The intensity of the spectral line was studied as a function of time delay as depicted in Figure 4.43. For time delay < 400 ns, the spectrum is masked by the continuum and therefore the emission intensities couldn't be measured. However at later times, the continuum rapidly drops as a result of the expansion, cooling of the plasma and its recombination into ground state ions and excited atoms. The ionic lines disappear and the neutral lead line becomes stronger and more intense peaking at 600 ns after which it decays. For chromium detection the grating was centered at 425.4 nm and the intensity of the chromium spectral line studied as a function of time/gate delay, the curve peaks at 800 ns and then decays as observed in Figure 4.44. Therefore 600 ns and 800 ns were selected as the optimal time delays for lead (Pb) and chromium (Cr) detection respectively.

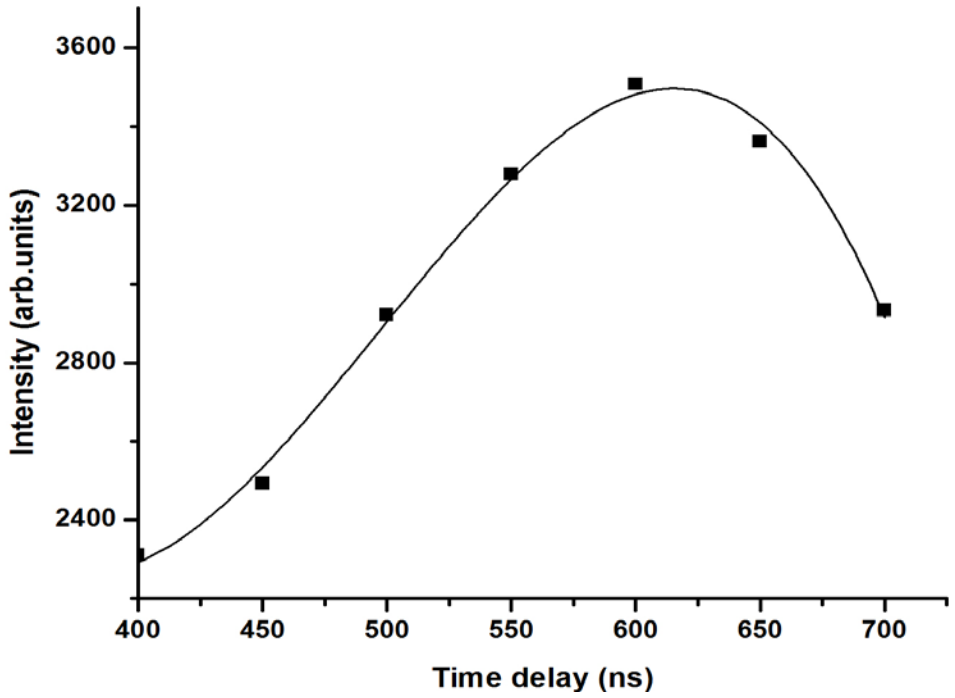

Figure 4. 43: Gate/time delay optimization for PbI at 405.7 nm using kohl sample #1.

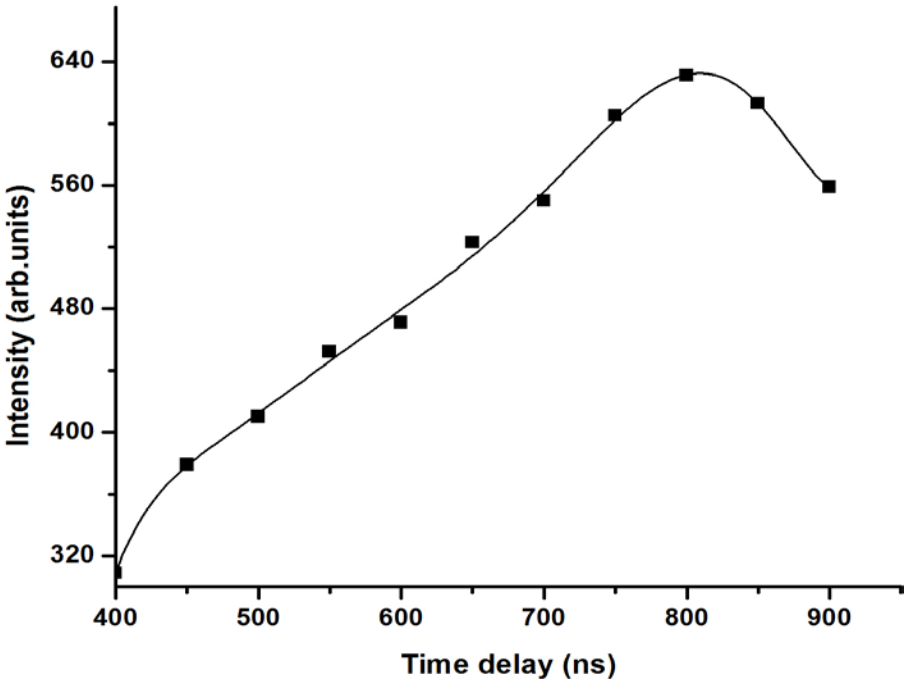

Figure 4. 44: Gate/time delay optimization for Cr I at425.4 nm) using kohl sample #1.

4.2.3.4 Laser energy optimization for kohl samples

The intensity of light emitted by laser produced plasma depends on the number density of the emitting species, degree of excitation/ionization and temperature of the plasma. The number density depends on the total mass ablated by the incident radiation from the surface of the material [141-144]. The vaporized mass produced above the surface of the material is dependent on the absorption of laser radiation by the material which is dependent on the laser fluence (energy). In order to optimize the laser fluence of our LIBS detector, the intensity of the lead (Pb) atomic transition line as a function of laser fluence was studied. The grating of the spectrometer was centered at a wavelength of 405.7 nm and its intensities corresponding to laser fluencies in the range 18-26 Jcm^{-2} obtained. From Figure 4.45, as expected the emission intensity increased with increase in the laser fluence due to the increase in the amount of the ablated material, however beyond 24 J/cm^{-2} a saturation regime is reached which is explicitly confirmed

by the leveling off of the curve. This is due to the absorption of the laser beam by the plasma formed in front of the surface of the material. Hence 24 Jcm^{-2} was identified as the optimum laser fluence for our LIBS system.

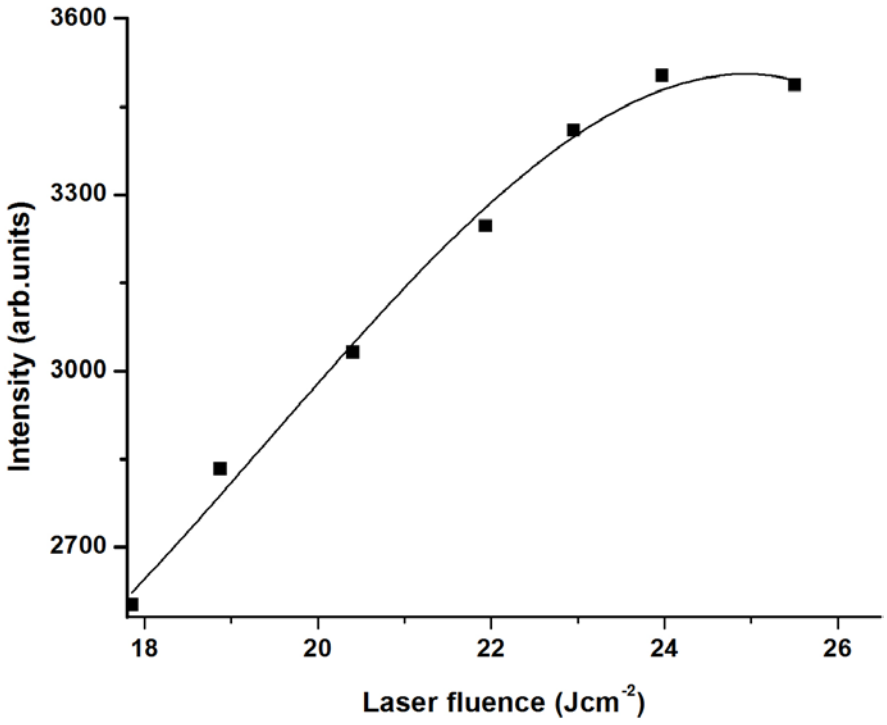

Figure 4. 45: Laser fluence optimization for the LIBS system Pb I at 405.7 nm using kohl sample #1.

4.2.3.5 Detection of chromium (Cr) and lead (Pb) in kohl eyeliners

In this case, the optimum experimental parameters discussed previously were used. To further consolidate on the presence of lead and chromium, samples having relatively different concentrations of lead and chromium in parts per million were prepared appropriately by contaminating the base material (kohl sample #1) with lead sulphate and chromium sulphate respectively. To confirm the presence of lead in the kohl samples, the grating of the spectrometer was adjusted to a center wavelength of 405.7 nm and respective spectra recorded as observed in

Figure 4.46. The intensity of the 405.7 nm lead atomic spectral line grows exactly and consistently at the same spectral position relative to the increase in the concentration of lead hence confirming the presence of lead in the kohl samples. On the other hand to confirm the presence of chromium in the kohl samples, the grating of the spectrometer was adjusted to a center wavelength of 425.4 nm chromium atomic transition and all the spectra of the respective samples recorded as depicted in Figure 4.47, the spectral line grows consistently and exactly at the same spot with respect to the increase in concentration of chromium. This confirms the presence of chromium in the kohl sample.

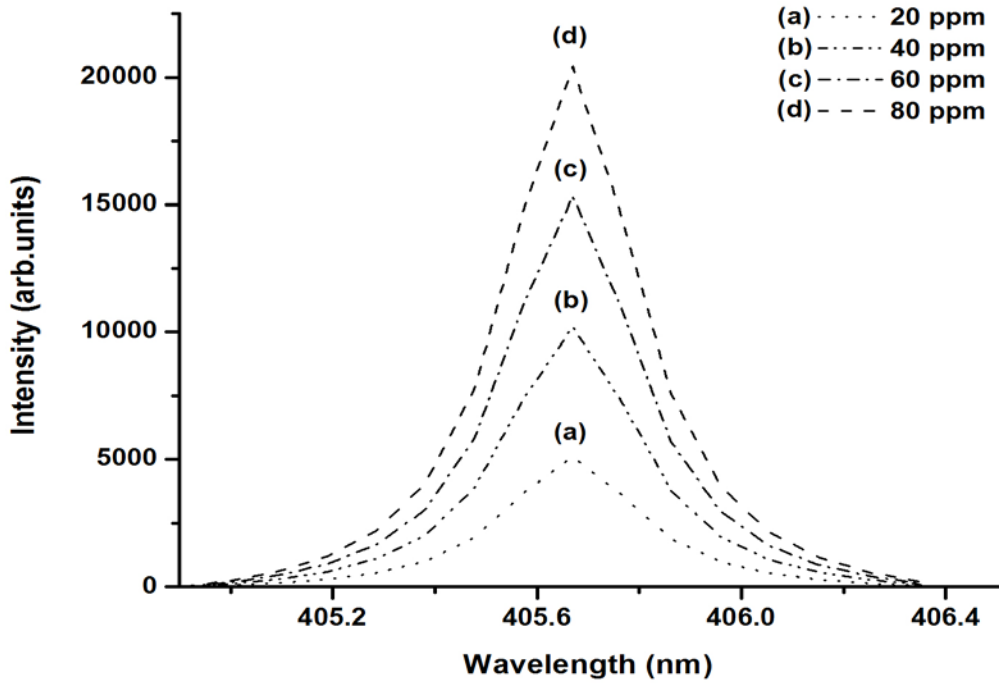

Figure 4. 46: Lead spectral marker (405.7 nm) peaks for different stoichiometric samples with kohl sample #1 as the base material.

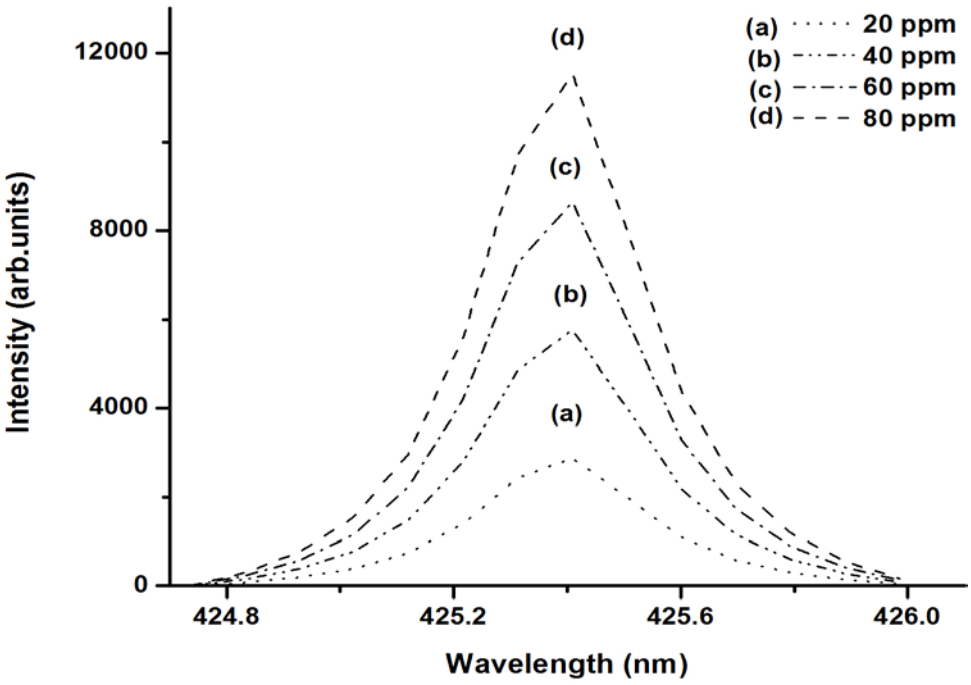

Figure 4. 47: Chromium spectral marker line (425.4 nm) peaks for different stoichiometric samples with kohl sample #1 as the base material

Laser induced plasma generated in LIBS is assumed to exist in local thermodynamic equilibrium. Therefore plotting a graph of Intensity of a spectral line as a function of the concentration yields a calibration curve which is used to estimate the concentration levels of an analyte provided its concentration is in the dynamic range of the curve and the experimental conditions are kept constant as shown in equation 10. To estimate quantitatively lead (Pb) and chromium (Cr) concentration levels in the kohl samples, the spectrometer was adjusted to a center wavelength of 405.4 nm and the LIBS spectra for all the lead calibration standards obtained. Intensities for the chromium (Cr) neutral atomic transition line 405.4 nm were recorded for each standard and a linear calibration curve established as illustrated in Figure 4.48 which was used to determine the lead concentration levels in all the kohl samples. For the chromium calibration standards the spectrometer was centered at 425.7 nm wavelength and intensities recorded for each standard. A

calibration curve was then established as shown in Figure 4.49 which was used to determine the chromium concentration levels in all the kohl samples. In addition to other optimum experimental parameters, a time/gate delay of 700ns was used to generate spectra in Figure 4.50 which clearly illustrates the comparison of the lead and chromium concentrations in all the kohl samples. The concentrations of lead and chromium in the kohl samples obtained using our LIBS detector is shown in Table 4-9.

In order to evaluate the sensitivity of our LIBS system the limits of detection were determined for lead (Pb) and chromium (Cr) using the calibration data and equation 14. The limits of detection are 1 ppm and 2 ppm for Chromium (Cr) and Lead (Pb), respectively.

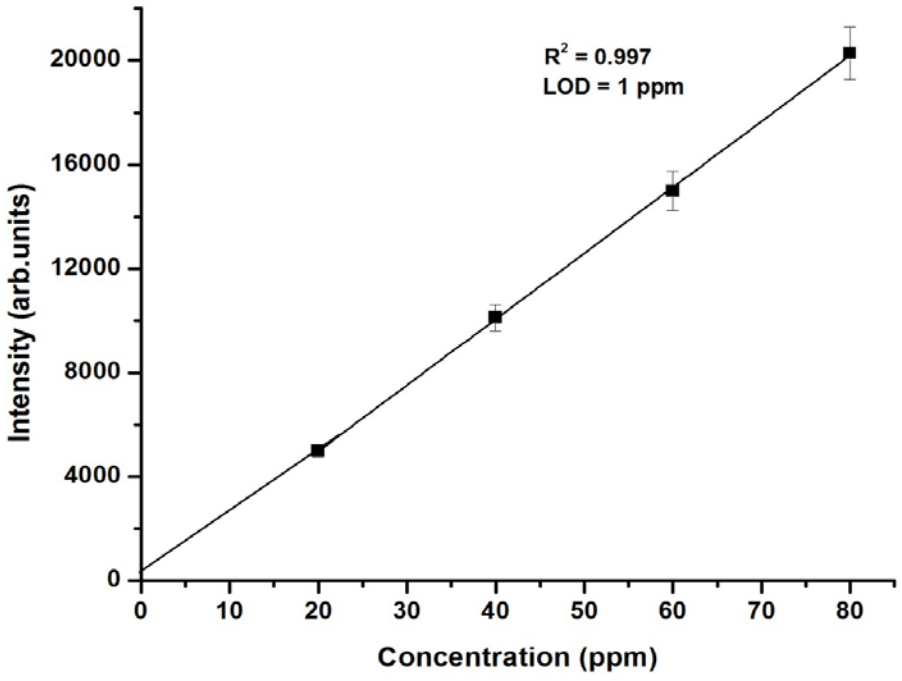

Figure 4. 48: Calibration curve for lead (Pb) in kohl with intensities (a.u) vs. concentration (ppm)

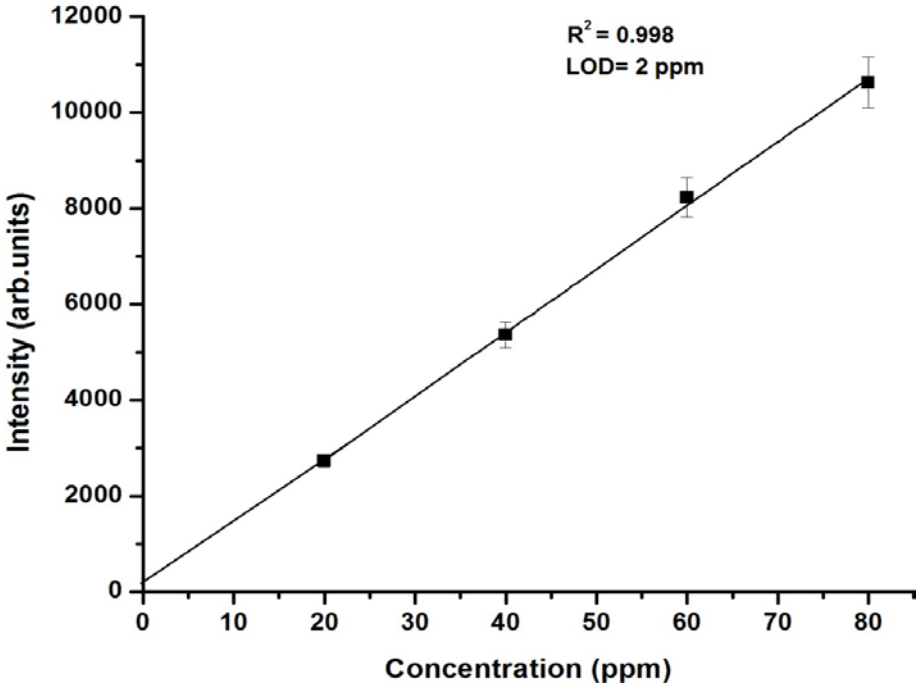

Figure 4. 49: Calibration curve for chromium (Cr) in kohl with intensities (a.u) vs. concentration (ppm)

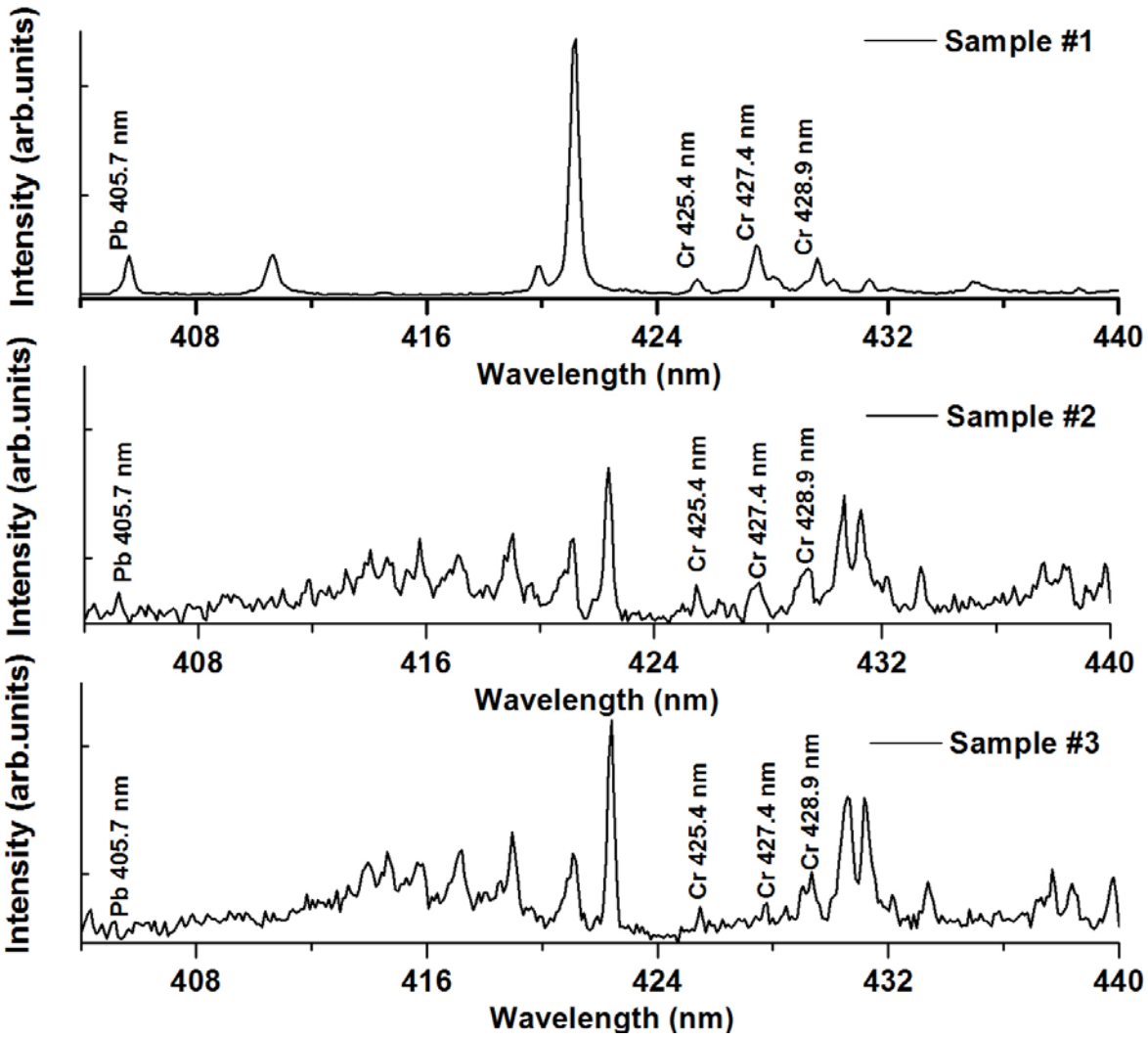

Figure 4. 50: Typical LIBS spectra in the wavelength range of 400 nm - 440nm for all the kohl samples obtained using optimal experimental conditions

To validate the results obtained by our LIBS system, its accuracy was estimated using equation 17. In this case the measured and reference values were obtained using LIBS and ICP-MS respectively. The residual error was calculated between both values yielding an accuracy in the range of 0.05 - 0.3 which is acceptable as clearly shown in Table 4 -9. This implies that both values are comparable with each other which is a worthy indicator that the LIBS spectrometer is a reliable tool for rapid analysis of toxic elements in the studied cosmetic products.

Table 4 - 9: Concentration levels of lead (Pb) and Chromium (Cr) present in the kohl samples

Element	Wavelength (nm)	Transition	Concentration (ppm)						LOD (ppm) for LIBS
			Sample #1		Sample #2		Sample #3		
			LIBS	ICP	LIBS	ICP	LIBS	ICP	
Lead	*405.7*	$6p_{1/2}6p_{3/2}$ to $6p_{1/2}7s_{1/2}$	*14*	*13.3*	*11*	*12.1*	*5*	*6.2*	*1*
Chromium	*425.7*	$3d^5(^6S)4s$ to $3d^5(^6S)4p$	*4*	*3.1*	*7*	*8*	*9*	*8.1*	*2*

4.2.4 Detection of Lead (Pb) and Chromium (Cr) in Talcum powder

4.2.4.1 Introduction

Talcum powder is made from finely ground talc, a very soft naturally occurring pearl white mineral found in deposits all over the world. Talc is derived from an Arabic word *talq* meaning pure. Its chemical composition is hydrated magnesium silicate (H_2Mg_3 $(SiO_3)_4$) and has a very unique property of absorbing moisture [199]. One of the most common uses of talcum powder is baby care, for fragrance and beauty purposes. It's also used to keep the body dry from sweat. Presence of heavy metals likes Lead (Pb), Chromium (Cr) etc, beyond the permissible limits in cosmetic products is of great concern. These heavy metals can be added as byproduct or are a natural part of the raw materials used in production. The human skin is permeable and so when the powder is applied onto the body, it penetrates the skin and finds its way into the blood stream [200]. Some harmful compounds are soluble in water and therefore dissolve in the sweat and penetrate into the body. Lead can cause many dangerous health conditions like disruption of the biosynthesis of hemoglobin, hypertension, kidney damage, disruption of the nervous system, brain damage and declined fertility of men through sperm damage [201, 202]. Lead poisoning in children is especially dangerous because it can cause learning problems and serious illness [203, 204]. The centers for disease control and prevention states that the level of lead in the blood above 0.1ppm is a cause for health concern. Chromium is another heavy metal present in cosmetic products, although the use of chromium is banned in most countries including the European Union and Canada. According to the Canadian national institute for occupational safety hexavalent chromium can cause adverse health problems like skin irritation, occupational asthma, rhinitis, nose bleed, sinus cancer, eye irritation and damage, epigastric pain and discoloration of teeth [205, 206]. In 1993, the European Chemical Industry Ecology and

Toxicology center recommended that chromium concentrations in consumer products should be as low as 1ppm [207, 208].

In the recent years LIBS technique has been applied in industrial materials analysis, prospecting and mining, environmental monitoring, homeland security, forensic analysis, pharmaceutical research, engine and crude oil analysis. Due to the above health concerns, in this section we have developed a highly sensitive laser induced break down spectrometer to detect lead and chromium concentration levels in talcum powder available on the local market.

4.2.4.2 LIBS spectra for talcum powder samples

The spectrometer parameters mentioned previously in the text which yield a good signal to noise ratio were used and spectra in the wavelength range of 250 – 600nm were recorded as shown in the Figures 4.51 – 4.53. The spectral data published by NIST was used to fully identify the elements corresponding to all the spectral lines in the spectra which are aluminum (Al), magnesium (Mg), sodium (Na), calcium (Ca), silicon (Si), titanium (Ti), chromium (Cr), lead (Pb). Lead (Pb) and chromium (Cr) atomic transitions at wavelengths 405.7nm and 425.4nm respectively were selected as the spectral marker lines because they are isolated, strongly intense and do not involve the ground state.

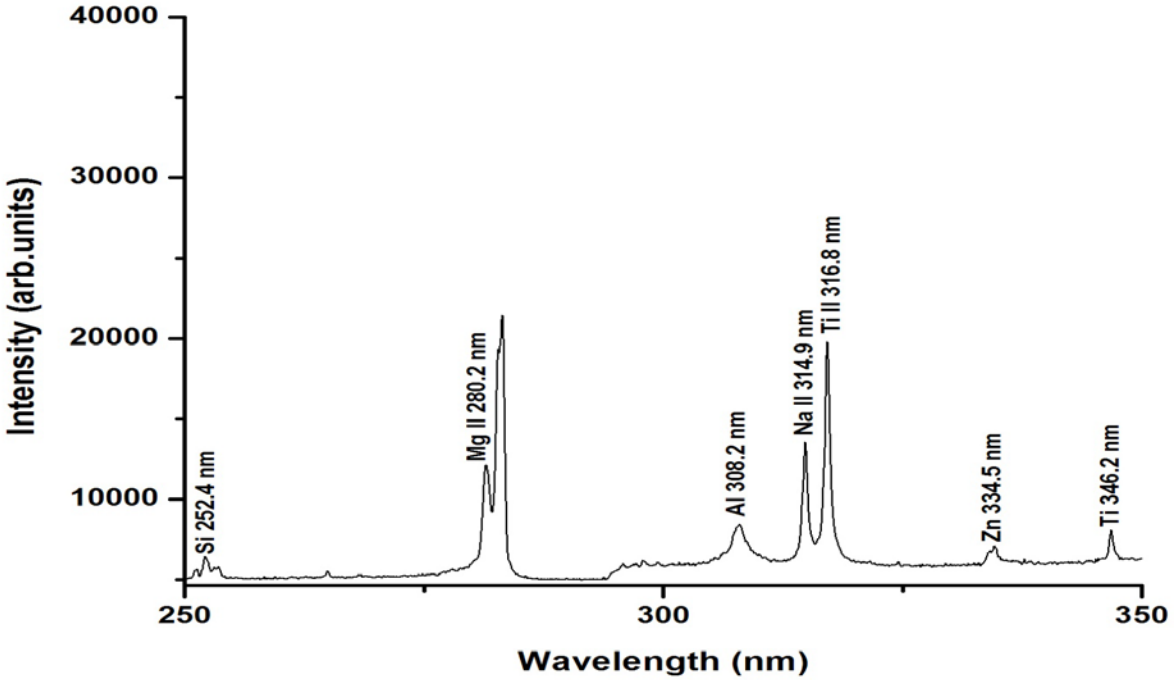

Figure 4. 51: Typical LIBS spectrum in the wavelength range of 250 – 350 nm for talcum powder sample #1.

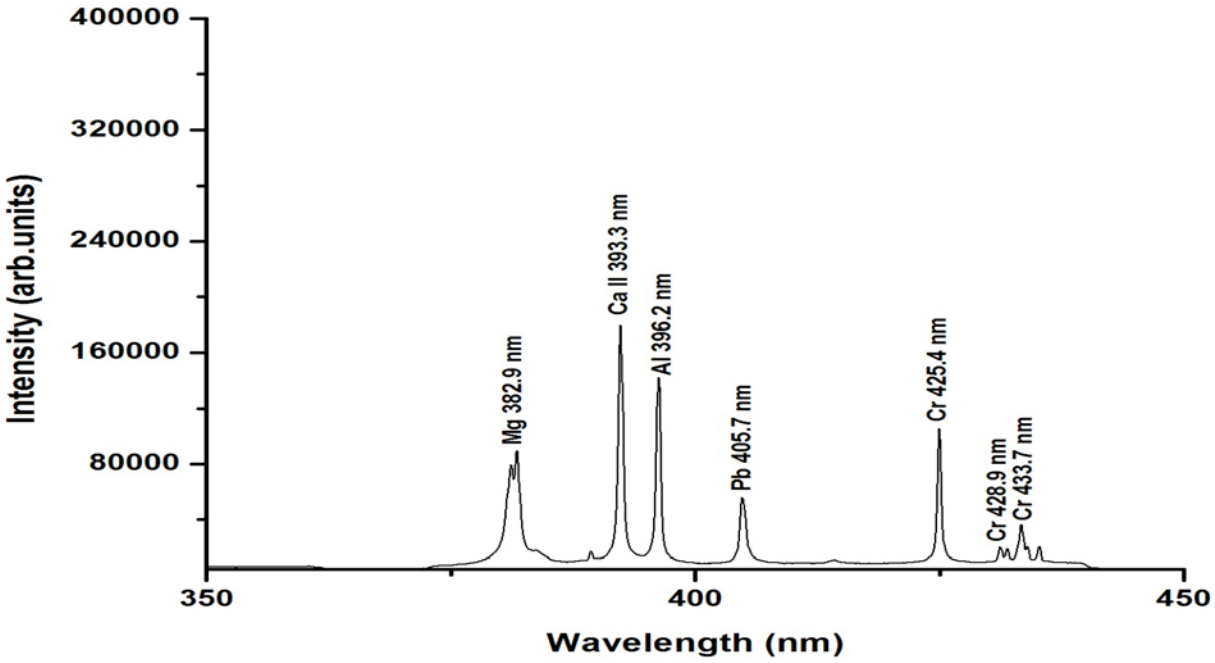

Figure 4. 52: Typical LIBS spectrum in the wavelength range of 350 – 450 nm for talcum powder sample #1.

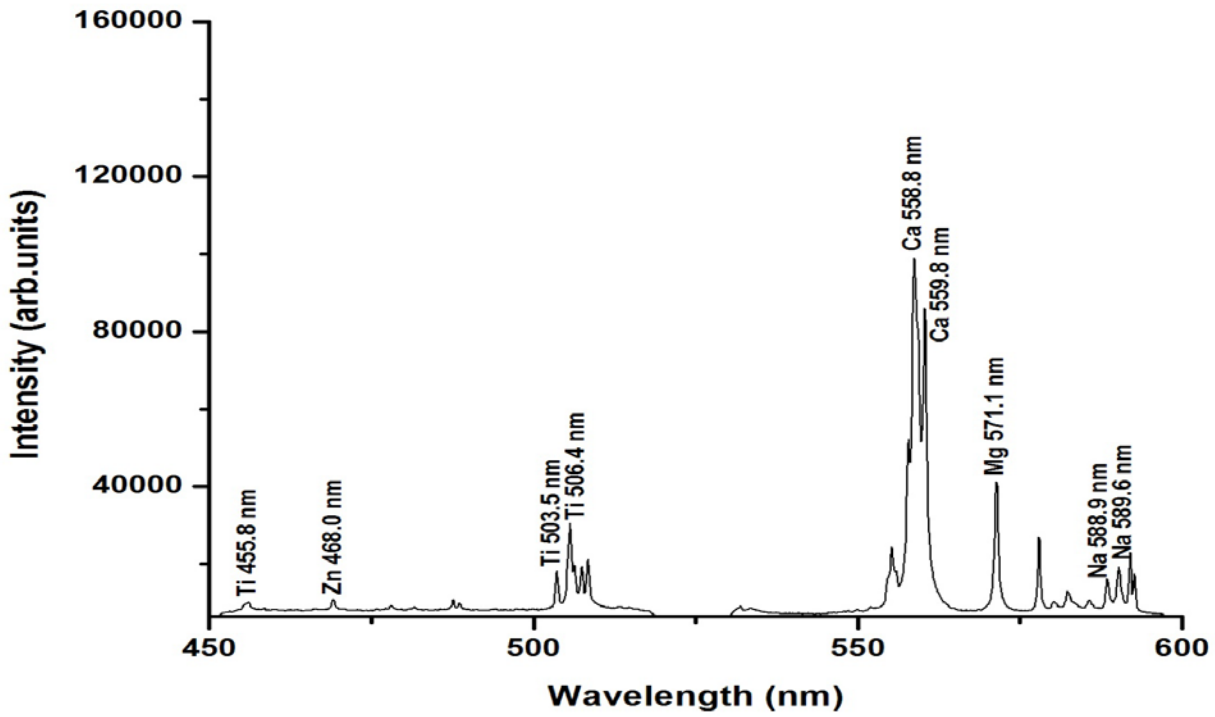

Figure 4. 53: Typical LIBS spectrum in the wavelength range of 450 – 600 nm for talcum powder sample #1.

4.2.4.3 Time delay optimization for talcum powder samples

In order to achieve a good signal to noise ratio (S/N), time/gate delay between laser excitation and acquisition of the spectrum was optimized. LIBS intensity for the spectral marker lines 405.7 nm and 425.4 nm for lead and chromium respectively as a function of time/gate delay was studied. From Figure 4.54 and 4.555, the intensities for the lead and chromium spectral marker line peak at 600ns and 800ns respectively as found in the previous section. Therefore these are the optimum time delays for detection and quantification of lead (Pb) and chromium (Cr) in all the talcum powder samples using our LIBS system. At these specific time/gate delays the signal intensity of the marker lines is a maximum across the entire time/gate delay range. It's worth

noting that the marker lines exhibit a difference in optimum time delays due to the fact that lead and chromium have different transitional probabilities.

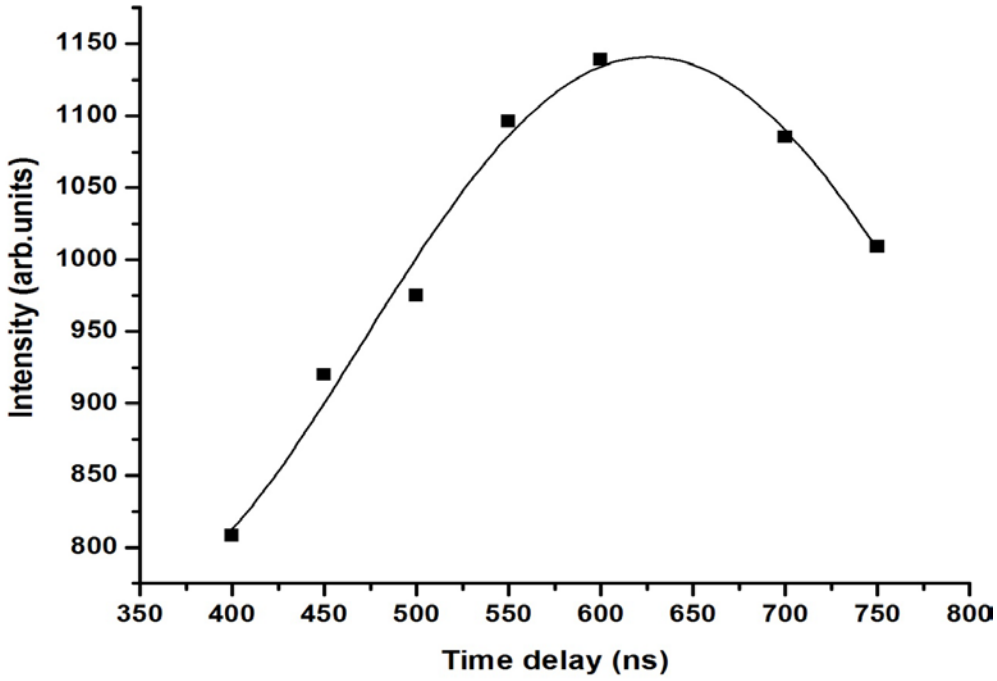

Figure 4. 54: Intensity dependence on time delay for the lead spectral line at 405.7 nm using talcum powder sample # 1

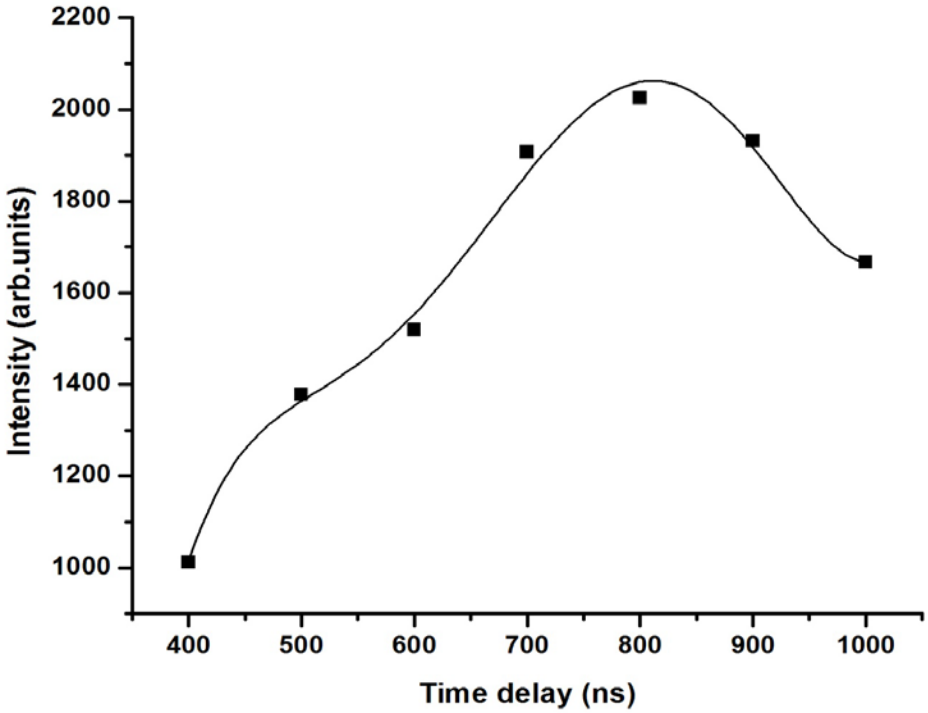

Figure 4. 55: Intensity dependence on time delay for the Chromium (Cr) spectral marker line at 425.4 nm using talcum powder sample #1

4.2.4.4 Laser energy optimization for talcum powder samples

Optimization of the laser energy of the incident pulse is very vital in order to maximize the intensity of the LIBS signal; this significantly improves on the limit of detection of the LIBS system. The intensity of the lead spectral marker line at a wavelength of 405.7 nm was studied as a function of the laser fluence as depicted in Figure 4.56. It is observed that the LIBS intensity increases with increase in laser fluence and at 24.4 Jcm^{-2} the rate of increase of the intensity with respect to the laser fluence drops and later the curve levels off due to self absorption. Therefore 24.4 Jcm^{-2} was identified and used as the optimum laser fluence to detect and quantify lead and chromium in all the talcum powder samples.

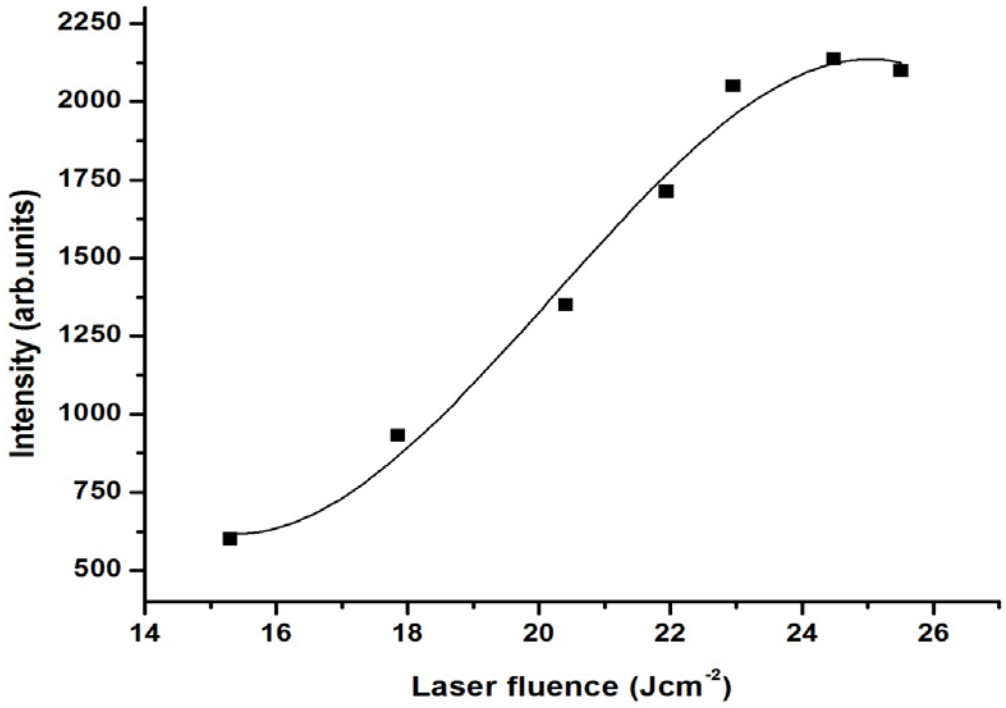

Figure 4. 56: Intensity as a function of laser fluence for the lead (Pb) spectral marker line using talcum powder sample # 1

4.2.4.5 Detection of lead (Pb) and chromium (Cr) concentration levels in talcum powder samples

In this case, the optimum experimental parameters mentioned previously in the text were used. For lead, the spectrograph was adjusted to a center wavelength of 405.7 nm and spectra for all the lead calibration standards were the recorded. For quantification of chromium the spectrograph was adjusted to a center wavelength of 425.4 nm and spectra also recorded for all the chromium calibration standards. All the data collected was then analyzed using Origin 8.0 Software and Intensities corresponding to each set of calibration standard for lead and chromium recorded respectively. In LIBS the laser induced plasma generated by a high power pulsed laser is optically thin and exists in local thermodynamic equilibrium. Therefore from equation 14, a plot of LIBS intensity (arb.units) as a function of concentration (ppm) yields a calibration curve.

The calibration curves of lead and chromium as shown in Figures 4.57 and 4. 58 respectively were established in order to estimate the concentration levels of lead and chromium in all the talcum samples. In order to evaluate the sensitivity of the LIBS system, the limits of detection were determined for lead and chromium using the calibration data and equation 15. The limits of detection are 1.96 ppm and 1.72 ppm for Lead and Chromium respectively. From Figure 4.59 Typical LIBS spectra in the wavelength range of 400- 430 nm for all the talcum powder samples were recorded using the optimum set of conditions discussed previously. The emission intensities for the lead and chromium spectral marker lines were measured and their corresponding concentration determined using the calibration curves. Lead and chromium was detected in the range of 14 - 17 ppm and 23 - 21 ppm respectively as shown in Table 4-10.

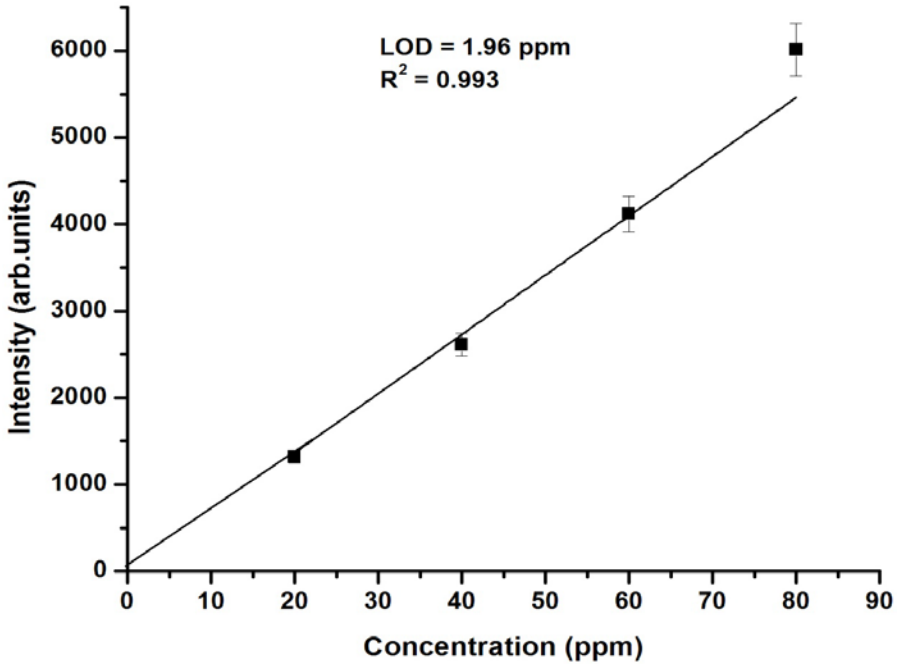

Figure 4. 57: Calibration curve for lead (Pb) in Talcum powder

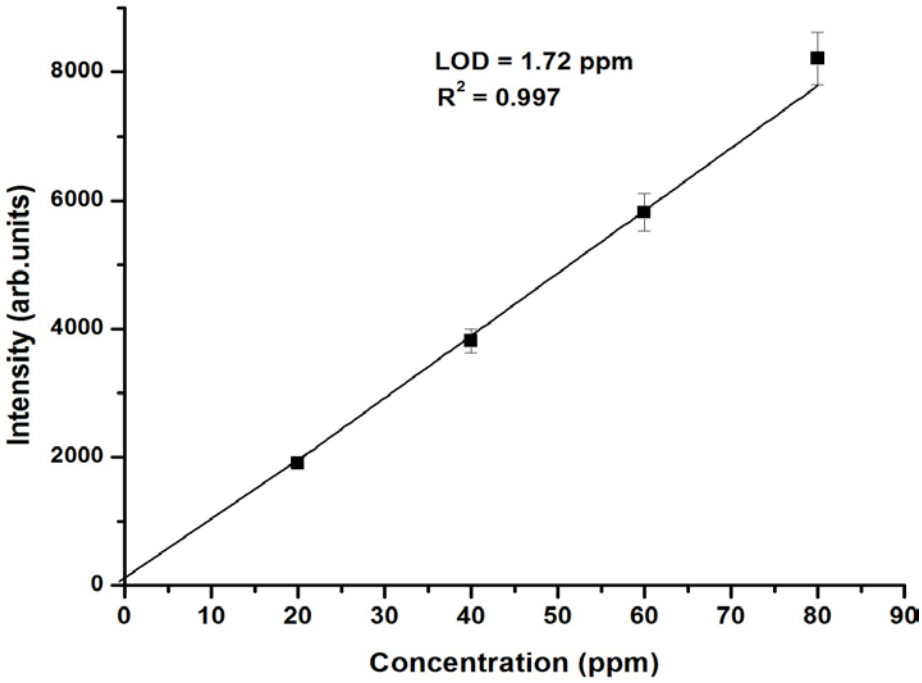

Figure 4. 58: Calibration curve for Chromium (Cr) in Talcum powder

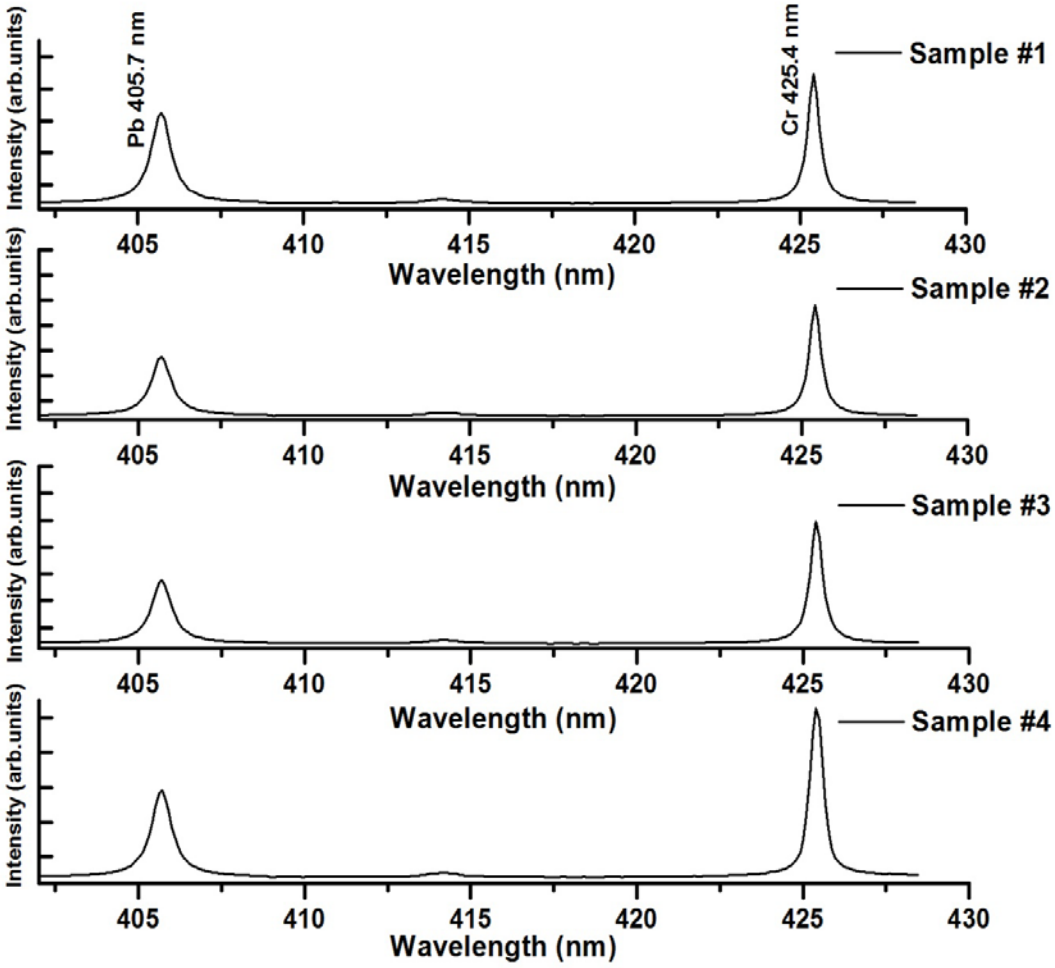

Figure 4. 59: Typical LIBS spectra in the wavelength range of 400 nm - 440nm for all the Talcum powder samples obtained using optimal experimental conditions

Table 4 - 10: Concentration levels of lead (Pb) and Chromium (Cr) present in the talcum powder samples

Element	Wavelength (nm)	Concentration (ppm)				LOD (ppm)
		Sample #1	Sample #2	Sample #3	Sample #4	
Lead	405.7	17	14	14	15	1.96
Chromium	425.7	21	23	26	29	1.72

CHAPTER 5

CONCLUSION

A high resolution and high sensitivity sensor based on laser induced breakdown spectroscopy (LIBS) was developed and applied successfully for the analysis of cosmetic products of daily use specifically for detection of trace amount of toxic elements such as fluoride (F), lead (Pb) and chromium (Cr) present in tooth pastes, synthetic hair dyes, kohl eye liners and talcum powders. Prior to the application to these cosmetic products, the optimum parameters of the LIBs system were investigated. For this purpose, we investigated the role of excitation laser wavelength, laser fluence and gate/time delay (time between laser excitation and spectrum acquisition) on plasma parameters under ambient conditions.

The laser induced plasma was generated using a fundamental (1064 nm), second (532 nm) and fourth harmonic (266 nm) Nd: YAG laser wavelengths as the excitation sources to ablate semi fluid samples. Optical emission spectroscopy provided us important information about the temperature (T) and electron density (n_e) of the plasmas during plume expansion. T and n_e showed a decrease with respect to increase in gate/time delay and then leveled off exhibiting a t^{-2} dependence for all wavelengths but 1064 nm and 266 nm consistently showed the lowest and highest values respectively. This is due to the differences in laser-target and laser- plasma coupling at different wavelengths. T and n_e increased with respect to the increase in laser fluence and leveled off at higher fluencies due to the saturation effect. However in this case, also 1064 nm and 266nm persistently showed the lowest and highest values respectively. Hence a 266 nm

wavelength excitation source was selected to develop our laser induced breakdown spectrometer for detection of toxic elements in cosmetic products.

A laser induced break down spectrometer for the detection of fluoride (F), lead (Pb) and chromium (Cr) levels in tooth pastes, synthetic hair dyes, kohl eyeliners and talcum powders was developed using a 266 nm wavelength Nd: YAG laser excitation source in conjunction with a high resolution spectrograph coupled with an ICCD camera. The vital experimental parameters such as gate/time delay and laser fluence were optimized to achieve a good signal to noise ratio, maximum intensities of the spectral marker lines and optically thin plasma in LTE. The choice of the selected parameters was validated using the Mcwhirter criterion. This further improved on the sensitivity of the LIBS system that is the limits of detection. For toothpaste, the atomic transition line at 731.102 nm (F I) is used as the marker line for detection of fluoride in the toothpaste samples. This study revealed that few brands of toothpaste available on the local market contain quite high fluoride levels which can be dangerous to human health. The limit of detection (LOD) of our LIBS system for the detection of fluoride in tooth paste was estimated to be 156 ppm. For the synthetic hair dyes, chromium (Cr) was detected and quantified using the atomic transition at a wavelength of 427.5 nm. Our calibrated LIBS system with a limit of detection of 1.2 ppm detected chromium (Cr) concentration levels in the range of 5 - 11 ppm. The LIBS results were compared with those obtained using ICP spectrometry, a standard technique and were in excellent agreement. However, they are above the acceptable limit of 1ppm set by the Environmental Agency (E.A) and other regulatory organizations. Hence use of synthetic hair dyes can be hazardous to human health. For kohl eyeliners, lead (Pb) and chromium (Cr) were detected and quantified using atomic transitions at wavelengths 405.7 nm and 425.4 nm as the spectral marker lines respectively. Lead (Pb) levels were estimated in the

range of 7 ppm-12 ppm and chromium (Cr) levels in the range of 15 ppm-20 ppm which are above the permissible limits set by OSHA of 0.5 ppm and 1 ppm of lead (Pb) and chromium (Cr) respectively. Our results were confirmed with those obtained using ICP-MS and were in good agreement. Therefore persistent use of kohl can have a negative impact on human health. For the talcum powders, lead (Pb) and chromium (Cr) levels were estimated using atomic transitions at wavelengths 405.7 nm and 425.4 nm as the spectral marker lines respectively. Lead (Pb) levels were estimated in the range of 15 ppm - 17 ppm and chromium (Cr) levels in the range of 21 ppm - 29 ppm which are above the safe permissible limits. This renders talcum powders dangerous to human health.

For future works, a double pulsed LIBS system capable of further improving on the limits of detection (sensitivity) can be developed. Also using a vacuum sample holder in LIBS analysis should be considered so as to improve on the signal to noise ratio (S/N) and signal intensities of the spectral lines. LIBS studies can also be extended to study toxicity levels of pharmaceutical products which are commercially available on the market. Presence of toxic elements in human body organs such as teeth, kidneys is worth studying to provide us with baseline data which can be used to minimize excessive intake of specific elements in the body which can be disastrous to the human body.

REFERENCES

[1] D.A.Cremers and L.J.Radziemski,"Hand book of Laser Induced Break down spectroscopy", John Wiley and Sons ,2006

[2] Alvey.D.C, Morton.K, Harmon.R.S, Gottfried.J.L, Remus.J.J and Collins.L.M," LIBS based geochemical fingerprinting for rapid analysis and discrimination of minerals-Example of Garnet", J. Appl opt, vol 49, pp. C168 - C180, 2010

[3] Bakry,A.H & Razvi.M.A.N ,"Detection of heavy toxic metals in water samples by laser induced breakdown spectroscopy(LIBS)" J. appl optics, vol 8, pp. 202-208, 2009

[4] Gondal.M.A, Hussain.T, Ahmed .Z and Bakry.A.H,"Detection of contaminants in ore samples using laser induced break down spectroscopy", J.Environ Sci&Health,vol 42, pp. 879-887, 2007

[5] Asimellis.G, Michos.N, Fasaki.I & Kompistas.M,"Platinum group metals bulk analysis in automobile catalyst recycling material by laser induced breakdown spectroscopy", J. spectrochimica, vol 63, pp.1338-1343, 2008

[6] Charlton. B, Fisher.A.S, Goodall.P.S, Hindis.M.W, Lancaster.S & Shore.S,"Atomic spectroscopy update. Industrial analysis: Metals, chemicals and advanced materials", JAAS: J of Anal. At spectrosc, vol 23,pp. 1636-1692, 2008

[7] Carvalho,Gabriel,Nunes,Lidiane,Souza,Paulino,Krug,J.Francisco,Alegre,Thaisa &Santos Jr,"Evaluation of laser induced break down spectrometry for determination of macro and micro nutrients in pharmaceutical tablets", J.Anal.At.Spectrom, vol 25, pp. 803-809, 2010

[8] Wu.J.Zhang,W.Shao,X.Lin.Z,Liu.X,"Simulated body fluid by laser induced breakdown spectroscopy", J.Laser.B, vol35, pp. 445-447, 2008

[9] Sarkar,Arnab, Aggarwal,K.S & Alamelu.D,"Laser induced break down spectroscopy for rapid identification of different types of paper for forensic application", J. Anal.Methods, vol 2, pp. 32-36, 2010

[10] Wise,S.H &Almirall.J.R, "Chemical taggant detection and analysis by laser induced breakdown spectroscopy", J. Appl.Optic vol 35, pp. 445-447, 2008

[11] Nina.L.Lanza,R.C.W Samuel,M.C.Ann, M.O.Seth, D.H.Horton, E.N &James E.B,"Calibration the chemCam laser induced break down spectroscopy instrument for carbonate minerals on Mars", J. Appl Optics, vol 49, pp. C211-C217, 2010

[12] Panne,U.,"Analysis of glass and glass melts during the vitrification of fly and bottom ashes by LIBS.Part II.Process analysis",J. Spectrochimica ActaB, vol 53 pp.1969, 1998

[13] K.W.Jackson,T.M.Mahmood,"Atomic absorption, Atomic emission and flame emission spectrometry" J. Anal.Chem vol 66, no.12, pp. 252R-279R, 1994

[14] A. Ciucci, M. Corsi, V. Palleschi, S. Rastelli, A. Salvetti, and E. Tognoni,"New procedure for quantitative elemental analysis by laser induced plasma spectroscopy", J. Appl. Spectrosc, vol 53, pp. 960-964, 1999

[15] J. Cu˜ nat, F. J. Fortes, J. J. Lasagna," Real time and in situ determination of road sediments using a man portable laser induced breakdown spectroscopy analyzer", J. Anal. Chim. Acta vol 633, pp. 38-42, 2009

[16] Nek. M. Shaikh, S Hafeez and M. A. Baig, "Comparison of zinc and cadmium plasma parameters produced by laser-ablation", J. Spectrochim. Acta Part B: vol 62, pp. 1311-1320, 2007

[17] S. Laville, M. Sabsabi, F. R. Doucet," Multi elemental analysis of solidified mineral melt samples by laser induced breakdown spectroscopy coupled with a linear multivariate calibration", J. Spectrochimica Acta Part B, vol 62, pp. 1557-1566, 2007

[18] NIST Atomic spectra databasehttp://www.nist.gov/physlab/data/asd.cfm

[19] Loree.T.R & Radziemski.L.J,"Laser induced break down spectroscopy: time integrated applications", J. Plasma Chem. Plasma Proc,vol 1, pp. 271-280, 1981

[20] Ko, J.B, Sdorra, W & Niemax K," on the internal standardization in optical spectrometry of micro plasmas produced by laser ablation of solid samples", J. FreseniusZ.Anal.Chem, vol 335, pp. 648-651, 1989

[21] Radziemski, L.J,"Review of selected analytical applications of plasmas and laser ablation", vol 50, pp. 218:234, 1987-1994

[22] Lee.Y.I,Song.K &Sneddon.J,"Laser induced break down spectrometry, New York, Nova Science Publishers, 2000

[23] Rusak.D.A,Castle.B.C,Smith.B.W &Wineforder.J.D,"Fundermentals and Applications of laser induced break down spectroscopy", J. Critical reviews in analytical chemistry, vol 27,pp. 257-290, 1997

[24] Corsi.M.V, Palleschi &Tognoni,E,"Special Issue,1st International Conference on Laser Induced Plasma Spectroscopy", J. Spectrochim.ActaPartB,vol 50, pp. 565-1034, 2001

[25] Hahn.D.W,Miziolek,A.W & Palleschi.V,"Special issue LIBS2002", J.Appl opt, vol 42,pp. 5933-6225, 2003

[26] Yang,Ningfang,Eash Neal,S.Lee,Jaehoon,Martin,Madhavi,Z.Zhang,Yong-Seon,Walker Forbes.R & Yang.J.E,"Multivariate analysis of laser induced breakdown spectroscopy spectra of soil samples", J.Soil science, vol175, pp. 447-452, 2010

[27] Tameze.C,Vincelette.R.Melikechi,N.Zeljkovic.V&Izquierdo.E,"Emprical analysis of LIBS images for ovarian cancer detection, In 8th international workshop on image analysis for multimedia interactive services", IEEE:Piscataway,NJ,USA,pp. 300-303, 2008

[28] Cremers.D.A & Chinni.R.C,"Laser Induced Breakdown spectroscopy capabilities and limitations", J. Appl spectrosc. rev, vol 44, pp. 457-506, 2009

[29] B.leDrogoff, J.Margot, F.Vidal, S.Laville, M.Charker,M.Sabsabi, T.W.Johnston and O.Barthelemy, “Influence of the laser pulse duration on laser produced plasma properties”, J. Plasma sources sci.Technol,vol13, pp. 233, 2004

[30] T.L.Thiem,Y.Lee and J.Sneddon,“Lasers in atomic spectrometry:selected applications”, J. Microchem, vol 45, pp 1-35, 1992

[31] Z.W.Huang, Y.Y.Teng, K.P.Li,J.Sneddon, “ Interaction of a laser beam with metals. Part 1: Quantitative studies of plasma emission”, J. Appl.spectrosc, vol45, pp. 432-441, 1991

[32] L.M.Cabali and J.J.Larsena,” Experimental determination of laser induced break down thresholds of metals under nanosecond Q-Switched laser operation spectroscopy”, J. Spectrochimica Acta B, vol 53, pp. 723 -726, 1998

[33] E.H .Prepmeier,”Laser ablation for atomic spectroscopy” Analytical Applications of Lasers(Ed.E.H.Premeier) Wiley Newyork(1988)

[34] C.D.Allemand,” Spectrocopy of single spike laser generated plamas”, J. Spectrochim ActaB, vol 27, pp 185-188, 1972

[35] A.M.Pnochov, V.A.Batanov, F.V.Bunklin, V.B Fedorov, “ Metal evapouration under powerful optical radiation”, IEEE.J.Quant Electron Q.E , vol 9, pp. 503-510, 1973

[36] A.S.Eppler, D.A.Creners, D.D.Hicknott, M.J Fenis, A.C.Koskelo., “ Matrix effects in the detection of Pb and Ba in soils using laser induced breakdown spectroscopy”, J. Appl Spectrosc, vol 50, pp. 1175-1181. 1996

[37] R.Wisburn, I.Schechter, R.Niesner, H.Schroder, K.L.Kompa,“Detector for trace elemental analysis of solid environmental samples by laser plasma spectroscopy”, J.Anal chem, vol 66, pp. 2964-2975, 1994

[38] C.Aragon,J.A.Aguilera,F.Penalba.” Improvements in quantitative analysis of composition of steel composition by laser induced breakdown spectroscopy at atmospheric pressure using an infrared Nd:YAG laser”, J.Appl Spectrosc, vol 53, pp. 1259 – 1267, 1999

[39] C.Chaleard,P.Mauchien,N.Andre,J.Uebbig,J.LlLacour,C.Cpectsen, “ Correction of matrix effects in qualitative analysis with laser ablation optical emission spectrometry”, J.Anal At Spectrom, vol 12, pp. 183- 188, 1997

[40] R.Krazniker,V.Blato,I.Schecher,” Study of matrix effect in laser plasma spectroscopy by shock wave propagation”, J. Spectrochim ActaB, vol 56, pp. 609-618, 2001

[41] A.Ciucci,V.Palleschi,S.Ratelli,R.Barbin,R.Fautous,A.Palluci,S.Ribezzo and H.J.L.Vander steen,” Trace pollutants analysis in soil by time resolved laser induced breakdown spectroscopy technique”, J. Appl.Phy.B, vol63, pp 185- 190, 1996

[42] Mikio kuzuya, Hitoshi Matsumoto, Hideaki Takechi and Osamu Mikami, “ Effect of laser energy and atmosphere on the emission characteristics of laser induced plasma”, J.Appl Spectrosc, vol47, pp. 1659-1664, 1993

[43] J.A.Bolger,"Semiquantitative laser induced break down spectroscopy for analysis of mineral drill core", J. Appl spectrosc, vol 54, pp. 181-189, 2000

[44] M.A.Gondal, T.Hussein,Yamani ZH, M.A.Baig," Role of binding materials for trace elemental analyisis of powder samples using LIBS", J. Talanta vol 72,no 2, pp 642-649

[45] L. Moenke-Blankenburg,"Laser micro analysis, "John Wiley, New York , pp.225,1989

[46] Cremers.D.A and A.K.Night,"Laser Induced breakdown spectroscopy. In Encyclopedia of Analytical chemistry ed.R.A.Meyers. John Wiley &Sons Ltd Chichester 95-9613

[47] Radziemski L., Cremers D., Benelli K., Khoo C., and Harris R.D."Use of the vacuum ultraviolet spectral region for LIBS-based Martian geology and exploration", J. Spectrochimica Acta B,vol 60, pp. 237-248, 2005

[48] Myers.M.J,Myres.J.D,Guo.B.P,Yang.C.X,Hardy,C.R.Meryers,J.A,MyersA.G& Christian S.M,"Non-invasive insitu detection of malignant skin tissue and other abnormalities using portable LIBS system with fibre spectrometer and eye-safe erbium glass laser", J. Proc.Soc.Photo.Opt.Instrum.Eng, vol 6863, pp.W8630-W8630, 2008

[49] S.S.Harilal, C.V Bindhu, V.P.N.Nampoori and C.P.G Vallabhan,"Temporal and spatial behavior of electron density and temperature in a laser produced plasma from YBa2Cu3O7", J. Appl spectrosc, vol 52, pp. 449-455, 1998

[50] V. K. Unnikrishnan, V. B. Kamlesh alti, C. Kartha, Santhosh, G.P. Gupta and B.M Suri, "Measurement of plasma temperature and electron density in laser induced copper plasma by time resolved spectroscopy of neutral atom and ion emissions", Pramana J. of phys. vol 74, pp 983-993, 2010

[51] H.R.Griem,"PrinciplesofPlasmaspectroscopy,"CambridgeUniversity Press,Cambrige,1997

[52] Young June Hong, Gi Chung Kwon, Guangsup Cho, Hee Myoung Shin and Eun Ha Choi,"Measurement of electron temperature and density using Stark broadening of the coaxial focused plasma for extreme ultraviolet lithography", IEEE transactions on plasma science, vol 38, pp. 1111-1117, 2010

[53] A.E.Hussein, P.K.Diwakar, S.S.Harilal and A.Hassanein," Role of laser wavelength on plasma generation and expansion of ablation plumes in air", J.Appl.Phys, vol 113, pp. 143305, 2013

[54] M.Milan, J.J.Laserna,"Diagnostics of silicon plasmas produced by visible nanosecond laser ablation", J. Spectrochimica Acta Part B vol 56, pp 275-288, 2001

[55] B.LeDrogoff,J.Margot,M.Chaker,M.Sabsabi,O.Barthlemy,T.W.Johnston, S.Laville, F.Vidal, Y.von Kaenel," Temporal characterization of femtosecond laser pulses induced plasma for spectrochemical analysis of aluminum alloys", J.Spectrochimica Acta Part B vol 56, pp. 987-1002, 2001

[56] Marwa A. Ismail, Hisham Imam, Asmaa Elhassan, Walid T.Younisss and Mohamed Harith ,"LIBS limit of detection and plasma parameters of some elements in two different metallic matrices", J.anal.at.spectrom vol 19, pp. 489-494, 2004

[57] Cremers.D.A & Radziemski.L.J,"History and fundermentals of LIBS. Laser induced breakdownspectroscopy fundermentals and applications, Cambridge University Press, 2006

[58] Song.K.Lee,Y.I &Sneddon.J,"Applications of laser induced breakdown spectrometry", J. Appl.Spectrosc. Rev, vol 32, pp. 83-235, 1997

[59] Gottfried ,Jennifer&DeLucia.F,"Laser induced breakdown spectroscopy:capabilities and applications",Army Research Laboratory,vol.ARL-TR-5238, 2010

[60] Brech.F and Cross.L,"Optical Microemission simulated by a Ruby laser", J. Appl.Spectrosc, vol16, pp. 59, 1963

[61] Radziemski.L.J,"from laser to LIBS, the path of technology development", J. Spectrochim. Acta PartB, vol 57, pp. 1109-1114, 2002

[62] Fantoni.R.Caneve,L.Colao.F,Fornarimi,L.Lazic &Spizzichino.V,"Methodologies for laboratory laser induced break down spectroscopy semi quantitative and quantitative analysis-A review", J. Spectrochim.ActaB, vol 63,pp. 1097-1108, 2008

[63] Tognoni.E, Palleschi.V,Corsi.M&Cristoforettti.G,"Quantitative micro analysis by laser induced breakdown spectroscopy, a review of the experimental approaches", Spectrochim.ActaB, vol 57, pp. 1115-1130, 2002

[64] Noda.M.Deguchi, Y.Iwasaki.S &Yoshikawa.N,"Detection of carbon content in a high temperature and high pressure environment using laser induced breakdown spectroscopy", Spectrochim.ActaB, vol 57, pp. 701-709, 2002

[65] Michel.A.P.M, Lawrence-Snyder,M.Angel,S.M &Chave.A.D,"Laser induced break down spectroscopy in the determination of gem provenance: Beryls", J. Appl.Optic, pp. 47,G72-G79, 2008

[66] Goujon.J,Giakoumaki.A, Pinon.V, Musset.O, Anglos.D. Georgiou.E and Boquillon.J.P ", A compact and portable laser induced break down spectroscopy instrument for single and double pulse applications", J. Spectrochim.ActaB, vol 63,pp. 1091-1096, 2008

[67] A. Ciucci, V. Palleschi, S. Rastelli et al., Trace pollutions analysis in a soil by a time-resolved laser-induced breakdown spectroscopy technique, J. Appl. Phys. BLas.Opt. vol 63, pp. 185-190, 1996

[68] J.M.Vadillo and J.J.Larsena,"Laser induced breakdown spectroscopy of silicate,vanadate and sulfide rocks," J. Talanta , vol 43, pp. 1149-1154, 1996

[69] Song, K.; Lee, Y. I.; Sneddon, J," Applications of Laser-Induced Breakdown Spectrometry," J. Appl spectrosc.Rev, vol 32, no. 3, pp. 183-235, 1997

[70] Fiona J.Wallis, Bruce L.Chadwick and Richard J.S.Morrison," Analysis of lignite using laser induced breakdown spectroscopy,"Appl Spectrosc, Vol. 54, no. 8, pp. 1231-1235, 2000

[71] Fichet P, Mauchien P., Wagner J.-F., and Moulin C. (2001)," Quantitative elemental determination in water and oil by laser-induced breakdown spectroscopy," Analytica chimica acta 429(22) 269-278.

[72] Charif, B. and Harith, M.A," Panoramic laser-induced breakdown spectroscopy of water," Spectrochimica Acta part B. vol 57, pp. 1141-1153, 2002

[73] K.Kuzuya, M,Murakami, M,Maruyama," Quantitative analysis of ceramics using laser induced break down spectroscopy," Spectromica acta partB: J. Atomic spectrosc, vol 58, no.5, pp. 957-965, 2003

[74] M. Corsi, G. Cristoforetti, M. Giuffrida, M. Hidalgo, S. Legnaioli, V. Palleschi, A. Salvetti, E. Tognoni and C. Vallebona, "Three-Dimensional Analysis of Laser Induced Plasmas in Single and Double Pulse Configuration," Spectrochimica Acta Part B, vol. 59, No. 5, 2004, pp. 723-735. doi:10.1016/j.sab.2004.02.001

[75] Boudjemai, S., Gasmi, T., Boushaki, R., Kasbadji, R. and Medjahed, F. (2004). " Laserinduced break down spectroscopy in water", J.Appl Sci.Environ, vol 8, pp. 13-15 ,2004

[76] Lazic, V., F. Colao, et al. (2005). "Recognition of archeological materials underwater by laser induced breakdown spectroscopy." J. Spectrochim. Acta, Part B, vol 60, pp.7-8, 2005

[77] Russell.S.H, Frank C.D, Andrzej.W.M, Kevin L.M, Macnesbey R.A, Patrick.D.F,"Laser induced break down spectroscopy (LIBS) an emerging field portable sensor technology for real time in situ geochemical and environmental analysis, Geochemistry, exploration, environment analysis" 5:21-28, (2005)

[78] M.A.Gondal, T.Hussain, Z.H Yamani. Detection of heavy metals in Arabian crude oil residue using laser induced breakdown spectroscopy. J. Talanta, vol 69, pp. 1072-1078, 2006

[79] Lawrence-Snyder, M., J. Scaffidi, et al. (2007). "Sequential-pulse laser-induced breakdown spectroscopy of high-pressure bulk aqueous solutions." J. Appl. Spectrosc, vol 61, no. 2: pp. 171, 2007.

[80] T.Hussain, M.A.Gondal, Z.H.Yamani, "Measurement of nutrients in green house soil with laser breakdown spectroscopy", J. Environ Monit Assess,vol 24, pp. 131-139, 2007

[81] M.A Gondal, T. Hussain, Z H. Yamani."Determination of Toxic metals in petroleum, cultivated land and ore samples using laser induced breakdown spectroscopy", J.Bull Environ contam toxicol, vol 78, pp. 270-274, 2007

[82] M.A.Gondal, T.Hussain.”Determination of poisonous metals in waste water collected from paint manufacturing plant using laser induced breakdown spectroscopy,”J. Talanta, vol 71, pp. 73-80, 2007

[83] T.Hussain, M.A Gondal “Monitoring and assessment of toxic metals in gulf war oil spill contaminated soil using laser induced break down spectroscopy”, J. Environ Monit Assess, vol 36, pp. 391-399, 2008

[84] M.N.Siddiqui, M.A.Gondal, M.M.Nasr. “Determination of trace metals using laser induced breakdown spectroscopy in insoluble organic materials obtained from pyrolysis of plastic waste”, J. Bull Environ contam Toxicol, vol 83, pp. 141-145, 2009

[85] M.M Naser. M.A.Gondal “Detection of hazardous pollutants in chrome tanned leather using locally developed laser induced break down spectrometer”, J. Environ Monit Assess, vol 175, pp. 387-395, 2011

[86] M.A.Gondal. M.H.Shwehdi. A.A.Khalil. “Application of LIBS for determination of ionic species (NaCl) in electrical cables for investigation of electrical breakdown”, J. Appl PhysB, vol 105, pp. 915-922, 2011

[87] BHymer,Clayton,Judith A.Brisbin,Karen L Sutton and Joseph A.Caruso.”New approaches for elemental speciation using plasma mass spectrometry”J. American Laboratory , vol 32, no.3, pp.17-32, 2000

[88] Jarvis KE,Al Gray and RS Houk.Handbook of inductively coupled plasma mass spectrometry.Chapman and Hall: Newyork, 1992.

[89] J.Radzienski and D.A.Cremers, Laser induced plasmas and applications,Marcel Dekker Inc.,NewYork, 1989.

[90] A .W.Miziolek,V.Pallesschi and I.Schecchter, Laser induced breakdown spectroscopy, Cambrige University Press, Cambrige, 2006.

[91] Young June Hong, Gi Chung Kwon, Guangsup Cho, Hee Myoung Shin and Eun Ha Choi,”Measurement of electron temperature and density using Stark broadening of the coaxial focused plasma for extreme ultraviolet lithography, IEEE transactions on plasma science 38(2010)1111-1117.

[92] S.Y.Moon,W.Choe,H.S.Uhm,Y.S.Hwang and J.J Choi,”Characteristics of an atmospheric microwave induced plasma,” Phys.Plasmas, vol 9, pp. 4045, 2002.

[93] Y.Noguchi,A.Matsuoka,K.UchinoandK.Muraoka,” Direct measurement of electron density and temperature distributions in micro discharge plasma for a plasma discharge panel,”J.Appl.Phys, vol 91, pp.613, 2002.

[94] B.Qi,J.J.Huang,L.Gao and Y.M.Qui,”Electron density measurements in an atmospheric pressure argon discharge by means of plasma radiation,” Phys.Plasmas, vol 16, pp. 083301, 2009.

[95] J.Torres,J.Jonkers,M.J.van de sande,J.J.A.M.Van der Mullen,A.Gamero, and A.Sola,”An easy way to determine simultaneously the electron density and temperature

in high pressure plasmas using stark broadening," J.Phys.D.Appl.Phys, vol 36, pp. L55-L59, 2003.

[96] J.Torres,J.M Palomares, A.Sola ,J.J.A.M.Van der Mullen, and A.Gamero,"A stark broadening method to determine simultaneously electron temperature and density in high pressure microwave plasmas," J.Phys.D.Appl.Phys, vol 40, pp.5929, 2007.

[97] L.Cadwell,L.Huwel, "Time resolved emission spectroscopy in laser generated argon plasmas- determination of stark broadening parameters" ,J.Quant.Spectrosc.Radiant Trans, vol 83, pp. 579-598, 2004

[98] M.Sabsabi,P.Cielo,"Quantitative analysis of allumium alloys by laser induced break down spectroscopy and plasma characterization", J. Appl Spectrosc, vol 49, pp. 499-507, 1995

[99] P.T Rumsby and J.W.M.Paul," Temperature and density of expanding laser produced plasma", J. Plasma Phys, vol16, pp. 247 – 260, 1974

[100] A.Caruso and R.Gratton, " some properties of plasmas produced by irradiating light solids by laser pulses", J. Plasma Phys,vol10, pp. 867-877, 1968

[101] Y.B.Zeldovich and Y.P.Raizer,Physics of shock waves and high temperature hydrodynamic phenomena(Academic press,New york, 1966)

[102] J.Hoffman, T.Moscicki and Z.Szymanski, "The effect of laser wavelength on heating of ablated carbon plume", vol 104, pp. 815-819, 2011

[103] R.A.Burdt,S.Yuspeh,K.L.Sequoia,Y.Z.Tao.M.S.Tillack,F.Najmandi, " Experimental scaling law for mass ablation rate from a Sn plasma generated by 1064 nm laser", J.ApplPhys, vol106, pp. 033310, 2009

[104] W.M.Haynes,CRC Hand book of chemistry and Physics(CRC Press,Boca Raton,FL,2013)

[105] A.Bogaerts and Z.Y.Chen,Spectrochim.Acta, Part B 60,1280(2005)

[106] Genius.S.J, "The chemical erosion of human health: adverse environmental exposure and in utero pollution determinants of congenital disorders and chronic disease", J Prenat Med, vol 34, pp. 185-195, 2006.

[107] Genius.S.J, "Nowhere to hide: Chemical toxicants and the unborn child", J. Reprod Toxicol, vol 28, pp. 155-166, 2009

[108] Gilman, Alfred, Goodman, Louis, Gilman, Alfred Goodman, Goodman and Gilman's the pharmacological basis of therapeutics, New York: MacMillan Publishing, vol 1546, 1980

[109] Osuji O.O, Leake J.L, Chipman M.L, Nikiforuk.G, Locker.D, Levine.N, "Risk factors for dental flourosis in a fluoridated community", J Dent Res, vol 67, pp. 1488–92, 1988.

[110] Milsom K, Mitropoulos C.M," Enamel defects in 8-yearoldchildren in fluoridated and non-fluoridated parts of Cheshire", J. Caries Res, vol 24, pp. 286–289, 1990.

[111] Evans D.J, “A study of developmental defects in enamel in 10 year-old high social class children residing in a non-fluoridated area”, J. Community Dent Health, vol 8, pp. 31–38, 1991
[112] Riordan P.J. “Dental flourosis, dental caries and fluoride exposure among 7-year-olds”, J. Caries Res, vol 27, pp. 71–77, 1993
[113] Pendrys D.G, Katz R.V, Morse D.E, “Risk factors of enamel flourosis in a fluoridated population”, J. Dent Res, vol 72, pp. 109, 1993
[114] Lalumandier J.A, Rozier G.R, “The prevalence and risk factors of flourosis among patients in a pediatric dental practice”, J. Pediatric Dent, vol 17, pp. 19–25, 1995
[115] Blinkhorn A.S, “Influence of social norms on tooth brushing behavior of preschool children”, J. Community Dent Oral Epidemiol, vol 6, pp. 222–6, 19788
[116] Grytten .J, Rossow. I, Holst. D, Steele. L, “Longitudinal study of dental health behaviors and other caries predictors in early childhood”, J. Community Dent Oral Epidemiol, vol16, pp. 356–9, 1988.
[117] Levy S.M, Maurice T.J, Jakobsen J.R, “Dentifrice use among preschool children”, J. Am Dent Assoc, vol 124, pp. 57–60, 1993
[118] Levy S.M, Zarei-M.Z, “Retrospective evaluation of fluoride exposures in children”, J. Dent Child, vol 58, pp. 467–473, 1991.
[119] Dowell T.B, “The use of toothpaste in infancy”. J. Br Dent , vol 150, pp. 247–249, 1981
[120] Hargreaves J.A, Ingram G.S, Wagg B.J, “Excretion studies on the ingestion of a monofluorophosphate tooth paste by children”, J. Caries Res, vol 4, pp. 256–268, 1970.
[121] Baxter P.M, “Toothpaste ingestion during tooth brushing by school children”, J. Br Dent, vol 48, pp. 125–128, 1980.
[122] Naccache H, Simard P, Trahan L, Demers M, Lapointe C, Brodeur J.M, “Variability in the ingestion of toothpaste by preschool children”, J. Caries Res, vol 24, pp. 359–363, 1990
[123] Naccache H, Simard P, Trahan L, Brodeur J.M, Demers M, Lachapelle D, “Factors affecting the ingestion of fluoride dentifrice by children”, J. Public Health Dent, vol 52, pp. 222–226, 1992.
[124] Levy S.M, Maurice T.J, Jakobsen J.R,”A pilot study of preschoolers’ use of regular-flavored dentifrices and those flavored for children”, J. Pediatr Dent, vol 14, pp. 388–91, 1992.
[125] Burt B.A, “The changing patterns of systemic fluoride intake”, J. Dent Res, vol 71, pp. 1228-1237, 1992.
[126] Baelum V, Ferjeskov O, Manji F, Larsen M.J, “Dose of fluoride and dental flourosis” ,J. Tandlaegebladet, vol 91, pp. 452–456, 1987.
[127] Ripa L.W, “A critique of topical fluoride methods (dentifrices, mouth rinses, operator and self-applied gels) in an era of decreased caries and increased fluorosis prevalence”, J. Public Health Dent, vol51, pp. 23–41, 1991.

[128] Fejerskov O, Manji F, Baelum V, Moller I.J, Dental fluorosis– a handbook for health workers. Copenhagen: Munksgaard, 1988
[129] European archives of pediatric dentistry//10.3 2009
[130] Chioca L.R, Raupp I.M, Da Cunha C, Losso E.M, Andreatini R, "Sub chronic fluoride intake induces impairment in habituation and active avoidance tasks in rats", Eur J. Pharmacol, vol 579, pp. 196–201, 2008
[131] Zhang M, Wang A, Xia T, He P, "Effects of fluoride on DNA damage, S-phase cell-cycle arrest and the expression of NF-κB in primary cultured rat hippocampal neurons", J. Toxicol. Lett, vol 179, pp. 1–5, 2008
[132] Agency for Toxic Substances and Disease Registry. 2003. Toxicological Profile for Fluorides, Hydrogen Fluoride, and Fluorine (Update). Available: http://www.atsdr.cdc.gov/toxprofiles/tp11.pdf
[133] Grandjean P, Landrigan P, "Developmental neurotoxicity of industrial chemicals", J Lancet, vol, 368, pp. 2167–2178, 2006.
[134] Balabolkin M.I, Mikhaĭlets N.D, Lobovskaia R.N, "The interrelationship of the thyroid and immune statuses of workers with long-term fluorine exposure", J. Ter Arkh. Vol 67, pp. 41-42, 1995.
[135] Krishnamachari K.A, "Skeletal fluorosis in humans: a review of recent progress in the understanding of the disease", J. Prog Food Nutr Sci, vol 10, pp. 279-314, 1986.
[136] Yan X, Yan X, Morrison A, "Fluoride induces apoptosis and alters collagen I expression in rat osteoblasts", J. Toxicol. Lett, vol 5, pp.133-8, 2011
[137] Xu H, Wang CH, Zhao ZT, "Role of oxidative stress in osteoblasts exposed to sodium fluoride", J. Biol Trace Elem Res, vol 123,pp. 109-15, 2008
[138] Sandhu R, Lal H, Kundu Z.S, "Serum fluoride and sialic acid levels in osteosarcoma", J. Biol Trace Elem Res, 2009. Published Online Ahead of Print.
[139] Bassin E.B, Wypij D, Davis RB, "Age-specific fluoride exposure in drinking water and osteosarcoma (United States)", J. Cancer Causes Control, vol 17, pp. 421-8, 2006.
[140] M.S.Frant, J.P.Ross, "Electrode for sensing fluoride ion in solution", J. Science, vol 154, pp. 1553, 1966.
[141] W.Shen, X.D.Wang, R.W.Caittral. Electro analysis 7(1995) 10117
[142] M.Pavic, D.Carevic, Z.Cimerman, "Potentiometric determination of monofluorophosphate in dentirifice: A critical discussion an a proposal for new improved procedures", J.Pharm.Biomed.Anal, vol 20, pp. 565-571, 1999
[143] S.Tokalioglu, S.Kartal, U.Kartal, U.Sahin, "Determination of fluoride in various samples and some infusions using a fluoride selective electrode", Turk.J.Chem, vol 28 pp. 203-211, 2004.
[144] T.A.Biemer, N.Asral. A.sippy, "Ion chromatographic procedures for analysis of total fluoride content in dentifrices", J.Chromatogr.A, vol 771, pp. 355-359, 1997

[145] R.Michalski, B.Mathews, "Simultaneous determination of fluoride and monofluorophosphate in tooth pastes by suppressed ion chromatography", Cent.Eur.J.Chem, vol 4, pp. 798-807, 2006

[146] Heike Gleisner, Jurgen W.Einar,Silvane Mores, Bernhard Welz, Eduardo Carasek, "A fast and accurate method for determination of total and soluble fluorine in tooth paste using high resolution graphite furnace molecular absorption spectrometry and its comparison with established techniques", J. Pharm Biomed Anal, vol 54, pp. 1040-1046, 2011

[147] S.M.Seo, E.J.Cho, S.J.Lee, K.C.Nam, S.H.Park, J.H.Jung," A mesoporous silica functionalized by covalently bound naphalene- based receptor for selective optical detection of fluoride ion in water", J. Micropor.Mesopor.Mater, vol 114, pp. 448-454,, 2008

[148] Monika Cernanska, Peter Tomcik, Zuzana Janosikova, Miroslav Rievaj, Dusan Bustin, "Indirect voltammetric detection of fluoride ions in tooth paste o a comb-shaped interdigitated microelectrode array",J. Talanta, vol 83, pp. 1472-1475, 2011

[149] Sun M.Z, Wu F.Y. Wu Y.M, Liu W.M, " A ditopic calorimetric sensor for fluoride ion based on thiorea mercury", J. Spetrochim ActaA:Mol.Biomol Spectrosc, vol 71, no.3, pp. 814-817, 2008.

[150] Walid Tawfik Y.Mohamed, "Study of the matrix effect on the plasma characterization of six elements in aluminum alloys using LIBS with a portable echelle spectrometer", J. Progress in physics, vol 2**,** pp. 42-49, 2007

[151] R. Fantoni, L. Caneve, F. Colao, L. Fornarini, V. Lazic V, "Methodologies for laboratory laser induced break down spectroscopy semi quantitative and quantitative analysis -A review", J. Spectrochim Acta B At Spectrosc, vol 63, pp.1097-1108, 2008

[152] E. H. Evans, J.A. Day, C. Palmer, C.M. Smith, "Advances in atomic spectrometry and related techniques", J. Anal. At. Spectrom, vol 25, pp. 760-784, 2010.

[153] A. Ferrero, J. J. Laserna, "A theoretical study of atmospheric propagation of laser and return light for standoff laser induced breakdown spectroscopy purposes", J.Spectrochim. Acta PartB, vol 63, pp. 305-311, 2008.

[154] George Asimellis, Stephene Hamilton, Aggelos Giannoudakos, Micheal Kompitsas, "Controlled inert gas environment for enhanced chlorine and fluorine detection in the visible and near – infrared by laser induced break down spectroscopy", J. Spectrochimica Acta PartB, vol 60, pp.1132-1139, 2005

[155] S.Morel, M.Durand, P.Adam, J.Amouroux, "Analysis of fluorine, chlorine, sulphur, phosphorous and carbon in air by time resolved laser induced break down spectroscopy :E.Tognin (Ed) First international conference on laser induced plasma spectroscopy and applications", societa italiana di fisica,tirrenia ,pisa,Italy,2001,p.30

[156] M.A.Baig, Aisha Qamar, M.A Fareed, M.Anwar-ul-Haq and Raheel Ali, "Spatial diagnostics of the laser induced lithium fluoride plasma", J. Phys Plasmas. Vol 19, pp. 063304, 2012

[157] B.Le Drogoff. JMargot, M Chaker, M.Sabsabi, O.Barthelemy, T.W Johnston, S.Laville, F.Vidal, Y.Von Kaenel," Temporal characterization of femtosecond laser pulses induced plasma for spectrochemical analysis of aluminum alloys", J. Spectrochim Acta part B, vol 56, pp. 987-1002, 2001.

[158] Young June Hong, Gi Chung Kwon, Guangsup Cho, Hee Myoung Shin and Eun Ha Choi,"Measurement of electron temperature and density using Stark broadening of the coaxial focused plasma for extreme ultraviolet lithography", IEEE transactions on plasma science, vol 38, pp. 1111-1117, 2010.

[159] A.E.Hussein, P.K.Diwakar, S.S.Harilal and A.Hassanein," Role of laser wavelength on plasma generation and expansion of ablation plumes in air, "J.Appl.Phys vol 113,pp 143305, 2013

[160] M.Milan, J.J.Laserna,"Diagnostics of silicon plasmas produced by visible nanosecond laser ablation," J. Spectrochimica Acta Part B, vol 56, pp. 275-288, 2001

[161] M. A. Gondal, M.A. Dastageer, Naqvi A. A., A. A. Isab, and Y. W. Maganda, "Detection of toxic metals(lead and chromium) in talcum powder using laser induced break down spectroscopy," J. Applied Optics, vol 51, pp. 7395, 2012.

[162] Metin Denli, Rusen D, ZelihagulD, TucerD, Mehtap.A, Volkan B," Effect of long term use of hair dyes on the DNA damage in health female subjects," The medical journal of Kocatepe, vol 3**,** pp. 57-62, 2002

[163] I.C. Nnorom, J.C. Igwe, C.G. Oji-Nnorom," Trace metal of facial (make up) cosmetics commonly used in Nigeria," African J.Biotech, vol 4**,** pp. 1113-1138, 2005

[164] I. Al-Saleh, S. Al-Enazi, N. Shinwari, "Assessment of lead in cosmetic products," J. Regular Toxicol.Parmacol, vol 54**,** pp. 105-113, 2009

[165] P.Apostoli," Elements in environmental and occupational medicine," J of Chrom.B, vol 778**,** pp. 63-97, 2002

[166] G. Saxena, G.M. Kannan, N. Saksenad, R.J. Tirpude, S.J.S. Flora," Lead induced oxidative stress and DNA damage using comet assay in rat blood," J.Cell Tissue Res, vol 6, pp. 763-768, 2006

[167] Some metals and metallic compounds. Lyon, International Agency for Research on cancer,1980(IARC Monographs on the evaluation of the carcinogenic risk of chemicals to humans,vol.23)

[168] Health assessment document for chromium. Research Triangle Park.NC, United States environmental protection agency, 1984(final report No.EPA600/8-83-014F).

[169] Chromium, nickel and welding. Lyon, International Agency for Research on Cancer,1990,pp.463-474(IARC Monographs on the evaluation of carcinogenic risk of chemicals to humans,Vol.49)

[170] Richa shrivastava, R.K.Upreti, P.K.Seth, U.C.Chaturvedi, "Effects of chromium on the immune system," J. FEMS Immunology and Medical Microbiology, vol 34, pp. 1-7, 2002

[171] Bruyzee.D.P, Hennipmann.G and Van ketel, W.G (1988),"Irritant contact dermatitis and chromium passivated metal," J. Contact dermatitis, vol 19**,** pp. 175-179, 1988.
[172] Brieger H Zur Klinik der akuten Chromatvergiftung. Zeitchrift fur experimentelle pathologie und Therapie, vol 21, pp. 393-408, 1920
[173] G.J.Nohynek, R.Fautz, F.Benech-kieffer and H.Toutain,"Toxicity and human health risk of hair dyes," J. Food and Chemical Toxicology, vol 42, pp. 517-543, 2004
[174] M.A. Gondal, Z. Seddigi, M.M.Nasr, B.Gondal," Spectroscopic detection of health hazardous contaminants in Lipstick using laser induced breakdown spectroscopy," J. Hazard mat, vol 175, pp. 726-732, 2010
[175] G.Gillian, G.Duyckaerts and A.Disteche,"Direct and simultaneous determination Zn, Pb, Cd, Cu, Sb, Bi dissolved in sea water by differential pulse anodic stripping voltammetry with a hanging mercury drop electrode," J. Anal.Chim.Acta, vol 106**,** pp. 23, 1979
[176] Ying Shih, Jyh-MyngZen, Annamalai Senthil Kumar, Yi-Chien Lee and Hui-Rou Huang, "Determination of the Toxic lead level in cosmetic hair dye formulations using a screen printed silver electrode," J. Bull.chem.Soc.Jpn, vol 77, pp. 311-312, 2004
[177] Tande.T, "Simultaneous determination of Cr (III) and Cr (VI) in water by reversed phase HPLC, after chelating with sodium diethyldithiocarbamate," J. Chromatographia, vol 13, pp**.** 607-610, 1980
[178] Urasa.I.T and Nam.S.H, "Direct determination of Cr (III) and Cr (VI) with ion chromatography using direct current plasma emission as element selective detector," J. chromatographic science, vol 27, pp. 30-37, 1989
[179] Cinzia Tonetti, Riccardo Innocenti," Determination of heavy metals in textile materials by atomic absorption spectrometry: Verification of the test method," AUTEX research journal. Vol 9, 2009.
[180] R.K.Singh, O.W.Holland and J.Narayan ,"Theoretical model for deposition of superconducting thin film using pulsed laser evaporation technique," J. Appl Phys, vol 68, pp. 233, 1990
[181] A.P.Thorne,Spectrophysics,2nd edition, Chapman and Hall,London,1998
[182] M.A. Gondal, Z. Seddigi, M.M.Nasr, B.Gondal," Spectroscopic detection of health hazardous contaminants in Lipstick using laser induced breakdown spectroscopy," J. Hazard mat, vol 175, pp. 726-732, 2010
[183] G.J.Nohynek, R.Fautz, F.Benech-kieffer and H.Toutain,"Toxicity and human health risk of hair dyes," J. Food and Chemical Toxicology, vol 42, pp. 517-543, 2004
[184] R.M.Al-Ashban, M.Aslam, A.H.Shah,"Kohl(surma) a toxic traditional eye cosmetic study in Saudi Arabia, "J. Public Health, vol 118, pp. 292-298, 2004
[185] N.Ashoub, W.M.Abdel Aziz, A.Elkady and I.I.Bashter,"Study of the elemental content of some natural and synthetic eye cosmetics," J. Energy and environmental research, Vol 3,no.1, pp. 1927-0577, 2013

[186] Al Hazza.S.A and Krahn.P.M "Kohl: a hazardous eyeliner", J. inter ophthal, vol 19, no. 2, pp. 83-88, 1995

[187] Hardy.A.D, Walton.R.I and Vaishnave.R,"Composition of eye cosmetics (kohls) used in Cairo," J. Environ. Health Res , vol 14, no.1, pp. 83-91, 2004.

[188] Lekouch.N, Sedki.A, Nejmeddine.A and Gamon.S (2001) "Lead and traditional Moroccan pharmacopoeia", J. The science of the total environment, vol 280, pp. 39-34, 2001

[189] Pervaiz habibullah, Zafar alam mahmood, Mohammad sualeh and sms zoha,"Studies on the chemical composition of kohl stone by x-ray diffractometer," Pak.J.Pharm.Sci, Vol 23, pp. 48-52, 2010.

[190] Klaasen.C.D, Casarett and Doulls Toxicology, the basic science of poisons (5^{th} ed) New York: McGraw hill book company, 1996

[191] Al salehI, "Sources of lead in Saudi Arabia: a review,"J. Environ Pathol Toxicol Oncol, vol 17, pp. 17-35, 1998

[192] Hu H. "Poorly controlled hypertension in a painter with chronic lead toxicity",J. Environ Health Perspect, vol 109, pp. 95-99, 2001

[193] Rothenberg S.J, Schanaas L, Salgado-Valladares M, "Increased ERG *a* and *b* wave amplitudes in 7 to 10 year old children resulting from parent", Inv.Opth& vis sci, vol 43, no.6, pp. 2036-2044, 2002

[194] Al-Saleh I, Khalil M.A, Taylor A. "lead, erythrocyte protoporphyrin and hematological parameters in normal maternal and umbilical cord blood from subjects of the Riyadh region, Saudi Arabia", J. Arch Environ health, vol 50, pp. 66-73, 1995

[195] New York city department of health, Lead poisoning prevention program.Newyork:DOH;1999

[196] M.A. Gondal, Z. Seddigi, M.M.Nasr, B.Gondal," Spectroscopic detection of health hazardous contaminants in Lipstick using laser induced breakdown spectroscopy," J. Hazard mat, vol 175**,** pp. 726-732, 2010

[197] A.F.M.Y Haider, R.S.Lubna and K.M.Abedin,"Elemental analyses and determination of lead content in kohl(stone) by laser induced breakdown spectroscopy," J. Appl spectrosc 66,420-425(2012

[198] P.Stravropoulos, C.Palagas, G.N Angelopoulous, D.N Papamantellos, S.Couris, "Calibration measurements in laser induced break down spectroscopy using nanosecond and picoseconds lasers", J. Spectrochmica Acta Part B, vol 59, pp. 1885-1892, 2004

[199] J. J Hostynek. "Toxic potential from metals absorbed through the skin", J. Cosmetics & Toiletries, vol 113, pp. 33–43 ,1998

[200] J. J. Hostynek Lead, Manganese and Mercury: Metals in Personal-Care Products. J. Cosmetics and Toiletries Magazine. Vol 116, pp. 52-65. 2001

[201] Gruber, H.E., H.C. Gonick, F. Khalil-Manesh, T.V. Sanchez, S. Motsinger, M. Meyer, C.F. Sharp. “Osteopenia induced by long-term, low- and high-level exposure of the adult rat to lead”, J. Mineral & Electrolyte Metabolism, vol 236, pp. 45-73, 1997

[202] D. C. Rice, “Behavioural Impairment produced by developmental lead exposure: Evidence from primate research. In Human Lead Exposure”, ed H. L. Needleman, CRC Press, 1992.

[203] National Research Council (US). Measuring lead exposure in infants children and other sensitive populations. National Academy Press, Washington DC, 1993.

[204] M. A. Smith, L. D. Grant and A. Sors, “Lead exposure and child development: an international assessment”. Kleeven Academic Publishers, 1989.

[205] M. D. Cohen, B. Kargacin, C. B. Klein, and M. Costa, “Mechanisms of chromium carcinogenicity and toxicity.Crit. Rev”, J. Toxicol.,vol 23, pp. 255-281, 1993

[206] S. Langard “Chromium carcinogenicity: a review of experimental animal data”, J. Sci Total Environ, vol 71, pp. 341–350, 1988

[207] D. A Basketter, G. Briatico-Vangosa, W. Kaestner, C . Lally and W. J Bontinck. “Nickel, cobalt and chromium in consumer products: a role in allergic contact dermatitis” J. Contact Dermatitis, vol 28**,** pp. 15-25, 1993

[208] D. A. Basketter, G. Angelini, A. Ingber, P. S Kern and T. Menné,”Nickel, chromium and cobalt in consumer products: revisiting safe levels in the new millennium”, J. Contact Dermatitis, vol 49**,** pp 1-7, 2003

Vitae

Name	:Yasin Wandhami Maganda
Nationality	:Ugandan
Date of Birth	:1/13/1987
Email	:ymaganda@gmail.com
Address	:King Fahd University of Petroleum and Minerals Department of Physics, 31261 Dhahran- Saudi Arabia

Academic Background	: From February/2011 to October/2013 Master of Science in Physics, King Fahd University of Petroleum and Minerals, Dhahran- Saudi Arabia
	: From August/2006 to May/2009 Bachelors of Science in Physics, Makerere University, Kampala-Uganda

Publications

1. M.A. Gondal, M.A. Dastageer, A. **Y.W. Maganda** ,A.A. Naqvi and A. A. Isab, Detection of lead and chromium in talcum powder using Laser Induced Breakdown Spectroscopy (LIBS) with Pb I (405.7 nm) and Cr I (425.4 nm) atomic transition lines as spectral Markers, *J.Appl Optics*, **51**,7395 (2012).
2. M.A.Gondal, **Y.W.Maganda**, M.A.Dastageer, F.F.Adel, and A.A.Naqvi, Study of temporal evolution of electron density and temperature for atmospheric plasma generated from fluid samples using Laser Induced Break down Spectroscopy, *IEEE proceedings* (2013)
3. M.A.Gondal, **Y.W.Maganda**, M.A.Dastageer, F.F.Adel and A.A.Naqvi, Detection of level of fluoride in commercially available tooth paste using Laser Induced Breakdown Spectroscopy. *J. Optics and laser technology*. 57, 32-38 (2013)
4. M.A.Gondal, **Y.W.Maganda**, M.A.Dastageer, F.F.Adel and A.A.Naqvi, Detection of carcinogenic chromium (Cr) in synthetic hair dyes using Laser Induced Breakdown Spectroscopy. *J. Appl Optics* (submitted)
5. M.A.Gondal, **Y.W.Maganda**, M.A.Dastageer, F.F.Adel and A.A.Naqvi, "Development of a laser induced breakdown sensor for detection of carcinogenic chemicals in cosmetic products", *IEEE proceedings.*
6. M.A.Gondal, **Y.W.Maganda,** M.A.Dastageer, F.F.Al-Adel Detection of lead and chromium in commercially available kohl using Laser Induced Breakdown Spectroscopy", *Spectrochimica Acta part B* (being submitted)

7. M.A.Gondal, T.F.Qahtan, M.A.Dastageer, **Y.W.Maganda**, D.H.Arjun, ”Synthesis of Cu/Cu_2O nanoparticles by laser ablation in deionized water and their annealing transformation into CuO”, *J.NanoSci &Tech.* 13, 5759-5766 (2013)
8. M.A.Gondal, T.F.Qahtan, M.A.Dastageer, T.A.Saleh, **Y.W.Maganda, “**Effects of oxidizing medium on the composition, morphology and optical properties of copper oxide nano particles produced by laser ablation,” *J.Appl Surf Sci.* (2013)